University of Pannonia

Chemical Engineering and Material Sciences Doctoral School (CEMSDS)

PhD Dissertation

Energy-efficiency analysis of phase change thermal storage microcapsules in model houses

DOI:10.18136/PE.2026.997

Written by:

Monika Ferencz

Supervisor:

Tivadar Feczkó PhD

Veszprém

2026

Energy-efficiency analysis of phase change thermal storage microcapsules in model houses

The thesis was prepared for the award of a doctoral degree (PhD) within the framework of the Chemical Engineering and Material Sciences Doctoral School (CEMSDS) at University of Pannonia

in the discipline of Bio-, environmental and chemical engineering sciences

written by: Monika Ferencz

Supervisor[s]: Tivadar Feczkó PhD

I recommend the dissertation for acceptance: yes / no.

……
supervisor

I recommend the dissertation for peer review.

…….
chair of the DDHC

The PhD-candidate has achieved ……. % at the public debate.

The composition of the Final Examination Committee:

chair:…….…….
reviewers:.…….
members:……...

Veszprém,

……
chair of the committee

Qualification of degree: ….....

Veszprém,

…….
chair of the UDHC

Table of contents

List of figures

List of tables

List of abbreviations

PCM: phase change material (the PCM material itself, e.g., microencapsulated paraffin).

PCM house: the PCM-enhanced model house (the test case in which the interior gypsum-based lining contains PCM and is installed on the interior side of the vertical opaque walls).

> ***Clarity note:*** *Throughout the dissertation, "PCM" is used for the material; when "PCM" appears as a case label in figures or captions, it refers to the PCM-plastered house ("PCM house"), so the text explicitly uses "PCM material" vs "PCM house" where needed to avoid ambiguity.*

REF: reference house (baseline container unit without PCM-containing interior lining).

OSB: oriented strand board

SD: standard deviation

U-value (U): thermal transmittance

HVAC: heating, ventilation, and air conditioning

RMSE: root mean square error (statistical measure of prediction error, a variability around the fitted trend)

Type-K: thermocouple type K – measuring equipment

IEQ: indoor environmental quality

EDH: Exceeded Degree-Hours

Kivonat (Abstract in Hungarian)

Az értekezés tárgya a mikrokapszulázott fázisváltó anyagot tartalmazó vakolat hatásának vizsgálata könnyűszerkezetes épületek dinamikus hőviselkedésére. A kutatás célja annak meghatározása volt, hogy a PCM-et tartalmazó vakolat miként módosítja a beltéri hőmérséklet napi lefutását, a csúcshőmérsékletek időbeli helyzetét, a túlmelegedési kitettséget, valamint, hogy mérési adatok alapján mely tájolásoknál várható a legnagyobb gyakorlati hatás.

A vizsgálat alapját egy 2021-ben végzett, 105 napos mérési kampány képezte, amely két azonos könnyűszerkezetes modellházban zajlott. Az egyik ház belső falazatában mikrokapszulázott PCM-et tartalmazó vakolat volt, míg a másik referenciaház PCM nélküli kialakítású volt. A rendelkezésre álló nagy mennyiségű nyers szenzoradat feldolgozása Python-alapú, reprodukálható munkafolyamattal történt, több esetben statisztikai értékelési eljárások alkalmazásával. A hosszú idősorok dinamikus értelmezéséhez Poincaré-ábrázolás, a tájolásfüggő alkalmazhatóság értékeléséhez pedig jellemző hőmérséklet-különbség és jellemző hőáramsűrűség mutatók kerültek alkalmazásra.

Az eredmények igazolták, hogy a PCM vakolat jelentősen csökkenti a napi beltéri hőmérséklet-ingadozást. Kimutatható volt továbbá a csúcshőmérséklet későbbre tolódása, amely a komforttartományban töltött idő növekedésével és a túlmelegedési kitettség mérséklődésével járt együtt. A tájolás szerinti értékelés alapján a tető és a nyugati tájolás bizonyult a legkedvezőbb célfelületnek a PCM gyakorlati alkalmazása szempontjából.

A disszertáció fontos eredménye, hogy nagymintás, mérési adatokon alapuló értékeléssel igazolja a PCM vakolat hőmérsékletcsillapító, csúcsidei eltolódást okozó és komfortjavító hatását, valamint gyakorlati döntési alapot ad a célzott, tájolásfüggő alkalmazáshoz.

Abstract

The subject of the dissertation is the investigation of the effect of plaster with incorporated microencapsulated phase change material on the dynamic thermal behavior of lightweight buildings. The aim of the research was to determine how PCM-containing plaster modifies the daily course of indoor temperature, the temporal position of peak temperatures, overheating exposure, and, on the basis of measured data, which orientations are expected to provide the greatest practical benefit.

The investigation was based on a 105-day measurement campaign conducted in 2021 in two identical lightweight model houses. One house had plaster containing microencapsulated PCM in the indoor wall construction, while the other reference house had no PCM. The processing of the available large quantity of raw sensor data was carried out through a Python-based, reproducible workflow, in several cases using statistical evaluation procedures. Poincaré representation was applied for the dynamic interpretation of the long time series, and characteristic temperature difference and characteristic heat flux density indicators were used to evaluate orientation-dependent applicability.

The results confirmed that PCM plaster significantly reduces daily indoor temperature fluctuation. A shift of peak temperature to a later time was also identified, and this was associated with an increase in the proportion of time spent within the comfort range and a reduction in overheating exposure. Based on the evaluation by orientation, the roof and the west-facing orientation proved to be the most favorable target surfaces for the practical application of PCM.

An important result of the dissertation is that, through a large-sample evaluation based on measured data, it confirms the temperature-damping, peak-shifting, and comfort-improving effect of PCM plaster, and provides a practical basis for decision-making for targeted, orientation-dependent application.

Zusammenfassung (Abstract in German)

Die Dissertation untersucht den Einfluss eines mikrokapselhaltigen PCM-Putzes auf das dynamische thermische Verhalten von Leichtbaugebäuden.

Grundlage ist eine 105-tägige Messkampagne aus dem Jahr 2021 an zwei identischen Leichtbau-Modellhäusern, von denen eines PCM-Putz in der inneren Wandkonstruktion enthielt. Die Auswertung basiert auf einer großen Menge von Sensordaten und wurde mit einem reproduzierbaren, Python-basierten Verfahren durchgeführt. Die Ergebnisse zeigen, dass PCM-Putz die täglichen Schwankungen der Innenraumtemperatur verringert und die Temperaturspitzen zu späteren Tageszeiten verschiebt. Dies war mit mehr Zeit im Komfortbereich und geringerer Überhitzungsexposition verbunden.

Die orientierungsabhängige Analyse zeigte zudem, dass Dachflächen und Westausrichtung die günstigsten Anwendungsbereiche darstellen. Die Arbeit bestätigt damit auf Messdatenbasis die temperaturdämpfende, spitzenverschiebende und komfortverbessernde Wirkung von PCM-Putz.

Tiivistelmä (Abstract in Finnish)

Väitöskirjassa tarkastellaan mikrokapseloitua faasimuutosmateriaalia sisältävän laastin vaikutusta kevytrakenteisten rakennusten dynaamiseen lämpökäyttäytymiseen. Tutkimus perustuu vuonna 2021 toteutettuun 105 päivän mittauskampanjaan kahdessa keskenään identtisessä kevytrakenteisessa mallitalossa, joista toisessa sisäpuolisessa seinärakenteessa käytettiin PCM-laastia. Arviointi perustui suureen määrään anturidataa, joka käsiteltiin toistettavalla, Python-pohjaisella menetelmällä. Tulokset osoittavat, että PCM-laasti vähentää sisälämpötilan päivittäistä vaihtelua ja siirtää lämpötilahuiput myöhempään ajankohtaan. Tämä johti siihen, että mukavuusalueella vietetty aika piteni ja ylikuumenemisalttius pieneni

Ilmansuunnan mukainen analyysi osoitti lisäksi, että katto ja länsisuunta ovat edullisimmat kohteet käytännön soveltamiselle.

Työ vahvistaa siten mittausaineiston perusteella PCM-laastin lämpötilavaihtelua vaimentavan, huippuja siirtävän ja lämpöviihtyvyyttä parantavan vaikutuksen.

1. Introduction and contributions

Thermal energy storage has become a defining issue in building physics and building energy research. The thermal behavior of a building is determined not only by the magnitude of heat losses and heat gains, but also by the extent to which the structure can moderate their time-dependent effects. Thermal storage capacity is therefore not a secondary structural property, but one of the basic determinants of dynamic thermal behavior. This becomes especially important in situations where indoor conditions are shaped by rapidly changing loads and where the role of the structure is not to maintain a nearly steady thermal state, but to attenuate short-term thermal stress.

In this context, latent heat storage is of particular importance. While sensible heat storage is linked to a change in the temperature of the structural material, phase-change-based storage makes it possible for a significant amount of energy to be absorbed and released within a relatively narrow temperature interval. From the perspective of building physics, this is important, because the storage effect does not result simply from an increase in mass but appears in a temperature range that is directly related to indoor conditions and thermal comfort. This explains why phase change materials have become one of the most intensively studied areas of building-integrated thermal storage in recent years.

Among PCM-based solutions, plaster deserves special attention, because it provides a realistic and practical way to integrate latent heat storage into the indoor side of the wall construction. Plaster containing microencapsulated PCM does not simply add another material layer; it modifies the time-dependent thermal response of the structure. During warmer periods, it absorbs part of the incoming heat and releases it later, thereby directly influencing the daily course of indoor temperature. For this reason, the effect of PCM cannot be described adequately by comparing absolute maxima and minima alone. Its real importance lies in its ability to modify daily temperature amplitude, the timing of peaks, and the duration of thermally unfavorable periods.

This issue is especially important in lightweight buildings. Because of their low thermal mass, such structures respond rapidly to changing outdoor conditions. Under solar radiation, exterior surfaces can heat up significantly within a short time, and the resulting thermal load can quickly affect indoor conditions. In lightweight spaces with small indoor

volume, this often appears as larger daily indoor temperature swings and sharper temperature peaks. Under these conditions, dynamic behavior is more important than average values. A daily mean temperature may appear acceptable, while short but relevant periods of overheating still occur. The problem therefore cannot be described adequately by static indicators alone; it requires an evaluation that also captures the temporal structure of indoor temperature variation.

This is particularly true under free-running measurement conditions, where no active heating or cooling system masks the natural dynamic response of the building. In this situation, the measured indoor thermal behavior directly reflects the interaction between the structure, solar radiation, outdoor temperature variation, and thermal storage capacity. Free-running measurements are therefore especially suitable for examining the actual effect of structure-integrated PCM. At the same time, this also means that the interpretation must take natural weather variability into account. Evaluating PCM performance therefore requires not only measured data, but also an approach that can reveal consistent patterns in long and highly variable datasets.

The present work is based on a 105-day measurement campaign carried out in 2021 in two identical lightweight model houses. The geometry and structural build-up of the two houses were the same. The difference was that one house had plaster containing microencapsulated PCM in the indoor wall construction, while the reference house had no PCM. The available dataset consists of a large number of raw sensor records with 5-minute time resolution. The length and density of the time series make it possible to examine the thermal behavior of the two houses on the basis of the full monitoring period, which covers a wide range of naturally occurring outdoor conditions, rather than because of only a few selected days.

The processing and evaluation of the large sensor database, with 5-minute time resolution and a very high number of data points, were carried out through a Python-based, reproducible workflow, in several cases using statistical evaluation methods. This is particularly important, because the study does not draw conclusions from a few selected days or from isolated weather situations, but from a dataset that includes the natural meteorological variability of the full monitoring period. The large sample size and statistical processing together significantly increased the reliability of the identified relationships and provided a stronger basis for the professional conclusions. In this sense,

the handling of the large dataset was not merely a technical issue, but one of the key conditions for the validity of the conclusions drawn.

The evaluation carried out in the dissertation is organized around three closely related questions. The first question concerns the extent and form in which PCM plaster modifies the dynamic indoor temperature response of a lightweight model house under real and naturally varying outdoor conditions. The issue here is not simply whether the presence of PCM reduces daily extremes, but also how consistently this effect can be identified across the full monitoring period. The core of the problem is therefore not the comparison of a few striking individual days, but the understanding of how PCM changes the structure of the daily temperature profile under a large number of diverse meteorological situations. This question includes the reduction of daily amplitude, the moderation of the indoor temperature path, and the specific situation in which a lightweight house exhibits heat-trap-like behavior under solar radiation, with indoor temperatures becoming elevated relative to outdoor air temperature.

The second question focuses specifically on the temporal structure of the dynamic response. Its center is time lag, or peak shifting, that is, the fact that PCM modifies not only the magnitude of the indoor temperature peak but also shifts its timing to a later hour. From the perspective of building physics, this effect has independent significance, because it suggests that PCM does not simply attenuate thermal load but also redistributes the thermal response in time. The real importance of this question, however, lies in the relationship between this peak delay and thermal comfort. The analysis therefore also addresses how the later occurrence of the daily maximum influences the fraction of time spent within the comfort range and the degree of overheating exposure. In this context, the dissertation examines whether peak shifting is merely a descriptive dynamic feature or a mechanism that directly contributes to more favorable indoor thermal conditions.

The third question extends the investigation toward practical applicability. If the effect of PCM can be verified, the next step is to determine where in the structure the greatest benefit can be expected. This is particularly important, because exposure to solar radiation and the resulting thermal load differ strongly by orientation and by building elements. The dissertation therefore does not aim to define a general, average PCM effect, but to identify, through a large-sample method based on measured data, those orientations and building elements where PCM application is most favorable. In engineering terms, the question is

direct: if the amount of PCM, its location, or the treated surface area is limited, in what order should the surfaces be prioritized? The purpose of this part of the work is to derive, from measured temperature and heat-flux data, practical guidance that goes beyond general statements and directly supports targeted design decisions.

These three questions require different, but closely connected, evaluation approaches. The dynamic behavior of long indoor temperature time series must be represented in a form that remains interpretable even for large datasets; therefore, Poincaré representation is used. The comfort meaning of peak shifting must be linked to a metric that expresses both the intensity and the duration of overheating; for this reason, exceeded degree-hours (EDH) are used within an adaptive comfort interpretation. Orientation-dependent applicability must be described by indicators that remain meaningful from an engineering point of view; this is why characteristic temperature difference and characteristic heat flux density are introduced.

The dissertation is built on three published papers, all of which process the same 2021 measurement dataset, but from different perspectives. The first paper focuses on the measured indoor thermal behavior of the PCM house and the reference house, including the reduction of daily amplitude, the interpretation of long time series by means of Poincaré plots, and the interpretation of heat-trap behavior under solar radiation. The second paper examines time lag and peak shifting and links these dynamic effects to comfort-related outcomes, including the increase in the fraction of time spent within the comfort range and the use of EDH. The third paper develops a large-sample, measurement-based method to determine which orientations are optimal for PCM application in the wall construction, with particular emphasis on the practical importance of the roof and the west-facing orientation.

Together, the three papers define a coherent line of investigation. The starting point is to show how PCM modifies the measured indoor temperature dynamics of a lightweight structure. This is followed by clarifying how these time-dependent changes can be interpreted from the perspective of thermal comfort. Finally, the work reaches the question of practical application, namely how measured results can be translated into orientation-dependent conclusions that support engineering decisions. The purpose of the dissertation is therefore not merely to show that PCM affects thermal behavior, but also to clarify how

this effect appears in a measured lightweight structure, how it can be interpreted in relation to comfort, and how it can be used in practice.

2. Bibliographic review and critical synthesis

Editorial note on referencing strategy

This dissertation is based on three article-format studies that are included in revised and extended form. For editorial reasons, the external literature citations are consolidated in the chapter “Bibliographic review and critical synthesis,” which provides the broader scholarly context for the dissertation. This chapter integrates the relevant state of the art across the different topic areas addressed by the three studies, using a consistent author–date in-text citation format and a single alphabetized reference list. The chapter “Experimental basis, data provenance, and processing” documents the experimental context and the origin and handling of the datasets used in the dissertation. The “Results” chapter focuses on the methods and findings of the included studies, while the chapters “Synthesis,” “Limitations,” and “Conclusions” provide cross-study interpretation, discuss constraints, and summarize the overall contribution.

2.1 Phase change materials: fundamentals, advantages, and limitations

Phase change materials are thermal storage media that absorb and release heat through a phase transition, usually within a narrow temperature range. Their main advantage is that a relatively large amount of energy can be stored and released as latent heat with only limited temperature change. In buildings, this makes PCM attractive for increasing the effective thermal mass of lightweight structures, moderating indoor temperature fluctuations, and reducing or delaying peak thermal loads [Zalba et al., 2003; Khudhair and Farid, 2004; Baetens et al., 2010]. For this reason, PCM has been widely studied as a passive means of improving thermal comfort and reducing energy demand, especially in

building envelopes with low inherent heat storage capacity [Baetens et al., 2010; Kalnæs and Jelle, 2015].

The performance of a PCM depends strongly on its melting range, latent heat capacity, cycling stability, thermal conductivity, and compatibility with the host material [Cabeza et al., 2011; Pielichowska and Pielichowski, 2014]. The main PCM groups used in building applications are organic, inorganic, and eutectic materials. Organic PCM, such as paraffins and fatty acids, are often favored because of their chemical stability and suitable phase change range, although their low thermal conductivity and fire-related behavior must be considered. Inorganic PCM, such as salt hydrates, may offer higher volumetric storage density, but they are more prone to problems such as subcooling, phase segregation, and corrosion. Eutectic systems are used when a more specific melting temperature or property combination is needed, although their practical use is also limited by long-term stability and integration issues [Cabeza et al., 2011; Pielichowska and Pielichowski, 2014].

The main groups of phase change materials used in building-related latent heat storage applications are summarized in Table 1.

Table 1: Main groups of phase change materials used in building applications

PCM group	Typical examples	Main advantages for building applications	Main limitations
Organic PCM	Paraffins, fatty acids	Good chemical stability, congruent melting, limited subcooling, and phase-change temperature ranges suitable for indoor thermal comfort applications.	Low thermal conductivity, flammability concerns, and the need for encapsulation or stabilization to avoid leakage.
Inorganic PCM	Salt hydrates, metallics	Higher volumetric storage density and relatively high latent heat capacity.	Subcooling, phase segregation, corrosion risk, and more demanding long-term stability requirements.
Eutectic PCM	Organic–organic, inorganic–inorganic, and organic–inorganic mixtures	Tailorable melting temperature and the possibility of matching a specific application temperature range.	More complex formulation, limited long-term data, and material compatibility issues depending on the selected components.

This classification is relevant for building applications because the material group determines not only the phase-change temperature range and latent heat capacity, but also the practical integration route. In the present dissertation, the relevant category is organic PCM, more specifically paraffin-based microencapsulated PCM, because this material class is commonly used when the target is indoor thermal buffering close to the comfort-relevant temperature range.

In building practice, the challenge is not only how much heat a PCM can store, but how effectively that storage can be integrated into a real wall system. Because many PCMs have low thermal conductivity and may leak in liquid form, research has focused on encapsulation, shape-stabilized composites, and other methods that make them suitable for plasters, boards, and lining materials [Zalba et al., 2003; Konuklu et al., 2015]. From a design perspective, one of the key attractions of PCM is that a relatively thin latent heat storage layer can provide a thermal buffering effect comparable to that of much thicker conventional materials. A wall layer containing a common latent heat storage material and only a few centimeters in thickness may achieve a thermal storage effect comparable to about 24 cm of solid concrete, 36 cm of brick masonry, or even 226 cm of lightweight construction [Thermofoam et al., 2021]. At the same time, conventional brick and concrete walls have relatively low thermal resistance, so adequate control of heat loss still requires substantial additional insulation [Thermofoam et al., 2021].

Figure 1: Comparison of the required PCM layer thickness with other structural elements of equivalent thermal storage capacity (based on Thermofoam et al. 2021.)

This comparison helps explain why PCM-based layers are of particular interest in lightweight envelope systems: they can enhance thermal damping without relying solely on very large wall thicknesses or high-mass construction.

Given these material characteristics, the practical relevance of PCM depends largely on how it is integrated into building components and whether the phase change range matches the thermal conditions of use.

2.2 Microencapsulated PCM for building applications

In the most common approach, microencapsulated phase change material (microencapsulated PCM; MPCM) refers to a phase change material (PCM) whose "core" (the PCM that melts and solidifies) is enclosed by a capsule shell, typically in the micrometer to tens-of-micrometers size range, so the product can be handled as a powder- or granule-like additive and mixed into building materials [Konuklu et al., 2015]. In the system investigated in this dissertation, the core material of the microcapsules was a paraffin-based PCM, which undergoes melting and solidification in the temperature range relevant to indoor thermal buffering.

Microencapsulation is commonly achieved by forming a polymeric (or otherwise engineered) shell around the PCM core through dedicated encapsulation processes, creating a mechanically stable "container" that remains intact during repeated phase transitions. The primary motivation is leakage control: when the PCM is in the liquid phase, the shell prevents seepage into the surrounding matrix while preserving latent heat storage near indoor comfort temperatures [Konuklu et al., 2015; Baetens et al., 2010]. This is particularly important in building applications, because PCM is often incorporated directly into construction matrices (e.g., plasters, gypsum-based layers, or cement-based materials), where unencapsulated PCM can introduce major constructability and durability risks [Konuklu et al., 2015; Drissi et al., 2019]. Microencapsulation can also increase the effective heat transfer area, which may support faster charging–discharging (melting–solidification) dynamics, especially for lightweight envelope systems with limited inherent thermal mass [Konuklu et al., 2015]. From a building-physics perspective, the goal is typically to absorb heat through phase change during daily cycles, thereby reducing indoor temperature swings and attenuating and time-shifting heat-flux peaks [Baetens et al., 2010].

By 2010, the use of PCM in buildings had already been consolidated in state-of-the-art reviews, indicating that this is a mature research topic with multiple waves of development [Baetens et al., 2010]. Focused reviews specifically addressing microencapsulated PCM in building applications became particularly prominent by the mid-2010s, once the evidence base was large enough to evaluate both benefits and limitations in a structured way [Konuklu et al., 2015].

A practical advantage of microencapsulated PCM is that it can be dosed as an "additive," allowing installation and mixing workflows to remain closer to conventional plaster or mortar practice than macro-encapsulated or dedicated storage solutions [Kalnæs and Jelle, 2015]. At the same time, microencapsulated PCM integration usually involves trade-offs: in cement-based composites, for example, a reduction in mechanical strength is frequently reported, and the balance between thermal gains and altered material properties depends on capsule fraction, size distribution, and matrix–capsule interactions [Drissi et al., 2019]. Shell integrity and cycling stability over many melt–freeze cycles are also critical, because shell damage can reintroduce leakage and degrade long-term performance [Konuklu et al., 2015]. Applicability is further governed by how well the PCM melting range matches the targeted indoor temperature band, since latent storage is only effectively utilized if the daily temperature trajectory crosses that range [Baetens et al., 2010].

During the 2010s, the literature increasingly addressed not only experimental performance but also commercially available PCM products and practical implementation pathways, reflecting a shift from laboratory studies toward market-facing solutions [Kalnæs and Jelle, 2015]. In this context, microencapsulated PCM incorporated into interior gypsum plasters has been viewed as a particularly promising approach for lightweight constructions, where damping temperature variability is otherwise challenging due to limited thermal mass [Konuklu et al., 2015; Baetens et al., 2010]. Accordingly, the following subsections should narrow the discussion from the general concept of microencapsulated PCM toward building-relevant boundary conditions and design variables, especially the integration form (e.g., plaster), layer position within the assembly, and the expected thermal cycling regime. [Konuklu et al., 2015; Drissi et al., 2019]

2.3 Integration of microencapsulated PCM in indoor gypsum plaster layers

Gypsum-based indoor linings are a common host matrix for microencapsulated PCM. In this role, gypsum plaster is treated as a thin, workable layer on the indoor side of the envelope. It can couple efficiently to the indoor air temperature field, which is where thermal damping is typically desired. The literature shows several distinct integration routes for gypsum–PCM systems. These routes differ in how the PCM is retained, how the layer is formed, and whether the work represents material-scale specimens or an envelope-scale lining.

Serrano and co-workers compared multiple PCM incorporation routes within a gypsum matrix. When microencapsulated PCM was used, the procedure followed a standard plaster logic. Dry constituents were homogenized, water was added, and the gypsum layer was formed. The same study also considered configurations where the PCM was not microencapsulated, as well as cases where PCM was introduced after hardening by impregnation into the pore network of the gypsum. A layered solution was also reported. In that case, a PCM-free gypsum top layer was applied over the PCM-containing gypsum, and the rationale was linked to fire response [Serrano et al., 2016]. The parallel use of microencapsulated, suspended, and impregnated PCM routes allowed the influence of the integration method to be separated from the gypsum matrix itself. The presence of a separate gypsum cover layer indicates that, in paraffin-based gypsum systems, thermal aims may be accompanied by requirements related to fire performance and functional layer separation. Claude and co-workers addressed microencapsulated PCM in gypsum plaster from a plaster-technology perspective [Claude et al., 2021]. In their approach, PCM microspheres were mixed into fresh gypsum plaster as an additive. Practical processing issues were treated as central. Mix design and water–gypsum ratio were discussed, because microcapsules can shift fresh-state behavior. Workability, setting behavior, and the feasibility of applying the plaster layer were therefore considered alongside thermal performance. This framing keeps gypsum plaster in focus as a construction material, and it places microencapsulated PCM within a recipe-driven workflow that resembles standard plaster practice. Stejskalová and co-workers studied gypsum-based composites with microencapsulated PCM, with emphasis on the coupled thermal, mechanical and fire-related response [Stejskalová et al., 2022]. Sample preparation followed a typical gypsum

composite route. Dry ingredients were dosed and mixed, water was added, and specimens were cast. The results were interpreted as a composite-material problem. This is consistent with the view that microcapsules can change porosity, bulk density, and strength-related properties, not only heat storage. In this type of study, the gypsum–PCM layer is represented by laboratory specimens. The integration method is defined by the material recipe rather than by an envelope-scale lining strategy.

A separate stream of work treats gypsum–PCM as a board-type solution rather than a site-applied plaster layer [Zhou et al., 2007]. In that case, PCM is integrated into a gypsum mix, and a composite board is produced. The indoor lining is then implemented as a prefabricated element. In the literature, such systems are often assessed in controlled test rooms or box models, where damping of indoor temperature swings can be evaluated under repeated thermal cycles. Board-type solutions follow a different construction route than gypsum plaster. They can offer tighter control of thickness and composition, but they sit in a product and assembly context that differs from site-applied linings.

Leakage control and form stability are not handled only through microencapsulation. Some studies use a porous carrier to retain the PCM and then add that composite to gypsum plaster. In these shape-stabilized systems, the mixing steps may resemble plaster mixing, but the retention mechanism is different, because the PCM is held within the carrier pore structure. This change can affect both performance and long-term stability [Fořt et al., 2018; Karaipekli et al., 2016]. Compared with core-shell PCM, carrier-based systems rely on a different physical mechanism for retention, and they may lead to different matrix interactions and durability risks.

Comparability across studies is also shaped by how PCM content is reported [Serrano et al., 2016; Stejskalová et al., 2022]. Many papers use mass fraction or volume fraction. Envelope-scale implementations are often described through total installed mass and total latent heat capacity. A consistent basis is usually obtained by converting to area-specific quantities, such as kg/m² or kJ/m², once layer thickness and density are known. This step becomes important when the aim is to compare different plaster formulations and different levels of surface coverage.

Finally, the definition of surface coverage varies widely [Serrano et al., 2016; Claude et al., 2021]. In material-focused papers, geometry and boundary surfaces tend to remain

implicit. In envelope-scale linings, walls, roof, and floor can be treated as explicit boundary conditions. That choice has direct consequences for the interpretation of orientation-resolved effects, because it governs which surfaces are “treated” and which remain as controls within the same building.

A direct comparison of the efficiency of different PCM–gypsum systems is not straightforward, because the reported performance depends not only on the PCM itself but also on the host matrix, PCM fraction, layer thickness, surface coverage, boundary conditions, and the selected evaluation indicator. Some studies quantify efficiency through peak-temperature reduction, others through heat-flux attenuation, time lag, cooling or heating energy demand, or the number of hours within a comfort range. Nevertheless, the available literature indicates a consistent tendency: PCM systems are most effective when the phase-change range matches the actual daily temperature cycle and when the PCM layer is sufficiently coupled to the indoor thermal environment to complete regular charging and discharging. For this reason, the efficiency of applied PCM should be interpreted as a system-level property rather than as a fixed material parameter. [Ascione et al., 2014; Kalnæs and Jelle, 2015]

2.4. Reduction of indoor temperature extremes in PCM-integrated buildings

One of the main reasons for using PCM in buildings is to reduce indoor temperature extremes. This is especially important in lightweight buildings, where indoor conditions often respond quickly to changes in the outdoor environment. Under free-running operation, daily indoor maxima and minima may fluctuate considerably, and even short warm periods may lead to uncomfortable overheating. In this context, PCM is valued not only as a heat storage medium, but also as a way to moderate the daily indoor temperature cycle [Khudhair and Farid, 2004; Baetens et al., 2010; Kalnæs and Jelle, 2015].

The literature consistently shows that PCM can reduce the intensity of indoor temperature peaks. This effect has been reported in wall systems, plaster-based layers, concrete elements, brick-based solutions, and lightweight test structures. Although the material

systems differ, the central finding is similar: when the phase change range is well matched to the thermal conditions of use, PCM can reduce daytime indoor maxima and moderate short-term thermal excursions [Cabeza et al., 2007; Castell et al., 2010; Anter et al., 2023].

Several studies also indicate that the effect is not limited to the daily maxima. PCM may reduce excessive cooling during the night or early morning by releasing previously stored heat. This point is important, because thermal discomfort in free-running buildings is not caused only by overheating. During transitional periods, low indoor minima may also become relevant. For this reason, PCM performance is often interpreted in terms of overall daily moderation rather than peak reduction alone [de Gracia et al., 2011; Nghana and Tariku, 2016; Ranger et al., 2022]. This moderating effect has been observed in a wide range of envelope configurations. Cabeza et al. reported that microencapsulated PCM in concrete walls reduced indoor temperature variation and improved the dynamic thermal response of the wall system [Cabeza et al., 2007]. Castell et al. found that PCM incorporated into brick-based constructive solutions could reduce indoor peak temperatures under passive cooling conditions [Castell et al., 2010]. Similar results have been reported for PCM-integrated wall systems designed for hot climates, where the reduction of temperature fluctuation was associated with improved indoor conditions and lower cooling demand [Ascione et al., 2014; Al-Absi et al., 2022; Anter et al., 2023].

The same general pattern appears in lightweight construction. In such systems, low inherent thermal mass makes indoor temperature more sensitive to rapid external forcing. PCM can partly compensate for this limitation by adding latent storage capacity to the envelope. This has been demonstrated in both experimental and numerical studies. Al-Yasiri and Szabó showed that thin PCM-integrated envelope solutions can improve thermal behavior under severe hot conditions [Al-Yasiri and Szabó, 2023]. Fan et al. also reported a measurable reduction in indoor temperature fluctuation in a lightweight wall system containing PCM, even in the presence of other interacting mechanisms such as interlayer ventilation [Fan et al., 2023]. Bruno and Bevilacqua reached a similar conclusion in dry-assembled wooden wall systems using bio-PCM [Bruno and Bevilacqua, 2023].

At the same time, the literature makes clear that PCM effectiveness is not constant. The same material does not produce the same benefit under all conditions. The magnitude of the effect depends on outdoor temperature, solar exposure, ventilation, surface properties,

and the thermal characteristics of the surrounding assembly. It also depends on whether the PCM can complete both charging and discharging within the daily cycle. For this reason, PCM performance should not be treated as a fixed material property alone. It is better understood as the result of the interaction between material properties and boundary conditions [Ascione et al., 2014; Nghana and Tariku, 2016; Anter et al., 2023].

Another important issue is methodological. Many studies describe PCM performance through selected indicators such as peak temperature reduction, daily temperature range, or a small number of representative days. These indicators are useful, but they do not always show how stable the PCM effect remains over a longer interval. A strong result on a hot day does not automatically imply robust behavior under a wider range of weather conditions. This limitation appears in both experimental and simulation-based studies, especially when the analysis is restricted to a few critical cases [Al-Absi et al., 2022; Al-Yasiri and Szabó, 2023; Lee, 2022].

This issue becomes even more important in free-running lightweight buildings. In such buildings, indoor temperature extremes are highly sensitive to weather variability. Solar gains, cloudy periods, cool nights, and short warm spells may all influence the apparent effect of PCM from one day to the next. As a result, mean improvement alone is not sufficient. A design-relevant assessment should also consider variability and consistency over time. This need has become more visible in recent work that evaluates PCM performance over longer periods and interprets the results statistically rather than only through selected peak events [Németh et al., 2021], an approach that has also been reflected in my later related work [S1].

Taken together, the literature supports a clear conclusion. PCM can reduce indoor temperature extremes in buildings, and this effect has been demonstrated in a wide range of wall-related applications. However, the practical value of this reduction depends strongly on context. It depends on the material system, the envelope configuration, and the external thermal environment. For this reason, the reduction of indoor maxima and minima should be interpreted not as an isolated material effect, but as part of the broader thermal response of the building envelope under realistic operating conditions [Khudhair and Farid, 2004; Baetens et al., 2010; Kalnæs and Jelle, 2015].

2.5. Thermal time lag in PCM-integrated building envelopes

Thermal time lag is one of the most important dynamic indicators in PCM research. In building-envelope applications, it refers to the delay between the outdoor thermal peak and the corresponding indoor or inner-side peak. This delay matters because it affects when the highest thermal load reaches the occupied zone. In practical terms, a longer time lag may move the indoor maximum away from the hottest part of the day and toward a period when outdoor conditions are less severe [Mavromatidis et al., 2012; Toure et al., 2019].

In the PCM literature, time lag is usually discussed together with peak attenuation and decrement factor. These metrics are closely related, but they describe different aspects of dynamic behavior. Peak attenuation shows how much the thermal maximum is reduced. Time lag shows when that maximum occurs. A PCM layer may therefore improve performance in two ways at the same time. It may lower the peak, and it may also delay it. This combined effect is especially relevant in lightweight envelopes, where the daily thermal wave can otherwise pass through the assembly relatively quickly [Thiele et al., 2017; Sun et al., 2019; Xu et al., 2024].

The physical basis of time lag in PCM systems is well understood. When the material melts during the daily heating phase, part of the incoming heat is absorbed as latent heat instead of causing an immediate temperature rise. This slows the propagation of the thermal wave through the layer. During the later cooling period, the stored heat is released again. The indoor-side response therefore becomes both slower and smoother. Several studies have shown that this effect is strongest when the PCM can complete both melting and resolidification within the daily cycle. If cycling is incomplete, the latent contribution becomes weaker and the lag effect is reduced [Arıcı et al., 2020; Al-Rashed et al., 2021; Xu et al., 2024].

A recurring conclusion in the literature is that time lag depends strongly on PCM selection and layer design. One key parameter is the melting range. If the phase change interval overlaps the temperatures actually reached in the wall during the day, the latent effect becomes active when it is most useful. If the melting range is too low or too high, the PCM

remains mostly solid or mostly liquid, and the gain in time lag becomes much smaller. Similar sensitivity has been reported for layer thickness. A thicker PCM layer can increase delay, but only as long as the layer still cycles effectively under the given boundary conditions [Arıcı et al., 2020; Al-Yasiri and Szabó, 2023; Al-Rashed et al., 2021].

The literature also shows that time lag is strongly influenced by the way PCM is integrated into the envelope. Placement within the wall assembly matters, because the same PCM layer may behave differently depending on its thermal coupling to the incoming daily heat wave. This is one reason why time lag cannot be treated as a material property alone. It is a system-level response that depends on wall stratigraphy, surface exposure, and operating conditions. Numerical studies have been especially useful in this area, because they make it possible to examine the interaction of thickness, placement, and climatic forcing in a systematic way [Mavromatidis et al., 2012; Thiele et al., 2017; Lajimi and Boukadida, 2023; Hepple et al., 2024].

Experimental studies confirm that meaningful time delays can also be achieved in practice. Sun et al. reported time lags of about 1.5 to 2.25 h in lightweight wall systems containing PCM [Sun et al., 2019]. Zhuang et al. found even larger retardation values in PCM storage blocks combined with night ventilation, which highlighted the possible synergy between latent heat storage and passive cooling strategies [Zhuang et al., 2015]. Al-Absi et al. also showed that exterior PCM panels can reduce peak surface temperatures and heat flux, while improving the dynamic behavior of the wall system [Al-Absi et al., 2022]. Xu et al. reported that PCM–gypsum boards increased thermal lag while only marginally affecting the steady-state U-value, which reinforces the view that the benefit of PCM is mainly dynamic rather than static [Xu et al., 2024].

Time lag should therefore not be treated as an abstract thermal metric without practical meaning. The literature repeatedly links greater lag to lower daytime overheating, smoother heat-flow transmission, and a more favorable alignment between the indoor thermal peak and occupant use patterns. In hot climates, delaying the indoor maximum may reduce cooling demand during the most critical hours. In free-running buildings, it may extend the period during which indoor conditions remain acceptable without mechanical intervention. For this reason, time lag is often discussed not only in thermal-physics terms, but also in relation to comfort, passive cooling, and peak-load management

[Al-Yasiri and Szabó, 2023; Al-Absi et al., 2022; Grygierek and Sarna, 2020; Ferdyn-Grygierek et al., 2021].

At the same time, the literature reveals a methodological weakness. Many studies illustrate time lag using one or a few selected days. Such examples can be useful for visualization, but they do not fully represent the variability introduced by changing weather. Time lag is affected by outdoor temperature, solar gains, cloud cover, and the day-to-day completeness of PCM cycling. A single example may therefore be informative, but not representative. This limitation has increased the importance of longer monitoring campaigns and of statistical approaches that evaluate distributions and variability rather than relying only on isolated daily cases [Li et al., 2024; Al-Absi et al., 2022; Xu et al., 2024].

Another important point is that time lag should be interpreted in relation to thermal comfort rather than as an isolated wall-level response. A delayed peak is useful only if it improves the timing of indoor conditions in relation to the comfort range. This is why the broader comfort literature is relevant in PCM studies as well. Adaptive comfort studies and comfort reviews show that acceptable indoor conditions depend on both climate and occupant adaptation. From a PCM perspective, this means that the practical value of time lag depends not only on its magnitude, but also on whether the shifted temperature peak falls into a more favorable part of the daily comfort window [Arsad et al., 2023; Aqilah et al., 2022].

In free-running buildings, thermal comfort is usually interpreted differently from mechanically conditioned spaces with fixed setpoint temperatures. In the adaptive comfort approach used in EN 16798-1:2019, the acceptable indoor temperature depends on recent outdoor thermal conditions, and the comfort temperature is therefore treated as a moving reference value with an acceptable range around it [EN 16798-1:2019]. This distinction is relevant for PCM applications because a PCM layer affects not only the daily maximum indoor air temperature but also the timing and duration of temperature excursions near or above the comfort range. Consequently, comfort-oriented assessment should also consider time-dependent overheating indicators, such as exceeded degree-hours, which combine the magnitude and duration of overheating instead of relying only on isolated peak temperatures or daily averages.

Overall, the literature supports a clear conclusion. Thermal time lag is one of the central dynamic effects through which PCM improves building performance. Its magnitude depends on melting range, thickness, placement, daily cycling, and boundary conditions. When these factors are well matched, PCM can delay the indoor thermal peak, reduce the severity of daytime overheating, and support a more stable indoor thermal regime. For this reason, time lag should be treated as a comfort-relevant performance indicator, not merely as a descriptive thermal parameter [Arıcı et al., 2020; Sun et al., 2019; Al-Yasiri and Szabó, 2023; Xu et al., 2024].

2.6. Effect of wall orientation on PCM performance

Wall orientation is a major factor in the performance of PCM-integrated envelopes. It does not change the material itself, but it changes the thermal forcing acting on the wall. Solar gains differ strongly between north-, east-, south-, and west-facing surfaces, both in magnitude and timing. As a result, the same PCM layer may behave very differently depending on façade direction [Kuznik et al., 2011; Akeiber et al., 2014; Carlucci et al., 2021]. This is particularly important in lightweight buildings. In such envelopes, solar exposure can quickly alter surface temperature, and PCM activation becomes closely tied to the daily pattern of incident radiation. A wall exposed to strong afternoon sun may activate the PCM more effectively than a wall receiving weaker or shorter solar input. Several studies therefore treat façade direction not as a secondary design detail, but as a primary condition governing the actual benefit of PCM integration [Plytaria et al., 2019; Liu et al., 2022; Mahmoud et al., 2024].

In many cases, the strongest PCM effect is reported on the most solar-exposed façades. Lee et al. found substantial heat-transfer reduction when a thin PCM layer was integrated into residential wall assemblies, with the response depending on façade exposure and the timing of solar gains [Lee et al., 2015]. Liu et al. likewise reported clear directional differences in lightweight PCM walls, especially for east- and west-facing façades under summer conditions [Liu et al., 2022]. Mahmoud et al. confirmed that orientation alone can lead to marked differences in thermal response even when the wall build-up remains unchanged [Mahmoud et al., 2024].

West-facing walls are often identified as especially sensitive. In many climates, afternoon solar radiation coincides with high outdoor air temperature, which intensifies surface loading and increases the chance of effective PCM activation. Ferster et al., in a hot-climate modeling study, identified the west façade as one of the most favorable locations for passive cooling with PCM [Ferster et al., 2017]. Gounni and El Alami reached a related conclusion experimentally, showing that PCM placement in a composite wall could reduce surface temperature and heat flux most effectively under strong solar exposure [Gounni and El Alami, 2017]. These results suggest that west-facing walls may offer a particularly high return per treated area in lightweight systems with limited inherent thermal mass.

South-facing walls are also frequently reported as favorable, but the outcome is usually more climate-dependent. In some cases, the longer and more regular solar exposure of the south façade supports stable PCM activation and useful damping of daily gains. In other cases, the benefit is less pronounced than on the west side because the timing of the solar peak is less critical for indoor overheating. Plytaria et al. showed that the thermal behavior of a PCM-equipped building differed between the south and north wall even within the same overall configuration [Plytaria et al., 2019]. Mahmoud et al. similarly showed that orientation-based differences remained significant across alternative lightweight wall solutions [Mahmoud et al., 2024].

North-facing walls generally show weaker PCM-related gains. Their lower direct solar exposure limits the amplitude of the daily thermal cycle at the outer surface, which in turn reduces the likelihood of strong phase change. This does not mean that PCM becomes ineffective on such walls, but it usually means that the activation potential is smaller. Several numerical studies therefore suggest that north-facing façades are not the first priority when the aim is to maximize the benefit of a limited PCM quantity [Al-Absi et al., 2020]. From a design perspective, this is important, because it argues against assuming that uniform PCM application across all façades is automatically the most efficient solution.

The PCM systems discussed in orientation-related studies are not identical in material composition or integration form. In several cases, the investigated PCM is an organic or paraffin-based material, while other studies use commercial PCM products, shape-stabilized composites, PCM panels, or simplified numerical PCM layers rather than explicitly described microcapsules. Therefore, orientation-dependent performance cannot

be interpreted independently from the PCM material itself. The core material, melting range, latent heat capacity, encapsulation or stabilization method, layer thickness, and position within the wall all influence whether the daily thermal cycle can activate the PCM effectively. In the present dissertation, the relevant material system is a paraffin-based microencapsulated PCM incorporated into an indoor plaster layer; the cited orientation studies are therefore used mainly to support the role of façade exposure and thermal forcing, rather than to transfer their material-specific performance values directly [Al-Absi et al., 2020; Liu et al., 2022; Mahmoud et al., 2024].

Orientation, however, cannot be interpreted in isolation. Its effect interacts with PCM melting range, layer thickness, and layer position within the wall. Zhang et al. showed that wallboard performance depends on the dynamic temperature field across the assembly [Zhang et al., 2008]. Izquierdo-Barrientos et al. demonstrated that the same PCM may perform differently depending on its location within the wall [Izquierdo-Barrientos et al., 2012]. Similar conclusions were reached by Jin et al.., who showed that optimal placement is not fixed in absolute terms, but depends on thermal forcing and building context [Jin et al., 2016;]. Arıcı et al. further showed that multi-layer arrangements can improve performance when they are matched to the wall's thermal profile [Arıcı et al., 2022]. Orientation therefore acts as part of a coupled system rather than as a stand-alone variable.

At the same time, the evidence base has a clear limitation. Much of the available knowledge on orientation-dependent PCM performance comes from numerical studies, optimization analyses, or short-duration experiments [Izquierdo-Barrientos et al., 2012; Kishore et al., 2021; Mahmoud et al., 2024]. These studies are valuable, and in many cases they are the only practical way to test a large number of configurations. Still, they do not always capture the variability of real outdoor exposure over longer periods. Full-season, free-running measurements that compare all major wall orientations under identical boundary conditions remain relatively rare, especially for lightweight buildings [Childs and Stovall, 2012; Pomianowski et al., 2013]. This matters because PCM activation is highly sensitive to weather variability, and orientation effects that appear strong in simulation may prove less regular or less sharply separated under measured conditions.

A related issue is that some studies emphasize energy demand or peak heat-flux reduction more strongly than the daily activation pattern of the PCM itself. Yet this is central to orientation-dependent behavior. A façade may receive more solar energy overall, but if the PCM melts too early, too late, or only partially, the practical benefit may be smaller than expected. For this reason, validation under real outdoor exposure remains important. Experimental studies on test walls and model houses have begun to address this gap, but the available evidence is still much more limited than the modeling literature [Biswas and Abhari, 2014; Lachheb et al., 2017; Németh et al., 2021].

Overall, the literature supports a clear conclusion. Wall orientation has a strong influence on PCM performance because it governs the thermal forcing that drives phase change. In most cases, solar-exposed façades, especially west- and south-facing walls, offer the greatest potential for effective PCM use. The magnitude of this benefit, however, is not universal. It depends on PCM properties, wall build-up, and local climate. Just as importantly, much of the current evidence still comes from simulations or short-term tests rather than long free-running measurement campaigns. Orientation-specific PCM design is therefore well supported in principle, but its practical ranking and robustness still require careful experimental confirmation under realistic boundary conditions.

3. Experimental basis, data provenance, and processing

3.1 Model house design, test field implementation, and experimental context

The experimental infrastructure behind this dissertation was developed within a broader research program focusing on building-scale thermal storage using PCM microcapsules.

Within this program, four lightweight container-based model houses were built for repeatable, side-by-side comparisons of different indoor lining concepts. The container baseline, geometry, and external exposure were kept as similar as reasonably possible across all houses.

At the project level, the four configurations were defined as follows:

1. an unmodified baseline house with the original wall build-up retained; (as a reference)
2. a variant with an internal polyurethane foam lining containing PCM microcapsules;
3. a variant based on a gypsum-board interior lining containing PCM microcapsules applied on vertical walls; and
4. *planned:* a non-PCM “added thermal mass” variant using a hollow brick lining applied on the internal side of the vertical walls only - This model house was ultimately not constructed and remained at the design stage; however, this has no significance for the present dissertation. This variant is mentioned only to keep the description consistent with the broader/former experimental project documentation.

This wider experimental platform is mentioned here for traceability only. This study uses data from the 1. and 3. houses. (Figure 2.)

The experiments were carried out at the outdoor test site in Bácsalmás (SE Hungary; 46.127877° N, 19.332132° E) during a spring–early summer 2021. Both houses were co-located and identically oriented, remained unoccupied. No atypical operating events were observed that could bias the results.

Figure 2: The three experimental model houses installed at the Bácsalmás site

At the dissertation level, the present work is deliberately framed as a data-processing and analysis study built on an existing experimental platform. Although the model houses were constructed in 2020 and the monitoring dataset evaluated here was recorded in 2021, my contribution began in 2022 and focused on the systematic processing, validation, and interpretation of the measured time series. Accordingly, the analyses presented in this dissertation are based specifically on the reference house (REF) and the gypsum-plaster PCM house, while other experimental variants of the broader test field infrastructure are outside the scope of the processed dataset and are not discussed further in this chapter.

Other project variants are not evaluated in the dataset analyzed in this chapter and are therefore not discussed further beyond this contextual note.

3.2 Study object and baseline envelope specification

The experimental basis of this dissertation is a pair of lightweight modular model houses built from Mobilbox MB10-type container units and installed in an outdoor test field. The use of a standardized container shell is intentional: it provides a repeatable, industrially common envelope construction with limited intrinsic thermal mass, where latent-heat

storage in phase change materials (PCMs) can measurably reshape diurnal thermal dynamics under real weather exposure.

Each model house corresponds to a single MB10 unit with external dimensions of 3.0 m (length) × 2.4 m (width) × 2.6 m (height), yielding an internal usable floor area of approximately 7.2 m². (Figure 3.) The two houses were placed side-by-side in an open-air environment so that they experienced comparable boundary conditions (solar radiation, wind exposure, and ambient temperature, etc.). Care was taken to avoid shading; no adjacent obstacles or shading elements affected one house differently than the other during the monitored period.

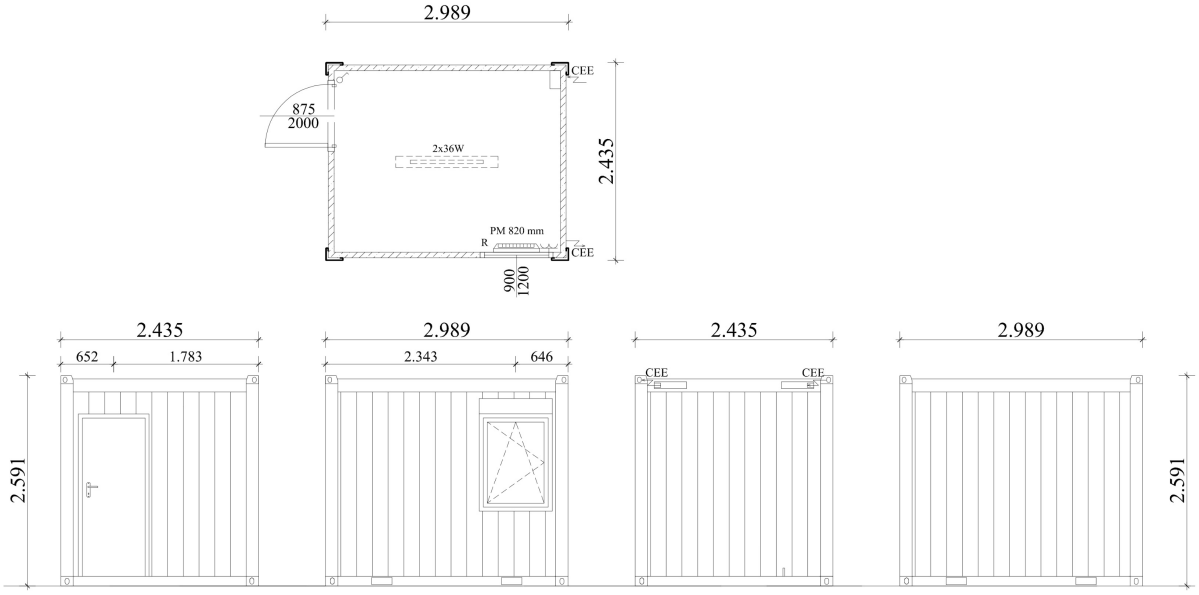

Figure 3: Layout and elevation drawings of the Mobilbox container model house (manufacturer's drawing)

Baseline envelope build-up and thermal transmittance were governed by the standard Mobilbox construction approach and the as-built interior finish used in the experiments. The Mobilbox MB10 specification defines an insulated panel concept with steel framing, replaceable wall elements, and mineral - wool thermal insulation (typical density range 16–24 kg/m³). In the standard configuration, the external wall panels comprise an exterior profiled galvanized painted steel sheet (~0.6 mm), an internal liner board (laminated decor board, 8 mm), and a mineral wool insulation core (60 mm), with a declared wall thermal

transmittance of approximately U ≈ 0.55 W/m²K; this value is used consistently as the wall heat-loss coefficient in the subsequent quasi-steady characteristic flux framework.

The roof assembly is built as an insulated panel and, per the Mobilbox specification, includes mineral-wool insulation (100 mm) with auxiliary insulation at frame profiles to mitigate thermal bridging, a vapor barrier foil, and an interior ceiling liner (laminated decor board, 8 mm).

The declared roof thermal transmittance is U ≈ 0.32 W/m²K. The floor assembly is a self-supporting base frame with a galvanized steel underside sheet (~0.5 mm), mineral-wool insulation (100 mm), and an interior floor board (water-resistant particleboard, 20 mm) with a thin resilient PVC floor covering (~1.5 mm). The declared floor thermal transmittance is U ≈ 0.45 W/m²K.

For clarity and traceability, the dissertation adopts the manufacturer-declared thermal transmittances (walls: 0.55 W/m²K, roof: 0.32 W/m²K, floor: 0.45 W/m²K) as the baseline envelope heat-loss coefficients of the model houses; these values were independently checked by calculation and are used directly in the subsequent analysis. Detailed layer descriptions serve primarily to

- justify the lightweight, low-thermal-mass character of the envelope and
- document the parameter provenance for the later simplified heat-flux estimation.

3.3 Reference vs PCM configuration

Two configurations were investigated: a reference house (REF) and a PCM-enhanced house (PCM). The houses were identical in geometry, placement, and baseline envelope construction. The sole intended difference between them was the presence of PCM plaster lining on the interior side of the vertical opaque walls in the PCM house.

In the PCM configuration, the latent-heat storage system was implemented as an interior gypsum-based lining containing microencapsulated RT25 paraffin PCM. Across the underlying publications, the PCM system is consistently characterized by

- the RT25 phase change material aligned with the indoor comfort-relevant temperature band, and

- a total installed PCM mass of 51.2 kg, corresponding to an overall latent heat capacity of approximately 8120 kJ.

The PCM plaster lining was mounted on the available interior side of the four vertical walls (north, east, south, west). Importantly, no PCM layer was installed on the floor or the ceiling/roof interior surface in the baseline time-lag configuration; this boundary condition is explicitly noted because it affects both the magnitude and the interpretability of orientation-resolved effects (the roof and floor remained non-PCM controls within the same building). The main material and integration parameters of the PCM-containing plaster lining are summarized in Table 2.

Table 2: Main material and integration parameters of the PCM plaster lining

Parameter	Value / description
PCM core material	RT 25 paraffin PCM
Microcapsule shell material	Poly(methyl methacrylate) (PMMA)
Microencapsulation method	Polymerization
Matrix material	Gypsum-based plaster panel
PCM microcapsule content in plaster elements	22 wt%
Panel thickness	25 mm
Total lined surface area	15 m²
Location in the model house	Available inner surfaces of the vertical walls
Total PCM content of installed panels	51.2 kg
Combined latent heat storage capacity	8120 kJ
Melting enthalpy of PCM-loaded microcapsules	106.9 J/g
Freezing enthalpy of PCM-loaded microcapsules	113.4 J/g
Melting enthalpy of PCM-microcapsule-loaded plaster elements	24.0 J/g
Freezing enthalpy of PCM-microcapsule-loaded plaster elements	23.9 J/g

These parameters characterize the PCM-containing plaster lining as an interior latent heat storage layer rather than as a separate insulation layer.

The reference house was retained in its original state (factory wall build-up with the same internal lining concept), with no PCM-containing lining applied. All other features relevant to passive thermal behavior—envelope U-values, envelope areas, positioning, and exposure—were kept as equivalent as practically possible so that differences in measured

thermal dynamics can be attributed to the latent-heat buffering and phase-change cycling of the PCM lining rather than to incidental geometric or construction variability.

3.4 Experimental Operation: Free-Running Boundary Conditions

The measurement campaign was designed to capture passive, free-running thermal behavior under real outdoor conditions. Throughout the monitoring period, both model houses were unoccupied and operated without active HVAC equipment and without internal heat sources, so that indoor air and surface temperatures evolved primarily as a response to outdoor temperature fluctuations, solar radiation, wind-driven convection, and long-wave radiative exchanges.

The monitored period covered 105 consecutive days in spring/early summer 2021 (29 March–11 July), providing a long dataset that spans variable weather regimes and enables statistical treatment beyond single-day illustrative examples. The site is reported as Bácsalmás, southeastern Hungary, which is favorable for such passive experiments due to high sunshine duration and pronounced diurnal forcing in the transitional season.

Operationally, the houses were kept in a closed, non-ventilated condition during the evaluated periods (doors and windows closed; no deliberate night ventilation), and precipitation effects were not explicitly modelled in the subsequent analysis. These constraints define the validity domain of later comfort and time-lag conclusions: the derived indicators quantify envelope-driven buffering and peak shifting under free-floating indoor air temperatures, rather than under controlled setpoints.

Wind speed was recorded as part of the external meteorological boundary conditions. Its effect was not evaluated as a separate variable in the present dissertation, because the aim was the comparative assessment of two co-located model houses exposed to the same outdoor environment. Since the reference and PCM-plastered houses had the same geometry, orientation, and site exposure, wind-driven convective effects were assumed to influence both configurations in a comparable way. Nevertheless, wind may have contributed to the day-to-day scatter of the measured surface and indoor air temperatures, especially during windy periods.

Although the model houses were equipped with air-conditioning and electric heating units, these systems were not operated during the measurement period analyzed in this dissertation. The two houses were therefore evaluated under free-running conditions, without active heating, cooling, or controlled mechanical operation.

3.5 Instrumentation and Measurement Layout

The experimental platform was developed to support long-term, multi-channel monitoring of both the building envelope response and the outdoor thermal and solar conditions.

The external meteorological data were recorded at the test site with a Vantage Pro2 weather station. The weather-station dataset provided several outdoor meteorological parameters; however, the dissertation used only those variables that directly entered the thermal evaluation of the model houses, primarily outdoor air temperature and solar radiation. Other recorded meteorological parameters were not evaluated as separate explanatory variables, because the two model houses were co-located and exposed to the same outdoor environment.

For the building response variables central to this dissertation, temperature measurements were planned and carried out using K-type thermocouples, with explicit measurement layouts designed for

1. exterior and interior surface temperatures of envelope elements and
2. indoor air temperature.

The instrumenting concept (Figure 4.) specifies diagonal placement patterns on vertical walls (typically three thermocouple pairs per side wall, with the door wall treated as an exception with fewer pairs), a thermocouple pair across the floor (external sensor routed through the floor to the underside, internal sensor fixed to the floor finish and mechanically protected), and three thermocouple pairs on the ceiling placed along defined diagonal lines. Indoor air temperature was measured using two thermocouples suspended from the ceiling to approximately 1.8 m above the floor; this height corresponds to the upper part of the occupied zone and was used as a representative level for evaluating the indoor thermal environment.

With this scheme, one house requires 14 thermocouple pairs (28 thermocouples) for surface temperature measurement plus 2 thermocouples for indoor air temperature, yielding 30 temperature measurement points per house.

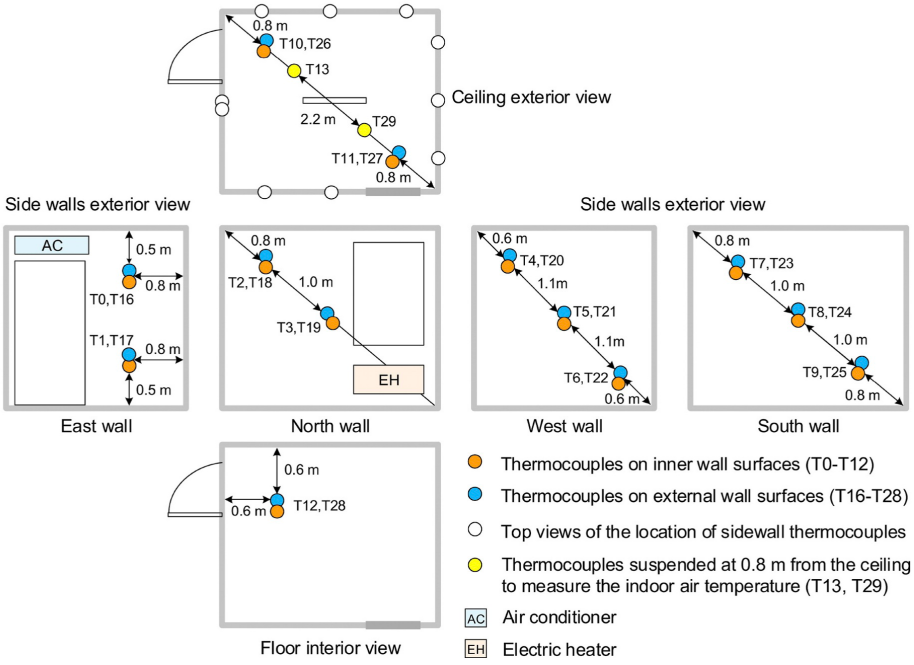

Figure 4: The measuring equipment layout in the model houses [Németh et al. 2021.]

Thermocouples were required to be in direct contact with the surface, and a thermally conductive paste could be applied between the surface and sensor to improve coupling. On the exterior side, a thin metallic cap fixed above the thermocouple was used as a protective cover intended to minimally disturb heat transfer; on the interior side, a thin protective cover plate was applied.

Outdoor weather conditions were monitored using a dedicated weather station system installed on a stable support structure, with software-based logging and local display.

All temperature channels were recorded synchronously at a 5-minute sampling interval throughout the campaign. After wiring the thermocouples to the measurement card, calibration measurements were performed and a software correction was applied, yielding an effective temperature accuracy within ±0.1 °C and a noise level of approximately 0.03 °C.

3.6 Data provenance, quality control, and validity domain

The present chapter describes the work of processing temperature and meteorological time series acquired under real outdoor exposure conditions, using synchronized logging across the two houses to ensure comparability. The measurement concept includes calibration before installation and recommends post-installation verification (e.g., cross-checks against infrared surface temperature readings) to support measurement credibility.

Quality control was applied in a manner consistent with the free-running nature of the experiment. Channel integrity and plausibility were checked to identify dropouts and obvious non-physical spikes, and the comparability of the two-house dataset was safeguarded through matched placement and the explicit effort to keep shading and exposure conditions similar during the monitored period.

The validity domain of the derived indicators is intentionally limited to free-running building behavior (no HVAC setpoints, no deliberate ventilation strategy) under the combined forcing of outdoor temperature variability, solar radiation, wind-driven convection, and long-wave radiative exchange. Results should therefore be interpreted as envelope-driven buffering and peak shifting, rather than as performance under controlled indoor setpoints or mixed-mode (heated or cooled) operation.

3.7 Computational post-processing environment

The post-processing and analysis workflow of this dissertation was implemented in Python, using widely adopted scientific-computing libraries. Python has become a de facto standard environment for reproducible data analysis in building-physics and energy-performance research, because it combines transparent, script-based workflows with a mature ecosystem for numerical computation, time-series handling, and visualization.

Numerical operations and feature extraction were performed with NumPy, while Pandas was used to structure the measurement data into time-indexed tables, enabling consistent resampling, aggregation, and daily-descriptor calculation across the full monitoring period. Plotting and figure generation were carried out with Matplotlib to produce publication-

ready visualizations under full programmatic control. This toolchain supports traceability because each preprocessing step (data cleaning, synchronization, filtering, and derived-metric calculation) is explicitly encoded in scripts, reducing the risk of manual spreadsheet errors and making analytical choices auditable.

Beyond practicality, the use of mainstream libraries matters because it increases interoperability and comparability with related studies: the same tools and data structures are commonly used for handling high-frequency sensor data, validating preprocessing pipelines, and generating figures and statistical summaries for peer-reviewed publications. It also strengthens scientific reproducibility: the analysis can be rerun on the same raw data to obtain identical results, and the workflow can be extended to additional periods, sensors, or alternative indicators without changing the underlying methodology.

3.8 Pre-processing and derived time-series features

Pre-processing was designed to preserve physical interpretability while enabling robust statistical aggregation across the long monitoring period. All channels were kept at their native sampling resolution and time-aligned across houses. Where solar irradiance exhibited high-frequency intermittency (e.g., cloud passages), a smoothed auxiliary representation can be used for day-to-day comparability while retaining the raw series for peak and timing analyses.

From the synchronized time series, daily extrema and daily descriptors were computed for each house and for the outdoor forcing variables: daily maximum and minimum indoor air temperature, daily maximum and minimum outdoor air temperature, and daily maximum solar irradiance. Daily amplitude (max–min) was derived as a compact descriptor of diurnal thermal swing. These daily features serve as the primary inputs to subsequent correlation and response-oriented analyses that relate indoor extremes to outdoor temperature and solar irradiation, and to quantify the damping benefit attributable to PCM under varying weather regimes.

To preserve traceability, feature definitions (extrema timing, amplitude, and aggregation window) are reported together with the operational constraints (no HVAC, no deliberate ventilation), because peak moderation and potential heat-trap behavior depend strongly on solar-driven exterior surface overheating and the absence of nighttime purge ventilation.

4. Results

The main results of the dissertation are summarized here, based on three published studies. The findings rely on experimental measurements and subsequent data analysis, focusing on the thermal response of lightweight building envelopes with PCM integration. The results show measurable impacts on peak thermal loads, the temporal dynamics of heat transfer, and indoor comfort indicators under free-running conditions. Performance is strongly dependent on boundary conditions, particularly solar exposure and façade orientation. The presented outcomes support the interpretation of PCM effectiveness and enable design-relevant conclusions. These results are referenced later when formulating recommendations and the overall conclusions.

4.1 Reduction of daily indoor temperature amplitude and extremes

The results presented in this section quantify how PCM integration affects the daily indoor temperature profile, with emphasis on extremes rather than average conditions. The evaluation focuses on daily minima, daily maxima, and the resulting daily indoor temperature amplitude as primary performance indicators. These metrics provide a direct, comparable basis for assessing peak damping under the variable boundary conditions observed during the monitoring period.

4.1.1 Definitions of daily extremes and peak-damping indicators

Peaks and extremes are handled in an operational, day-based manner. The hot-side “peak” is the daily maximum of the indoor air temperature, while the cold-side extreme is the daily minimum of the indoor air temperature. The same daily maxima and minima are evaluated for the outdoor air temperature, and solar exposure is represented by the day’s maximum global solar radiation power/intensity.

The peak-damping indicators are derived directly from these daily extremes. The daily temperature-fluctuation amplitude is defined as:

$$A = (T_{max} - T_{min}) / 2$$

This quantity is computed for both outdoor and indoor conditions (A_{out} and A_{in}).

The attenuation factor is then defined as:

$$M = (A_{out} / A_{in}) * 100\%$$

Values of M above 100% indicate amplification, meaning that the indoor daily swing exceeds the outdoor daily swing; this behavior is consistent with a heat-trap effect under free-running conditions without ventilation.

Reducing peaks is important because comfort and overheating risk are governed by extremes rather than mean values: acceptable average indoor temperatures can still coincide with excessive daily maxima. Therefore, the evaluation focuses on daily indoor maxima/minima and the derived amplitude and attenuation, while tracking solar radiation alongside temperature, since it is a dominant driver of indoor peaks and can otherwise bias the interpretation.

4.1.2 Dataset and analysis framing

The evaluation is based on a continuous spring monitoring period with high temporal resolution (5-minute sampling), yielding a large dataset suitable for robust day-by-day statistics rather than isolated "representative days." Over the full interval, each sensor provides more than 30,000 data points, which supports stable estimation of daily indicators and their variability. In its raw form, the time-series dataset is too dense to interpret reliably by visual inspection alone, because meaningful trends are obscured by the sheer volume of points and short-term fluctuations. Therefore, the analysis is based on daily summary indicators that condense the data into comparable descriptors (e.g., daily extremes and derived metrics) suitable for statistical evaluation across the full monitoring period.

For processing the large volume of data, the scientific Python libraries listed in Appendix 1 were used instead of Excel-based charting, whose limitations are illustrated in Figure 5.

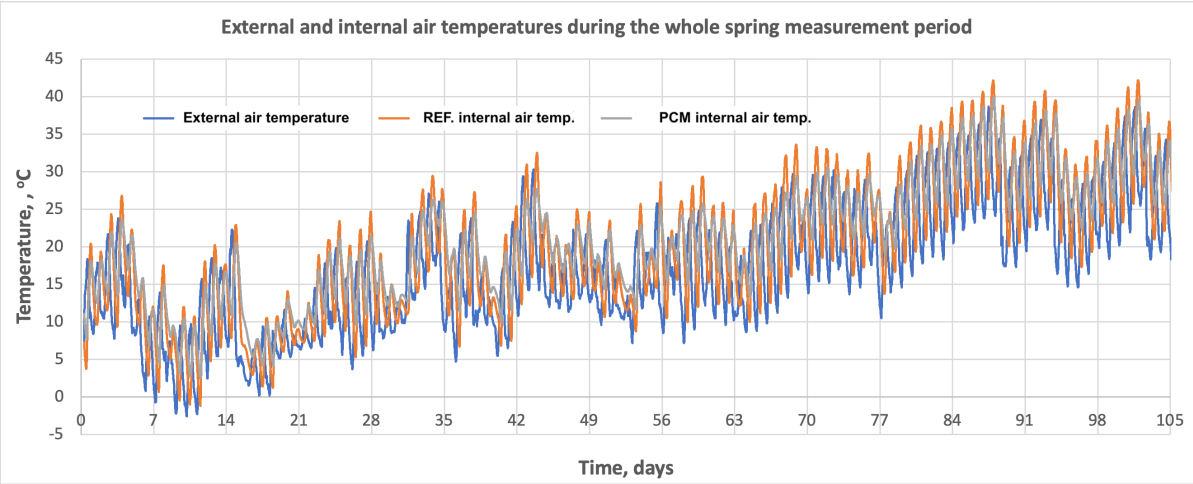

Figure 5: Abundance of data: the all-in temperature for illustration purposes

The raw time series are reduced to daily descriptors that are directly comparable across the monitoring period, most importantly daily maxima and minima and the derived daily amplitude and attenuation indicators defined in 4.1.1. To avoid overinterpreting day-to-day weather noise, the results are evaluated in relation to the main boundary conditions. Daily outdoor temperature extremes and daily solar exposure are therefore treated as the primary influencing factors when evaluating the level and variability of indoor extremes. Before computing daily indicators, the dataset is screened to remove obvious sensor dropouts and to handle short data gaps, so the aggregated metrics represent physical behavior rather than measurement artifacts.

Detailed instrumentation, sensor placement, and measurement protocol are documented in Chapter 3; only dataset properties required to interpret the results are stated here.

4.1.3 Reduction of daily indoor temperature amplitude

The primary performance indicator is the daily indoor temperature amplitude, defined from the daily extremes as

$A_{in} = (T_{in,max} - T_{in,min})/2$.

Across the full monitoring interval, the PCM-integrated model house exhibits a markedly smaller daily swing than the reference house, indicating that the indoor temperature trajectory is less “peaky” and less sensitive to short-term external forcing. In quantitative

terms, the mean daily indoor amplitude decreases from 6.3 °C (reference) to 3.6 °C (PCM), i.e., a reduction of 2.7 °C in the characteristic daily half-range. (Figure 6.)

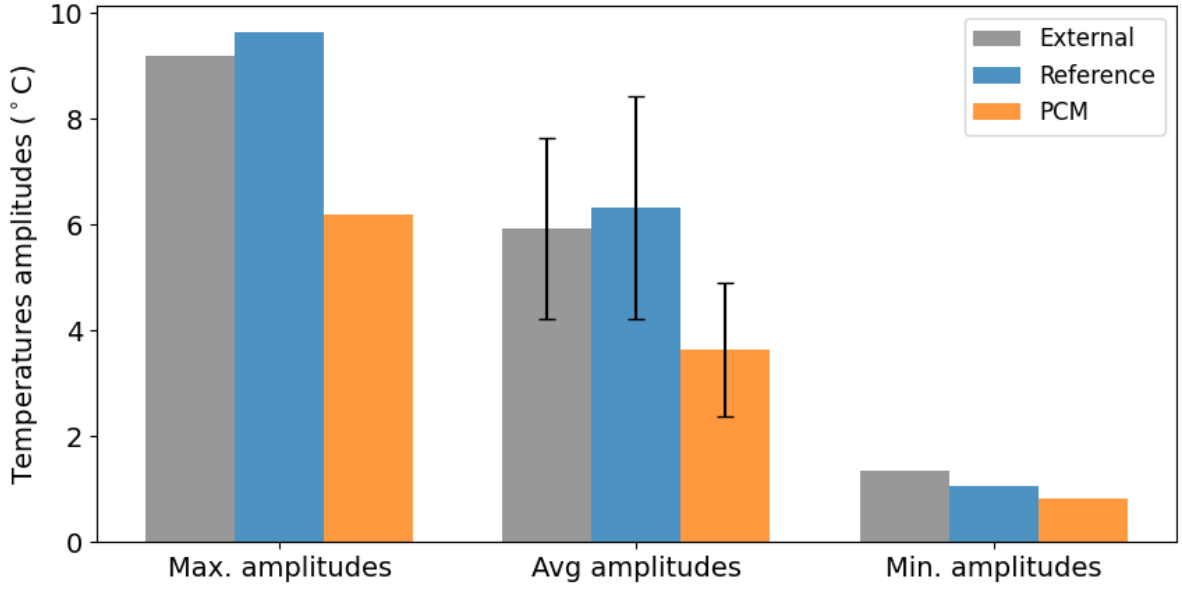

Figure 6: Daily indoor air temperature amplitudes, maxima, mean values, and minima in the reference and PCM-plastered model houses.

Expressed in relative terms, this corresponds to roughly a 43% decrease in the average daily indoor amplitude (2.7/6.3 ≈ 0.429), which is a substantial attenuation in day–night variability.

Interpreting this key performance indicator (KPI) in a physically meaningful way: a lower A_{in} implies that both sides of the daily cycle are moderated simultaneously: daytime overheating tendencies are reduced (lower propagation of high external loads into indoor maxima) and night/morning cooldown is less pronounced (higher persistence of indoor temperature during colder hours).

Importantly, this indicator is robust for long monitoring periods because it does not depend on selecting "representative" days; it aggregates daily behavior consistently even when boundary conditions vary strongly from one day to the next. For that reason, the amplitude-based KPI provides a compact, comparable summary of peak damping that can be used as the backbone metric for the subsequent results (e.g., variability, amplification cases, and boundary-condition mapping) without reintroducing methodological details already covered earlier.

4.1.4 Behavior of daily maxima and minima

Daily extreme values provide a direct view of how strongly external conditions propagate into the indoor environment. Over the monitoring period, daily indoor maxima in both cases frequently exceeded the daily outdoor maxima, which indicates that the indoor peak is not governed by outdoor air temperature alone; solar gains and the resulting inward heat flow can push indoor air temperatures above ambient levels. This “heat-trap” behavior is most apparent under free-running conditions without ventilation, and it is therefore not interpreted as attenuation during the warming phase, but rather as a form of amplification whose magnitude depends on the actual boundary conditions of the day.

The key result is that the PCM-integrated lining consistently moderates this peak build-up compared to the reference. While peak amplification can still occur, it is less pronounced: the daily maximum indoor temperature in the PCM case is systematically closer to the outdoor daily maximum than in the reference house. In absolute terms, the difference between the two indoor maxima can reach approximately 2.2 °C, with the PCM case remaining lower than the reference on the same day. This is the most direct peak-reduction statement: under identical external excitation, the PCM layer measurably limits how high the indoor maximum rises relative to the reference.

A similarly clear effect appears on the low-side extreme. Daily indoor minima remain above the outdoor minima in both cases, but the PCM-integrated case shows a stronger retention of indoor temperature during the cooling phase (night/morning). Practically, this means that the indoor air does not cool down to the same extent as in the reference, and the separation between the two cases can be substantial: the daily minimum indoor temperature can be higher by up to about 3.8 °C in the PCM plaster lining compared to the reference.

Interpreted in the context of daily comfort robustness, this reduction in low-temperature deviation is at least as important as peak reduction, because it stabilizes the lower end of the indoor temperature cycle without requiring active heating. The daily indoor air temperature maxima, minima, and the corresponding calculated standard deviations are summarized in Figure 7.

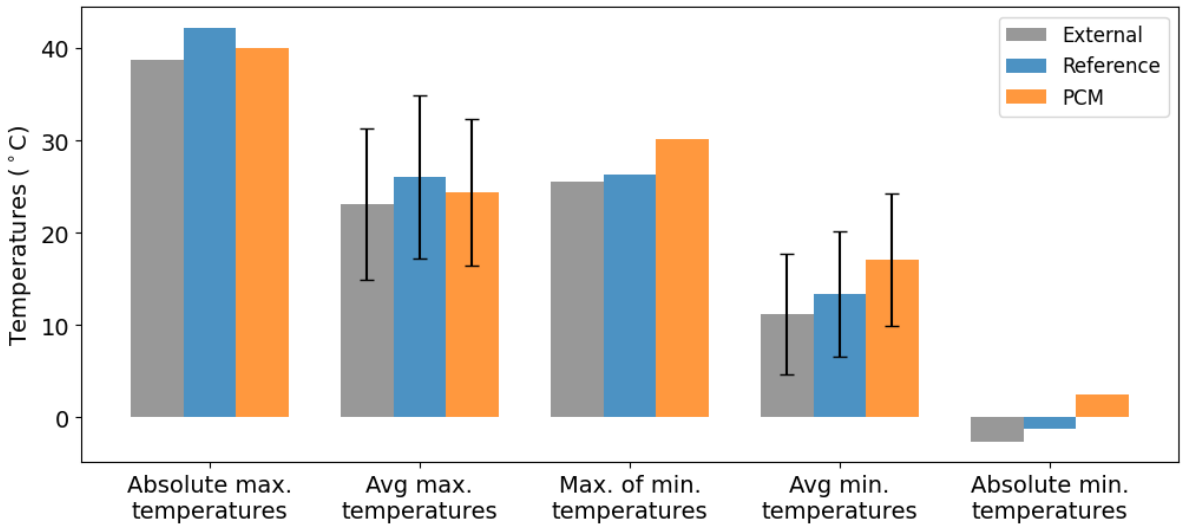

Figure 7: Daily indoor air temperature maxima and minima with the calculated standard deviations over the full measurement period for the reference and PCM-plastered model houses

4.1.5 Variability, robustness, and heat-trap behavior

Season-long monitoring makes it possible to evaluate peak damping as a distribution rather than as a single effect value. The daily extreme indicators (maxima, minima, and the derived amplitude and attenuation) show considerable fluctuation over the interval because the boundary conditions are not constant, particularly outdoor air temperature and solar exposure. As a result, robustness should be described not only by mean values but also by dispersion measures, such as standard deviations and variation around the mean trend.

When variability is summarized over the entire indoor and outdoor time series, the reference indoor case exhibits a higher standard deviation than the outdoor air series (8.96 °C vs 8.23 °C), while the PCM indoor case is lower (7.90 °C). This indicates that the indoor environment can amplify variability under free-running operation, and that PCM integration reduces that amplification when viewed across the full period.

A similar robustness pattern appears after daily summarization. For daily maxima (one value per day), the standard deviation remains high in all datasets, but the reference case shows the largest spread (daily-max standard deviation: outdoor 8.04 °C, reference 8.82 °C,

PCM 7.97 °C). For daily minima, the PCM case can exhibit a slightly higher spread than the reference (daily-min standard deviation: outdoor 6.52 °C, reference 6.75 °C, PCM 7.12 °C). This is consistent with the fact that low-side behavior depends on how fully latent storage is regenerated overnight under changing nights and changing solar-driven charging during the preceding day. The key point is that peak damping is not constant; it is condition-dependent and must be reported with dispersion.

Heat-trap behavior explains why indoor peaks can exceed outdoor peaks even when outdoor air temperature alone would not suggest it. Under free-running conditions without ventilation, short-wave gains increase inward heat flow and raise indoor air temperature peaks above ambient levels. In this regime, the amplitude-based attenuation factor can exceed 100%, which is interpreted as amplification rather than improved damping.

This distinction is reflected directly in the attenuation of statistics. Over the interval, the reference case shows an average attenuation of 106.2%, indicating net amplification on average, while the PCM case shows true attenuation, with the outdoor amplitude reduced to about 61% indoors on average. The day-to-day variability of these indicators also differs materially: the standard deviation of daily amplitudes is 2.11 °C in the reference case and 1.27 °C in the PCM case (outdoor is 1.67 °C). Together, these results show that PCM integration reduces not only the mean daily swing but also the variability of the swing, while heat-trap-driven amplification remains a boundary-condition-dependent regime that must be separated conceptually from attenuation.

4.1.6 Poincaré-based characterization of temporal changes and deviations

A Poincaré representation is used to compress large time series into a form that makes dispersion, persistence, and regime shifts comparable across datasets. Instead of plotting temperature versus time, successive samples of the same variable are plotted against each other, forming pairs of the form $(x_t, x_{t+\Delta t})$ at the native sampling interval. This mapping retains temporal adjacency while making the overall spread and the “randomness around the dominant trend” quantifiable.

Geometrically, if a sequence changes smoothly and quasi-periodically, points cluster near the identity line $x_{t+\Delta t} = x_t$, because successive values are similar. The endpoints of the cloud

correspond to the lowest and highest values observed over the interval. Since daily minima and maxima do not repeat at identical values each day, the cloud broadens near its lower and upper ends; this broadening is a visual signature of day-to-day variability in extremes. Point density along the cloud indicates how frequently certain temperature ranges occurred during the monitoring period. The resulting Poincaré representation of the outdoor and indoor temperature series is shown in Figure 8.

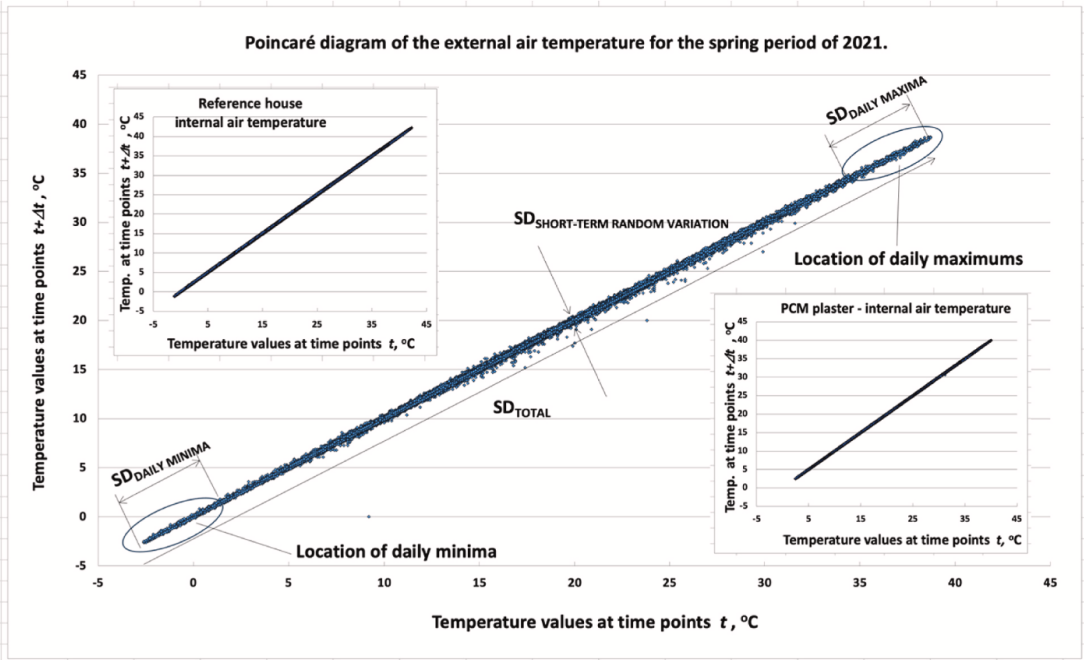

Figure 8: Outside and inside temperatures with the Poincaré visualization

Two forms of deviation are separated in the Poincaré framework. The first is a large-timescale deviation (SD2), describing how widely values spread along the dominant trend over the full period; it reflects slower shifts in the typical level of the process and the overall range of states explored. The second is a short-timescale random deviation (SD1), describing the thickness of the cloud perpendicular to the dominant trend; it reflects step-to-step irregularity and stochastic effects that cause consecutive values to differ more than expected from the quasi-periodic trajectory.

In implementation terms, for a time series x_i (i = 1…N), form pairs $p_i = (x_i, x_{\{i+1\}})$. (The index *i* denotes the temperature values corresponding to successive sampling times. The

shape of the diagram naturally depends on the sampling frequency; however, if the same approach is applied consistently to all datasets (outdoor and both indoor series), comparability is not compromised.)

Determine the dominant trend line through the cloud (often close to the identity line for quasi-periodic signals) and rotate the coordinate system so that one axis is parallel to this line and the other is perpendicular. Then SD2 is the standard deviation of the projected coordinates along the parallel axis, and SD1 is the standard deviation along the perpendicular axis. A numerically convenient equivalent formulation uses the standard deviation of the series and of its successive differences, preserving the same interpretation: SD1 is tied to step-to-step variability, while SD2 is tied to the overall spread of the process.

Within the dissertation framing, the Poincaré metrics serve three roles. First, they support robustness assessment: a reduction in mean peak indicators is more convincing when accompanied by a tighter scatter structure rather than being driven by a few atypical days. Second, they help diagnose heat-trap-driven amplification: strong peak escalation events widen the upper end of the cloud and can increase SD2 (broader range of explored high values) and, depending on frequency, can increase SD1 (more irregular step-to-step behavior). Third, they provide a PCM-versus-reference comparison that does not rely on hand-picked periods, because the ellipse-like geometry and dispersion parameters summarize the behavior over the full interval.

The Poincaré comparison is consistent with the daily-extreme and amplitude-based results: the reference case exhibits stronger upper-end expansion consistent with heat-trap amplification, while the PCM case shows a more constrained spread consistent with peak damping. Quantitatively, this aligns with the lower overall variability observed in the PCM case and with the reduced dispersion in daily amplitude and attenuation metrics compared to the reference.

4.1.7 Physical interpretation and significance of the saddle-type response surfaces

The response surfaces (Figure 9.) represent the statistical relationship between the daily maximum indoor air temperature and two independent boundary-condition descriptors:

- the daily maximum outdoor air temperature and
- the daily maximum specific power of incident solar radiation.

The physical rationale is that solar radiation contributes to indoor peak formation by warming the exterior wall surfaces, which increases inward heat flow (heat gain) into the indoor air; therefore, peak indoor temperatures cannot be interpreted credibly from outdoor air temperature alone.

The resulting surfaces exhibit a saddle-type shape, which is consistent with a coupled, two-parameter dependence: the influence of outdoor temperature maxima on indoor maxima changes with solar intensity, and the influence of solar intensity changes with the level of outdoor temperature. In the evaluated dataset, the relationship is close to linear between outdoor and indoor maxima when the daily maximum solar radiation level is fixed, but the slope increases markedly with increasing solar radiation at high outdoor temperature maxima. At low outdoor temperature maxima, solar radiation intensity has only a minor effect on indoor maxima.

The same relationship was confirmed through two independent analysis workflows. First, the visualization and response-surface regression were produced in StatSoft Statistica, a statistical analysis environment commonly used for multivariate regression and response surface modeling. Second, the regression was recalculated in Python using the scientific computing stack (e.g., NumPy, Pandas, SciPy, Matplotlib). (See Annex.1 about the software and versions.) The regression coefficients and regression equations obtained with the two approaches were the same, which supports that the observed surface geometry and conclusions are not artifacts of a single software tool or plotting routine.

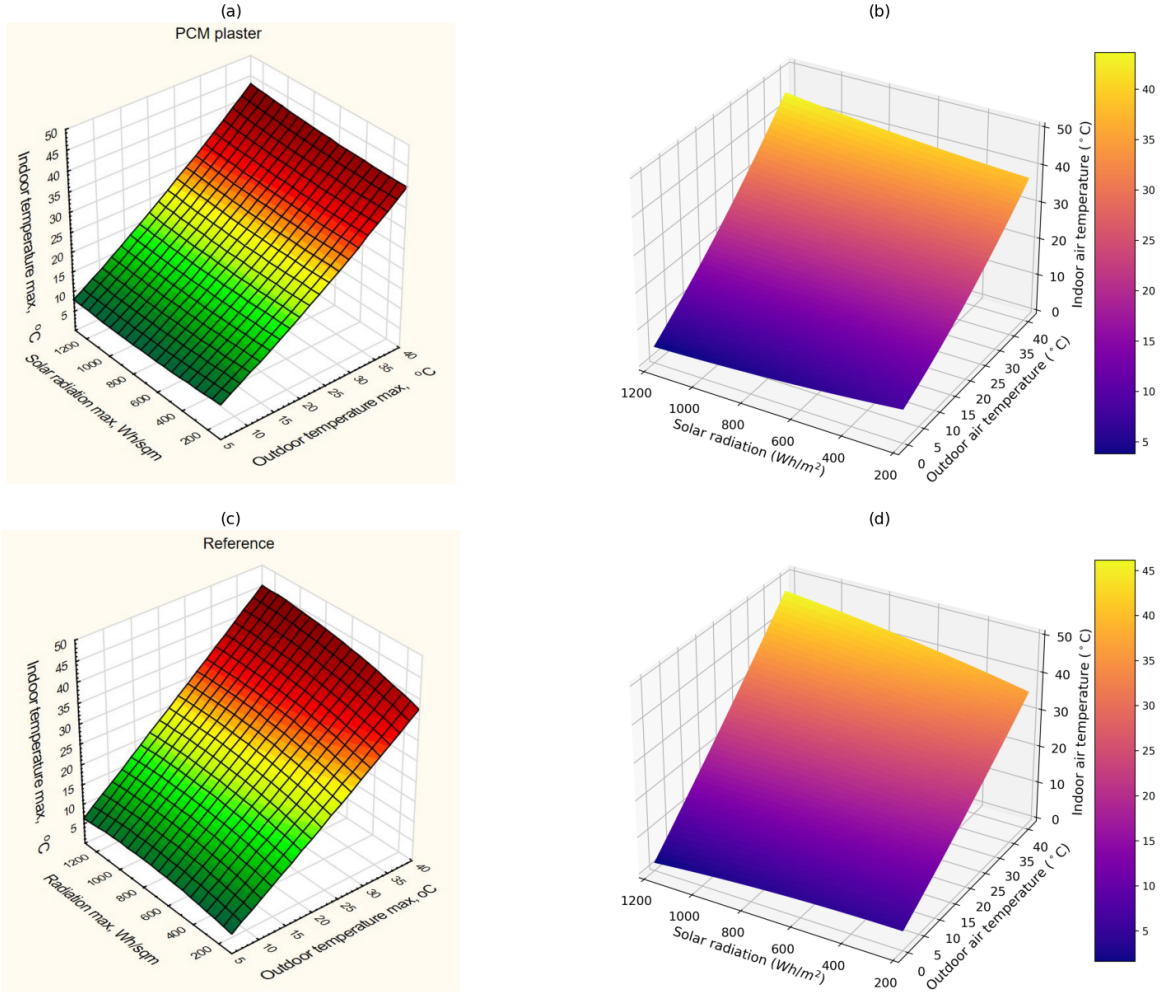

Figure 9: Relationship between daily maximum indoor air temperature, daily maximum outdoor air temperature, and daily maximum solar radiation in the PCM-plastered and reference model houses. Panels (a) and (c) were generated with Statistica, while panels (b) and (d) were generated with Python. Panels (a) and (b) show the PCM-plastered house, and panels (c) and (d) show the reference house.

The combined figure summarizes the response-surface regression for both configurations by mapping the daily maximum indoor air temperature as a joint function of the daily maximum outdoor air temperature (y) and the daily maximum solar radiation (x). In all panels, the fitted surface is expressed by a second-order polynomial that includes linear terms (x, y), quadratic terms (x^2, y^2), and the interaction term ($x \cdot y$), which together allow the indoor peak temperature to vary nonlinearly across the boundary-condition space. The key point of the visualization is that the indoor peak cannot be characterized by outdoor temperature alone: for a given outdoor maximum, increasing solar radiation shifts the predicted indoor maximum upward, while the sensitivity to solar radiation changes with the outdoor maximum level due to the interaction structure of the fit.

In Figure 9, panels (a) and (b) represent the PCM-plastered configuration, while panels (c) and (d) represent the reference configuration. The Statistica-based response surfaces are shown in panels (a) and (c), and the corresponding Python-based surfaces are shown in panels (b) and (d). Presenting the two fitted surfaces side by side makes the boundary-condition dependence directly comparable across cases without relying on selected days. In the PCM case, the fitted surface indicates reduced indoor peak levels in the high-stress region of the domain (higher outdoor maxima combined with higher solar radiation), consistent with the peak-damping behavior quantified earlier using daily extreme metrics.

The regression surface equations obtained with Statistica software and Python-based processing were practically identical. This indicates that the two separately applied methodological approaches produced consistent results and can therefore also be interpreted as a mutual validation of each other.

A key added step in the Python workflow is the subtraction (difference) surface, constructed point-by-point as the temperature difference between the PCM-lined and the reference case over the boundary-condition space as shown in Figure 10. This difference in surface highlights two effects: larger peak-reduction capacity at higher temperature conditions, and heat reservation (reduced cooling) under cold-weather conditions. In the modeled space, the indoor temperature difference between the two cases ranges roughly from about −4 °C to +2 °C, and the maximum variation reaches approximately 6 °C.

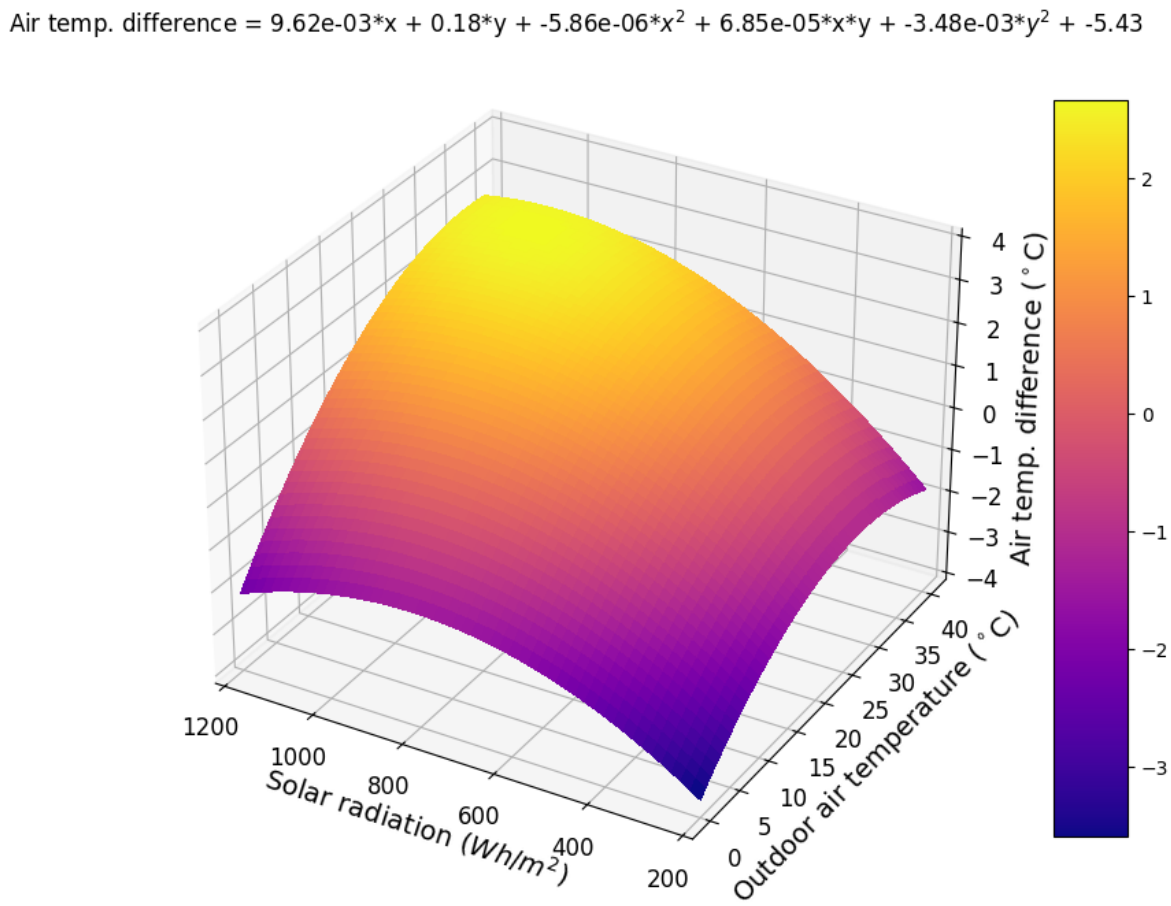

Figure 10: The difference surface shows the temperature difference between PCM plaster lined and reference houses on each point (generated from Fig. 9 data sources).

The reliability and significance of the fitted surfaces are supported by the reported approximation errors. The average regression-approximation error of the response surfaces is ±1.35 °C for the reference case and ±4.04 °C for the PCM case; the larger error in the PCM case is plausibly related to the fact that PCM phase changes do not occur to the same extent across all daily temperature ranges. Importantly, the variation attributed to the independent variables (solar radiation and outdoor temperature) is substantially larger than the estimation error, and the statistical relationship depicted by the surface is considered significant on this basis.

The physical implication of the difference surface is that the performance gap between the two cases is not uniform over the season. The indoor temperature difference is minimal around medium solar radiation and medium outdoor maximum temperatures, but it becomes increasingly significant as solar intensity and outdoor temperature deviate from

these medium values. Consequently, PCM lining provides optimal protection under extremely high or extremely low outdoor temperatures and under too low or too high solar radiation intensities. This trend illustrates both reduced internal cooling at lower outdoor temperatures and limited overheating at higher outdoor temperatures, implying improved protection against outdoor temperature fluctuations.

To summarize and interpret the physical meaning of the regression surfaces within the study, the response models are formulated as second-order polynomials with linear, quadratic, and interaction terms. The presence of the interaction term implies that the sensitivity of indoor peak temperature to one driver depends on the level of the other driver, which is the mathematical reason a saddle-type geometry can appear. The quadratic terms capture the nonlinearity of the response at low versus high boundary-condition levels and allow the surface curvature to change across the domain. The difference-surface equation provides a compact, pointwise description of how the PCM-related peak modification varies over the same boundary-condition space.

4.1.8 Summary of peak-damping performance and consolidated extreme-temperature relationships

The peak-damping performance is summarized using daily indicators of indoor extremes and daily swing, complemented by consolidated linear relationships for daily minima and maxima. Table 3 compiles the key temperature-based outcomes. The mean daily indoor amplitude decreases from 6.3 °C (reference) to 3.6 °C (PCM), confirming a substantial reduction of day–night variability. This is consistent with the observed separation of daily extremes: the PCM configuration yields lower daily indoor maxima (up to 2.2 °C below the reference) and higher daily indoor minima (up to 3.8 °C above the reference), indicating the moderation of overheating peaks and reduced overnight/morning cooldown.

Variability measures further support the stability of this effect over the full interval. The standard deviation of the full indoor temperature series decreases from 8.96 °C (reference) to 7.90 °C (PCM), while the dispersion of daily maxima is also reduced (8.82 °C to 7.97 °C). For the daily swing itself, the standard deviation of daily amplitude narrows from 2.11 °C (reference) to 1.27 °C (PCM), indicating that the reduction is not limited to mean

behavior but also manifests as a tighter day-to-day distribution. Using the attenuation-factor definition applied in this section, the reference case exhibits an average value of 106.2% (amplification by definition), whereas the PCM case indicates attenuation with the outdoor amplitude reduced to approximately 61% indoors on average.

Table 3: Main metrics of the temperatures statistics in both houses

Metric	**Reference house**	**PCM house**
Mean daily indoor amplitude A_{in} (°C)	6.3	3.6
Std. dev. of full indoor temperature series (°C)	8.96	7.90
Std. dev. of daily indoor maxima (°C)	8.82	7.97
Std. dev. of daily indoor minima (°C)	6.75	7.12
Std. dev. of daily indoor amplitude A (°C)	2.11	1.27
Mean attenuation factor M (%)	106.2	61

The consolidated regressions in Figure 11. provide a compact closing view of the same conclusions in the space of daily extremes. The outdoor-to-indoor minimum regressions show near-unity slopes for both configurations but a higher intercept in the PCM case, consistent with elevated indoor minima at comparable outdoor minima. The reference-to-PCM extreme regressions further separate the two effects: daily minima are shifted upward, while daily maxima exhibit a slope below unity, indicating stronger suppression as reference peaks increase.

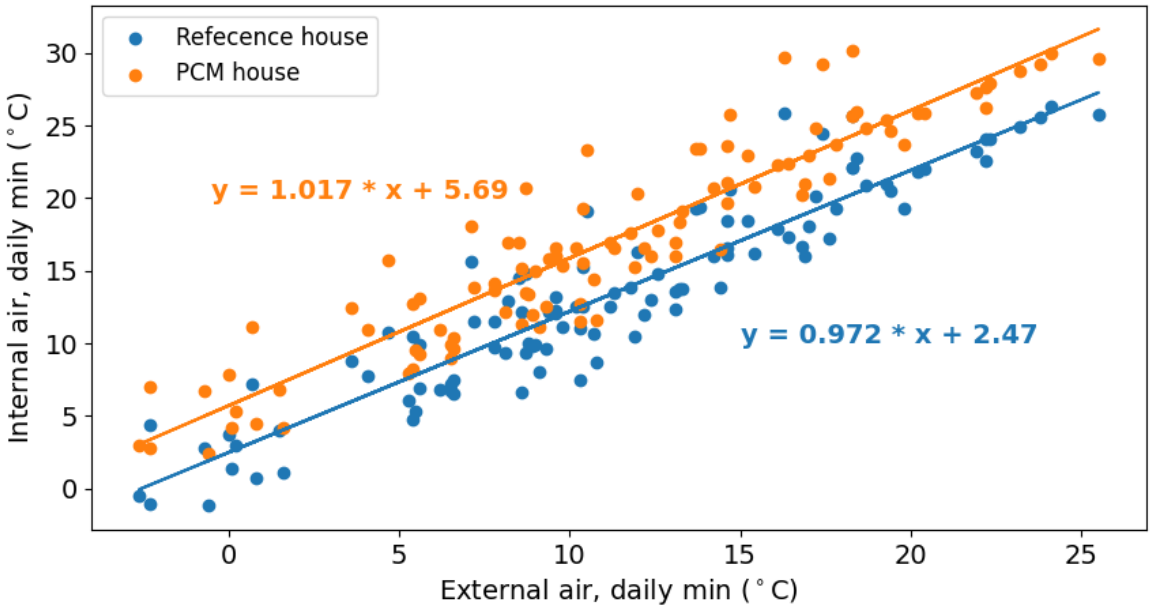

Figure 11: The relationship between daily minimum temperature of indoor air in the PCM plaster and reference houses and daily minimum temperature of external air (with the regression equation between the variables displayed).

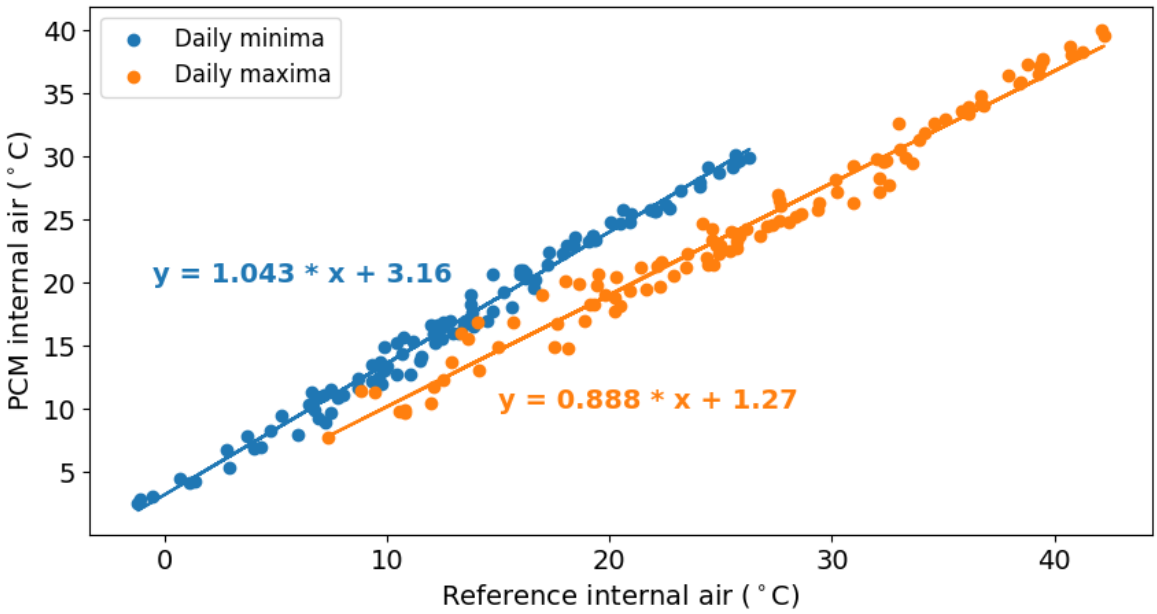

Figure 12: Relationship between daily minima and maxima of indoor air with the regressions.

According to the interpretation in the conclusions, the regression-based summary of daily extremes is important, because it compactly and quantitatively captures the two principal components of the PCM effect: heat retention on the minimum side and peak damping on the maximum side. The near-unity slopes obtained for daily minima indicate that indoor

minima still co-vary strongly with outdoor minima, while the higher intercept for the PCM house shows that higher indoor minima are maintained at comparable outdoor minima. This is consistent with the physical picture in which heat absorbed during the day (partly stored in latent form) contributes to reducing night-time and early-morning cooldown.

The direct comparison of indoor extremes further clarifies that the effect is asymmetric: the fitted slope for minima is slightly above unity, whereas the fitted slope for maxima is below unity. This indicates that the PCM suppresses higher overheating peaks proportionally more strongly, while the uplift in minima is not necessarily representable as a simple constant offset over the full range. In conclusion, this behavior is linked to a radiation-driven “heat-trap” mechanism: during the warmest hours, the PCM absorbs part of the inward heat gain, thereby limiting the rise of indoor maxima, and part of the stored heat is released later. Overall, the regression summary is consistent with the PCM compressing the indoor operating temperature band from both sides, with an effect of magnitude that can vary with the thermal loading state.

4.1.9 Overall conclusion of the peak-damping study

Across the monitoring period under free-running operation, the PCM-lined house exhibits a consistently damped indoor temperature operating band relative to the reference house. The results converge across daily indicators: the mean daily indoor amplitude is substantially reduced, daily maxima are moderated during warm load conditions, and daily minima are elevated, indicating reduced night-time and early-morning cooldown. Variability metrics support that this effect is not limited to average behavior but also manifests as a narrower day-to-day distribution of indoor swing, while the attenuation-factor evaluation distinguishes amplification in the reference house from attenuation in the PCM-lined house by definition. The consolidated regression view of daily extremes further supports an asymmetric response: indoor minima are shifted upward, whereas higher indoor peaks are suppressed more strongly as reference peaks increase. Taken together, the findings show that PCM plaster provides a passive stabilization effect that mitigates peak overheating while improving low-side temperature retention, forming a quantitative basis for the subsequent analysis of time-shift and comfort-related performance.

4.2 Time lag phenomenon and its significance

4.2.1 Interpretation of time lag and the issue of excessively high indoor temperatures

Due to latent heat storage, PCMs not only reduce the magnitude of daily temperature fluctuations but also shift the occurrence of temperature peaks to later times. The essence of this phenomenon is that the temporal evolution of thermal loads changes: maxima and minima do not emerge at the same time as they do without PCM. In this sense, the time lag is a key descriptor of dynamic thermal behavior, because it reorganizes the timing of extremes rather than merely altering their amplitude. During warm periods, this has direct relevance for thermal comfort, since excessively high indoor temperatures constitute a primary driver of discomfort and overheating risk. If the indoor maximum is delayed, more favorable indoor conditions may prevail during the most critical hours of the day. Consequently, the observed delay is not simply a "lag" in a narrow sense, but a meaningful redistribution of the daily load profile. The combined effect of peak attenuation and time shifting is illustrated schematically in Figure 13.

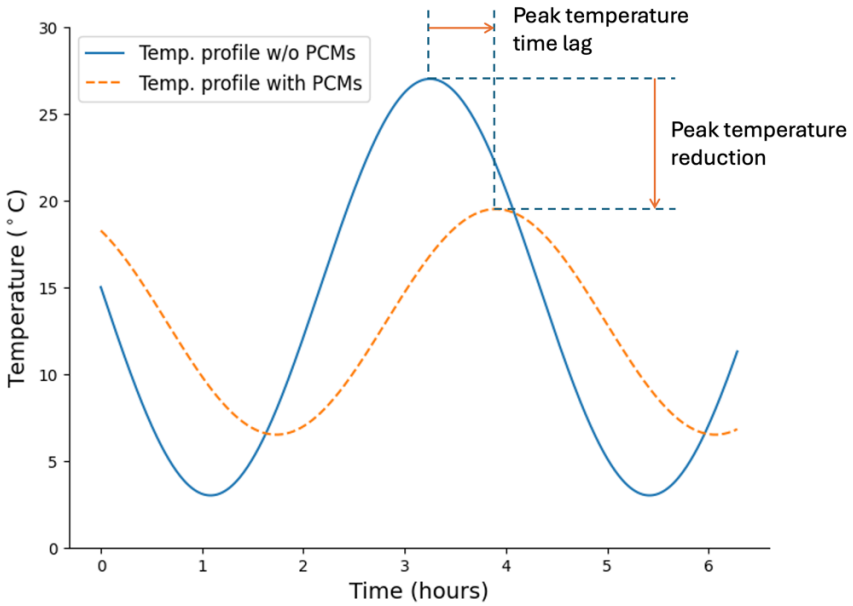

Figure 13: Illustration: the application of the PCM attenuates (reduction) and shifts (time lag) of the thermal peaks in model houses.

From a practical perspective, this implies that the most severe loads can be displaced toward time windows when outdoor conditions may already be less adverse. Time lag describes the timing of thermal stress, whereas peak reduction describes its magnitude. The magnitude of the time lag, however, is clearly design-sensitive and depends on multiple factors, meaning it cannot be treated as a universal outcome that applies identically across all configurations.

In the literature, time lag is often illustrated using arbitrarily selected individual days, even though the phenomenon is influenced by several weather drivers that vary stochastically. This creates a methodological risk, because an illustrative day may not represent typical behavior. For this reason, the evaluation of time lag is best supported by long time series, where the phenomenon can be characterized statistically rather than only demonstrated qualitatively. In this chapter, time lag is interpreted within such a free-running measurement framework, with a specific emphasis on implications that are relevant to periods of excessively high indoor temperatures.

4.2.2 Data processing and peak position identification for time lag estimation

This analysis is likewise based on the 105-day free-running measurement campaign and the corresponding high-resolution sensor data. In this section, however, the primary target is not the magnitude of daily temperature swings, but the reliable identification of the timing of daily extrema. Time lag is defined through the temporal position of peaks, so even a small error in locating the peak can propagate directly into the estimated delay. Although the temperature signal exhibits an overall quasi-periodic diurnal pattern, determining the peak position is not trivial in practice.

With a 5-minute sampling interval, the signal near the top of the daily cycle often appears jagged, and several closely spaced local maxima can occur around the warmest hours. During hot periods, the peak region may contain numerous short-term fluctuations, and multiple candidate peaks can emerge within a relatively narrow time window. In such cases, a simple “global maximum” search becomes unstable, because the selected time stamp may be driven by short-lived variations rather than the dominant diurnal behavior. To address this issue, peak identification is preceded by curve smoothing. The purpose of

smoothing is not to alter the underlying physical behavior of the signal, but to suppress short-period variability so that the diurnal maxima can be interpreted consistently. Following the approach described in the paper, a moving-average filter is applied to reduce high-frequency fluctuations while preserving the daily trend. Specifically, a centered 9-point moving average is used. Given the 5-minute sampling interval, this corresponds to an effective low-pass filtering of the measured time series. The 9-point averaging attenuates the short-term oscillations that would otherwise generate multiple spurious local maxima around the peak region.

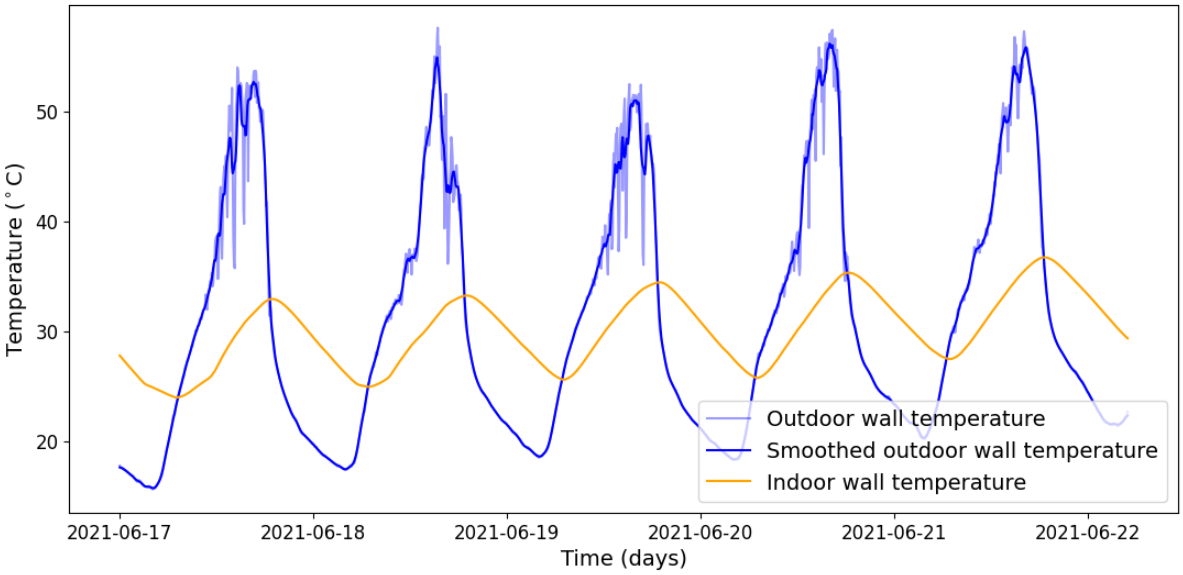

Figure 14: Raw outdoor and indoor wall temperature data and moving-average-smoothed outdoor wall temperature used for peak detection.

As a result, both the timing and the magnitude of daily peaks become more clearly identifiable on the smoothed curve, improving the stability of peak position detection. This is particularly important when peak times must be determined repeatedly on a day-by-day basis and subsequently used to compute time lag. At the same time, smoothing can raise a methodological concern, because an inappropriate filter may distort amplitudes and, in principle, introduce artificial phase shifts. For this reason, the paper explicitly considers whether the selected window size introduces systematic bias into peak timing. The conclusion is that the centered 9-point moving average does not meaningfully distort the data and, crucially for the present objective, does not alter the physical timing of the peaks.

Consequently, time lag can be estimated with minute-level resolution while limiting the sensitivity of the procedure to weather-driven and measurement-related fluctuations. The smoothing step is illustrated in the accompanying figure (Figure 14), where the raw signal and the filtered curve are shown together to demonstrate that peak position identification is not an ad hoc choice, but a reproducible data-processing procedure.

4.2.3 Relevance of time lag

The practical relevance of time lag lies primarily in shifting the timing of maximum temperatures at interior surfaces and in the indoor air, so the peak thermal load does not necessarily coincide with the most critical outdoor conditions. This delay effectively redistributes the daily profile of comfort-driven cooling load, meaning it influences when an air-conditioning system would, in principle, need to operate at its highest capacity. It is important to emphasize that the present measurement campaign was conducted under free-running conditions: no heating, cooling, or any other HVAC components were used.

Accordingly, any statements related to air-conditioning are theoretical implications derived from the measured temperature trajectories rather than observations of actual system operation. A later-occurring peak can be relevant because air-conditioning efficiency is typically sensitive to outdoor temperature, so a delayed peak may coincide with more favorable operating conditions. In parallel, a reduction or temporal spreading of the peak demand can lessen the concentration of cooling needs during the hottest hours, which is relevant from the perspective of sizing and peak-capacity requirements for comfort-oriented air-conditioning.

Beyond cooling, time lag can be interpreted more generally as a modification of the timing of thermal extremes, aligning the building's thermal response differently within the daily cycle. From a comfort perspective, the delay is significant because indoor temperatures change less abruptly: more favorable (lower) conditions may persist during the critical peak period, while nighttime cooling of the indoor environment may proceed more slowly. As a consequence, fewer hours may fall outside the comfort range, thereby reducing the theoretical need for comfort-restoring intervention.

Time lag also acts as an indicator of buffering behavior, expressing the extent to which the envelope can temporally moderate external temperature variations. In the logic of latent

heat storage, delayed energy release manifests as a delayed thermal response, so a larger time lag is consistent with stronger buffering performance. At the system level, this temporal shift can be advantageous because comfort-driven air-conditioning would, in principle, be less forced to deliver its maximum intervention during the most extreme hours, resulting in a more even load profile.

4.2.4 The importance of the comfort temperature

Within this experimental framework, the relevance of comfort temperature arises from the fact that describing indoor conditions solely through daily maxima and minima is insufficient to judge practical usability. From an occupant perspective, the indoor temperature trajectory is favorable only to the extent that it remains within an acceptable range, or—when excursions occur—those excursions are limited in both magnitude and duration. Under free-running operation, indoor conditions respond directly to external driving forces, so comfort assessment requires a reference framework that is appropriate for naturally ventilated or non-air-conditioned buildings. For this reason, an adaptive comfort approach is suitable, because the comfort temperature is not treated as a fixed setpoint but as a quantity that varies with the outdoor environment, commonly expressed through a running-mean outdoor temperature. This allows the same indoor temperature level to be interpreted differently in a mild transition period than during a hot summer episode. Comfort temperature therefore functions as a dynamic interpretive layer that assigns meaning to measured indoor data, rather than as a single target value.

In this context, the “excessively high indoor temperature” problem is not governed only by the peak temperature itself, but also by how long indoor conditions remain above the upper comfort limit. The same logic applies on the cold side: during transition periods and under free-running conditions, indoor temperatures may remain below the comfort range for extended periods, which reflects the operating mode rather than a failure of the envelope concept. Consequently, comfort temperature plays a dual role. First, it delineates when overheating risk is present; second, it helps identify those days and ranges in which free-running performance can be interpreted meaningfully from a comfort standpoint. Comfort-based evaluation also emphasizes that discomfort is inherently time-dependent: brief excursions and persistent exceedances are qualitatively different even if they share

similar peak values. This is essential for interpreting the effect of PCM beyond a generic "temperature reduction," and instead in terms of the fraction of time spent in acceptable indoor conditions and the persistence of periods outside the comfort range.

Using a comfort framework also improves methodological transparency and comparability. It anchors the comparison of the investigated configurations to a common, standardized reference, making the interpretation reproducible across the full measurement period. In this framing, PCM performance is favorable when the indoor temperature trajectory exceeds the upper comfort limit by a smaller margin and/or for a shorter duration, particularly during the warm load periods that are most relevant for overheating. Ultimately, comfort temperature links measured time series to the occupant-relevant meaning of "better indoor conditions," and it prevents qualitative labels such as "too high" or "acceptable" from becoming arbitrary by providing a consistent basis for evaluation.

4.2.5 Adaptive comfort range based on EN 16798-1:2019

The EN 16798 series provides a harmonized European framework for defining indoor environmental input parameters in buildings. Within this series, EN 16798-1:2019 defines categories and assessment conditions for thermal comfort, together with requirements related to other aspects of indoor environmental quality (IEQ). In the present work, the adaptive comfort model is the relevant component because the measurement campaign was conducted under free-running conditions, i.e., indoor temperatures were not controlled by any HVAC system toward a fixed setpoint. Under such operation, comfort assessment against a constant target temperature is not methodologically justified, since indoor conditions evolve in response to external driving forces and the building's dynamic thermal behavior. The adaptive model therefore provides an outdoor-contextualized reference by defining a comfort temperature and an associated acceptability band that vary with prevailing outdoor conditions.

For periods without mechanical cooling, the adaptive centerline (comfort temperature) is calculated as:

$T_{comf} = 0.33\ T_{rm} + 18.8$

where T_{rm} is the running-mean outdoor temperature. The adaptive model is applied within its validity range, approximately $10 \leq T_{rm} \leq 30$ °C. In the present evaluation, the running-mean outdoor temperature is computed using a weighted formulation based on the daily mean outdoor air temperatures from the preceding days:

$$T_{rm} = (T_{ed-1} + 0.8\ T_{ed-2} + 0.6\ T_{ed-3} + 0.5\ T_{ed-4} + 0.4\ T_{ed-5} + 0.3\ T_{ed-6} + 0.2\ T_{ed-7}) / 3.8 \quad (1)$$

where T_{ed-i} denotes the daily mean outdoor air temperature i days prior to the day being evaluated. Physically, this 7-day weighted form approximates short-term thermal acclimatization by giving greater influence to the most recent outdoor conditions while still retaining a diminishing memory of earlier days, and it is convenient in practice because it can be computed directly from standard daily mean weather data.

Acceptability is assessed using a ±3 °C band around the adaptive comfort temperature. Accordingly, at each time step, indoor air temperature is classified as acceptable if it lies within:

$$[T_{comf} - 3\ °C,\ T_{comf} + 3\ °C]$$

This definition avoids arbitrary absolute overheating thresholds and supports a consistent interpretation across the full monitoring period as outdoor conditions evolve. Overheating is therefore defined by exceedance of the adaptive upper boundary, and its interpretation is inherently relative to the prevailing outdoor context. Methodologically, both the magnitude of exceedance and its persistence are relevant for characterizing comfort performance under free-running conditions, because short excursions and sustained periods above the upper limit represent qualitatively different indoor environments even if peak temperatures are similar.

4.2.6 Results of time lag quantification

The quantification of time lag is based on comparing the timing of daily temperature peaks between characteristic outdoor and indoor temperature trajectories. For the assessment of dynamic response, the daily maximum of the external wall surface temperature is treated as the primary driving signal, as it is more directly related to heat transfer through the envelope and implicitly captures the combined effects of solar radiation, cloud cover, wind, and precipitation. By contrast, outdoor air temperature is typically more volatile; therefore,

peak timing is determined from wall-temperature signals, while solar-radiation behavior can be used as a consistency check for the timing of the diurnal forcing. For each day of the monitoring period, the time stamps of the daily maxima are identified and paired, and the daily time lag is calculated as the time difference between the outdoor-side and indoor-side peaks.

The evaluation focuses on the west-oriented façade. During the monitored spring–summer period, the maxima of outdoor air temperature and the external surface temperature of the west wall typically occur in the early afternoon, when the west façade is strongly affected by solar exposure; this provides a clear and physically meaningful context for interpreting the formation of indoor temperature peaks. On both the exterior and the interior reference side of the west wall, three calibrated temperature sensors were used; employing multiple measurement points reduces uncertainty associated with local inhomogeneities and supports a more robust identification of peak timing. For each day, the time of the outdoor-side maximum and the corresponding indoor-side maximum are determined, and their difference yields the daily time lag.

As shown in Figure 15, the daily time lag values are reported over the full monitoring period for both the reference configuration and the PCM-lined configuration. The comparison indicates a persistent and clearly discernible difference between the two cases: the PCM-lined house exhibits an approximately twofold increase in time lag relative to the reference case. Based on the time series in Figure 15, the reference configuration shows a typical time lag on the order of about 100 minutes, whereas the PCM configuration shows a typical value on the order of about 200 minutes. Importantly, this twofold character is not limited to a small subset of days but is sustained across the monitoring campaign, indicating a reproducible delay effect associated with latent heat storage rather than an episodic phenomenon. Consequently, Figure 15 serves as the primary results figure for the day-by-day quantification of time lag and provides direct numerical support for the magnitude of the delay effect observed for the PCM configuration under free-running conditions.

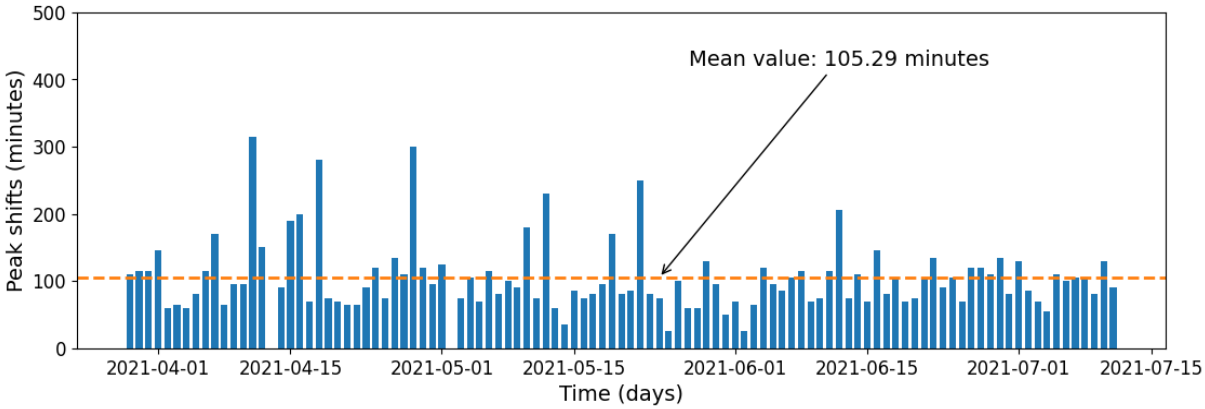

Reference

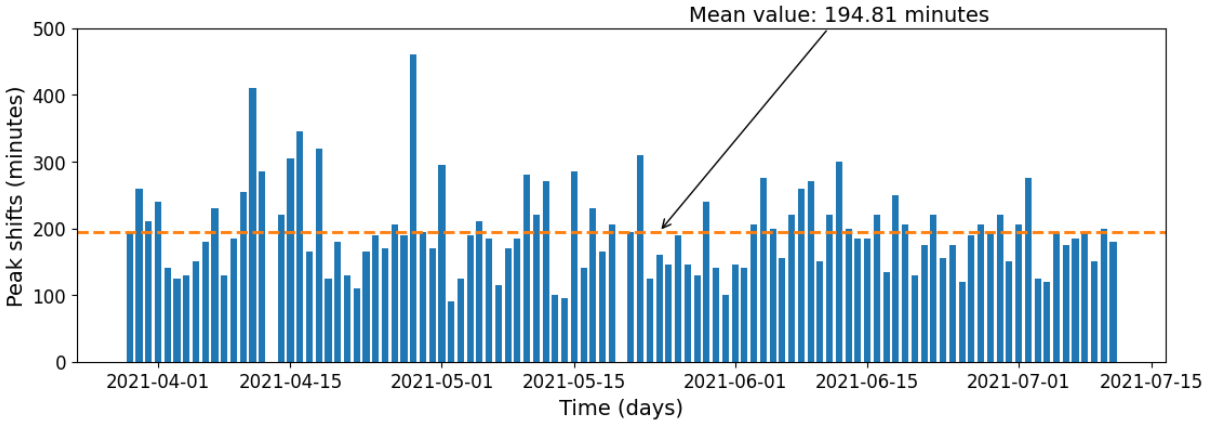

PCM

Figure 15: Temperature peak-time lags in the model houses (west wall outside–inside)

4.2.7 Statistical characterization of time lag based on a lognormal distribution

Day-by-day time lag values quantified in Section 4.2.6 were characterized statistically to describe the overall behavior across the monitoring period.

Time lag, as a dynamic response parameter, varies over time; therefore, describing performance over the full monitoring period requires a distribution-based characterization that captures central tendency and variability in a consistent manner. This approach is also necessary because the monitoring period encompasses multiple outdoor regimes, and a single “representative day” would not provide a firm, basis for inference. Treating time

lag as a stochastic outcome enables the comparison of houses on the level of population behavior rather than isolated events.

Figures 16a and 16b show the empirical frequency distributions of daily time lag values for the reference house and the PCM house, together with fitted distribution curves. The distributions are strictly positive and asymmetric, which motivates avoiding a normality assumption. The fitted curves indicate that the time lag values are adequately described by a lognormal distribution, consistent with the general observation that lognormality is common for quantities shaped by multiple coupled influences. In this context, the lognormal representation supports treating time lag as an integrated outcome of environmental forcing and the envelope's dynamic response, rather than as a fixed parameter. Importantly, the use of a common distribution family for both houses provides a coherent statistical basis for comparison, because differences can then be interpreted primarily through shifts in location and changes in deviation rather than through fundamentally different distributional forms.

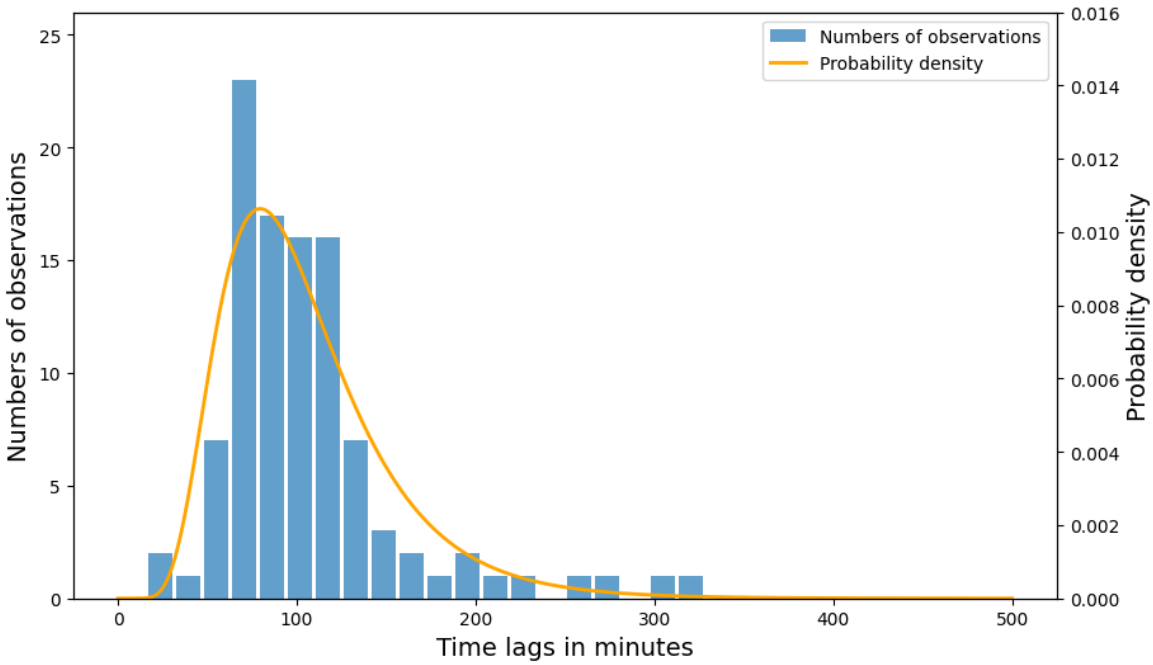

a.) Reference

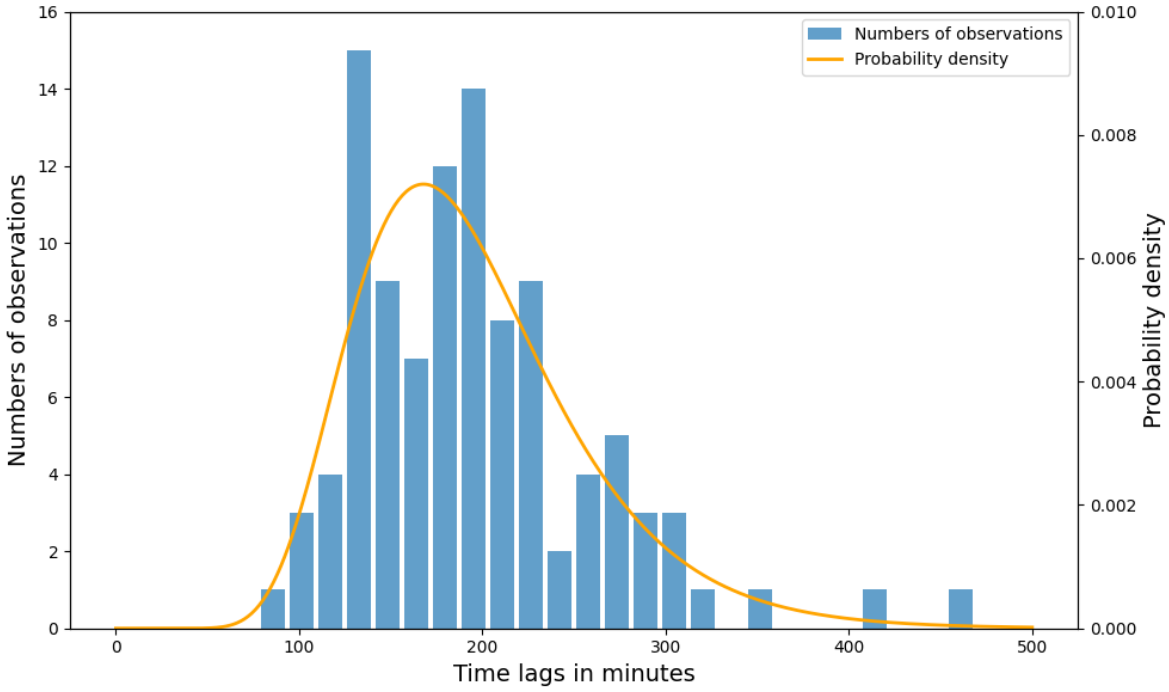

b.) PCM

Figure 16 a-b: Time lag histograms with lognormal deviation

Figure 17 summarizes the minimum, mean, and maximum time lag values for both houses and includes a lognormal deviation around the mean derived from the fitted distribution parameters. The PCM house exhibits higher values across all three summary metrics, indicating that the increase in time lag is not limited to a narrow subset of days. The reported lognormal deviation is smaller for the PCM house, which indicates that the increased delay is associated with a more concentrated distribution of daily values. From an interpretation standpoint, this combination implies not only a stronger delay effect but also a more stable one, in the sense that daily outcomes are less dispersed around the central tendency.

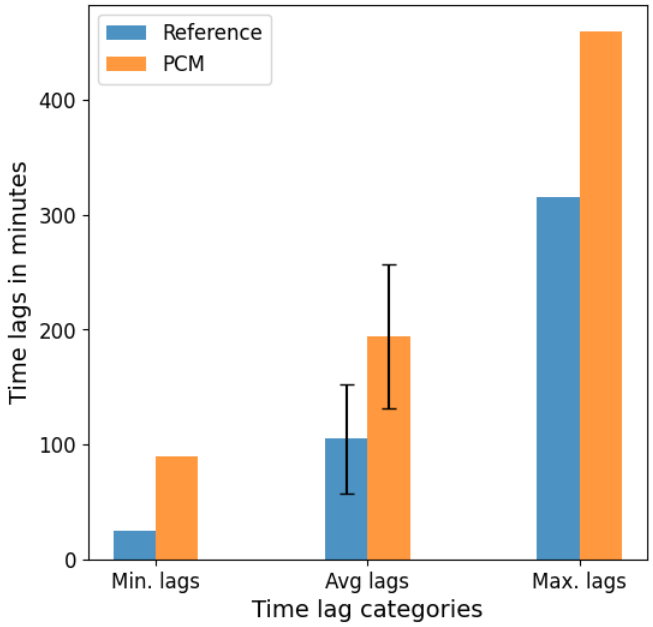

Figure 17: Minima, average and maxima of time lags in the model houses

Figure 18 provides a paired comparison by plotting the daily time lag in the reference house against the corresponding daily time lag in the PCM house. All paired observations lie above the y=x line, demonstrating that the PCM house yields a larger time lag for every observed day. The regression line further corroborates this relationship, with an approximately unit slope and a positive intercept that is consistent with the mean offset already quantified in Section 4.2.6, thereby providing a graphical consistency check of the numerical procedure. The paired formulation is particularly informative because it suppresses day-to-day meteorological variability as a confounding factor and directly evaluates the between-house difference under matched external conditions.

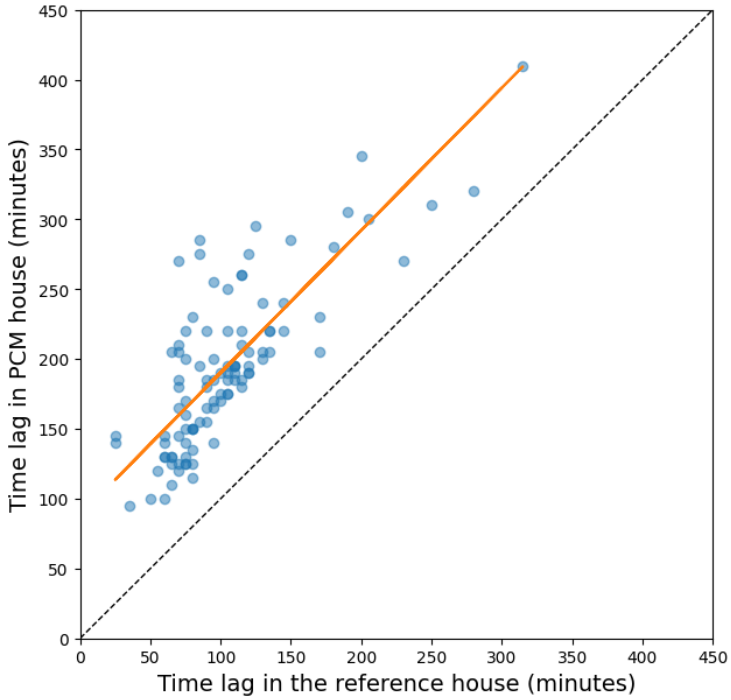

Figure 18:The connection between the PCM and reference time lags.

Overall, the results indicate that time lag is well represented by a lognormal distribution for both houses, while the PCM house exhibits systematically larger delays together with a smaller lognormal deviation, and the paired comparison confirms the direction and coherence of the quantified difference at the level of daily observations.

4.2.8 The relevance of time lag for thermal comfort

Time lag, as a dynamic response indicator, describes the temporal shift of temperature peaks; however, its comfort-related interpretation is only methodologically sound when indoor time series are evaluated against a standardized reference range that is consistent with the outdoor context. This framework is provided by the EN 16798-1 adaptive comfort model, which is applicable to free-running operation where indoor temperature is not controlled by an HVAC system toward a fixed setpoint. According to the standard, the comfort temperature is derived from the running-mean outdoor temperature; in the present evaluation this running mean is computed using the 7-day weighted formulation. A direct consequence is that both the comfort centerline and the associated comfort band vary over time and change in a discrete, stepwise manner at a daily resolution: the reference remains

constant within a given day, and shifts on the next day as the running mean is updated. Thermal comfort assessment is therefore not tied to fixed thresholds but to a standard-defined, climate-responsive comfort range.

Figure 19 presents the indoor air temperature pattern of the reference house and the PCM house together with the adaptive comfort temperature and the comfort range. The reference house exhibits a pronounced diurnal cycle: daytime warm-up is faster, the temperature amplitude is larger, and peak formation follows the external forcing more closely. In contrast, the PCM house shows a more moderated trajectory: the rise is slower, extrema are attenuated, and the daily maxima occur later in time. Here, the delay does not appear as a single scalar value but as a relative shift between the peak timings of the two time series, consistent with the time lag differences quantified earlier. A comparable modification is visible around the minima as well: the PCM house cools less deeply, implying a compressed daily swing and reduced slopes of the temperature curve.

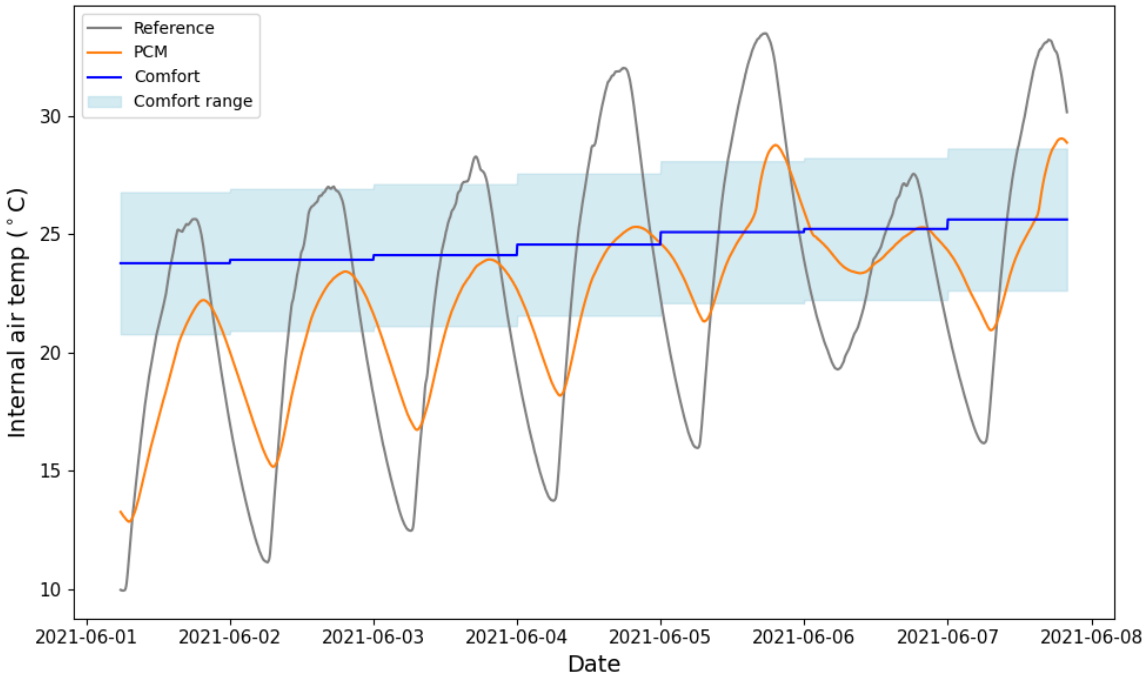

Figure 19: Internal temperature and the comfort range in the model houses. For illustrative purposes, it shows the daily temperature profile and the comfort range.

When interpreted relative to the comfort band, Figure 19 indicates that the temperature trajectory of the reference house crosses the comfort range more frequently and by a larger margin, particularly during daytime peak-load hours. The PCM house, by comparison,

remains within the comfort range for a longer portion of time, and conditions near the upper comfort boundary develop less abruptly. Because the monitoring was conducted under free-running operation, these comfort-related differences are not the outcome of active control but of the passive thermal response: the PCM modifies the shape and timing of the indoor temperature trajectory in a manner that improves alignment with the standard-defined adaptive range. Within this framework, the relevance of time lag is not limited to the fact that maxima occur "later," but lies in the restructuring of the thermal profile during critical periods: peaks are shifted in time, and the formation and persistence of out-of-range conditions are reduced.

Figure 19 also emphasizes that comfort evaluation cannot be reduced to a single absolute limit. Because the comfort reference varies over time, the same indoor temperature level can be classified differently across periods; accordingly, the PCM effect should not be described solely in terms of absolute maxima and minima. The illustrated time window shows that the PCM house is not simply "cooler" or "warmer," but that its dynamic timing contributes to a more favorable correspondence with the adaptive comfort range. In this sense, the comfort relevance of time lag can be expressed through the combined effect of peak shifting and trajectory moderation, which together increases the fraction of time spent in comfort-acceptable conditions over the monitored period. The key point is that this is about timing, not just temperature level. The PCM effect matters because it keeps the indoor temperature closer to the comfort band for longer, even when the absolute daily extremes change only slightly.

4.2.9 Conclusions on time lag

Beyond the mitigation of temperature extremities, a substantial temporal shift of temperature peaks is also observed in the PCM-lined experimental house. Based on the quantification of this effect and the demonstration of its relevance, the following conclusions can be drawn.

Time lag quantification was based on processing tens of thousands of raw sensor measurements recorded under free-running conditions. Because peak timing cannot always be identified unambiguously due to fluctuations in the measured signal, evaluation

was performed after statistical smoothing so that peak positions could be determined in a consistent and comparable manner for both houses.

The processed data indicate that the PCM house exhibits a meaningful increase in delay relative to the reference house; for the peak behavior evaluated on the west façade, the typical additional time lag is on the order of approximately 100 minutes. This difference is relevant at the scale of a free-running daily temperature profile because it represents a restructuring of the timing of indoor maxima rather than merely a change in peak amplitude. The paired graphical comparison also supports the internal coherence of the numerical results: the relationship between the daily time lag values of the reference and PCM houses remains consistent in direction, and the intercept of the linear fit agrees with the typical offset quantified earlier. Accordingly, the observed relationship provides a consistency check for the calculation procedure.

The statistical characterization further shows that daily time lag values can be described by a lognormal distribution for both the reference and PCM houses. This lognormality supports a distribution-based evaluation and indicates that the phenomenon should not be represented as a single constant parameter. When the distributions are compared, the PCM house is shifted toward larger time lag values, while the fitted lognormal deviation is smaller, implying a more concentrated day-to-day response. Interpreting minimum, mean, and maximum values together likewise indicates that the difference is not attributable to isolated extreme days but is consistently present across the observed range.

Comfort-related conclusions become interpretable under free-running operation by applying the adaptive comfort model of the European standard EN 16798-1:2019. The comfort reference temperature is derived from the running-mean outdoor temperature computed using the standard's 7-day weighted formulation, and the comfort range is defined as a ±3 °C band around the adaptive comfort temperature. Because the reference varies over time, comfort classification is not based on fixed absolute thresholds but on a range that is continuously aligned with prevailing outdoor conditions. Within this framework, the relevance of time lag lies in the fact that peak shifting and moderation of the indoor trajectory together lead to a more favorable alignment with the adaptive comfort range and, in turn, contribute to an increased fraction of time spent within comfort-acceptable conditions over the monitoring period.

Overall, time lag emerges as a relevant and measurable indicator of the dynamic PCM effect: it can be quantified after statistically smoothed peak identification, its magnitude is meaningful (≈100 minutes) on the west façade, it is robustly described using a distribution-based approach, and it is directly connected to the fraction of time within the adaptive comfort range under free-running conditions.

4.3 Effect of orientation on PCM plaster performance

4.3.1. The role of wall orientation in PCM plaster placement

During the statistical analysis of peak shifting presented in Section 4.2, it became evident that wall orientation may play a decisive role when PCM is placed within the envelope. Accordingly, the purpose of this subsection is to highlight the relevance of different orientations in a way that provides direct practical value for optimizing the placement strategy of PCM-based plaster. It should be emphasized that, in the investigated model house, PCM was applied only on the side walls, while the roof and the floor assemblies remained without PCM.

Wall orientation can be considered one of the most influential contextual variables affecting the performance of PCM. At mid-latitudes, the magnitude and temporal profile of incident solar radiation differ substantially across the north-, east-, south-, and west-facing façades, which leads to pronounced differences in the daily evolution of surface temperatures. Consequently, the thermal behavior of PCM-containing wall assemblies is orientation-dependent, and neglecting orientation may result in underperformance or misleading conclusions. An orientation-agnostic optimization of PCM layers cannot be regarded as generally valid, because the operating conditions for PCM differ across façades due to the unequal solar loads. Therefore, orientation should be treated as a primary design consideration for applying PCM plaster in building envelopes.

The physical basis of these orientation-driven differences can be captured through the interaction between solar gains and phase-change dynamics. PCM operation is governed by the extent and timing of phase-change activation and by whether the phase-change cycle is effectively completed under the daily load variations. Since solar exposure reaches

its maxima at different times of the day for different orientations, and exhibits different rise and decay rates, façade temperature time series also differ in shape. From the perspective of PCM, this implies that, on some façades, the temperature range and cycle duration may be more favorable for latent heat storage, whereas, on other orientations, the temperature profile may be less supportive of effective phase change. Orientation therefore directly affects when, and to what extent, the PCM is able to absorb and release latent heat, which can translate into distinct patterns in the delay and attenuation of heat-flux peaks.

Based on earlier measurements conducted under free-floating spring conditions in other studies, a delay of thermal peaks and an attenuation of indoor peak temperatures were observed for the PCM-plaster configuration; however, long-term experimental evidence based on free-running measurements has been largely lacking in the field. An increase in the number of comfort hours under variable weather conditions was also identified as a notable effect. By applying statistical analysis methods to season-long datasets, changes associated with PCM integration could be quantified, and a reduction in the calculated energy use was also indicated. Nevertheless, experimental substantiation of orientation-specific behavior in lightweight buildings remains limited, which supports the need to examine the role of orientation explicitly.

Accordingly, this subsection focuses on the role of orientation and illustrates how direction-dependent solar loads shape the operating conditions of PCM plaster, as well as the orientation-specific differences observed in temperature- and heat-flux-related indicators.

4.3.2. Measurement setup and data processing for the orientation-based thermal evaluation

The thermal behavior analysis of the sensor dataset made the role of orientation clearly assessable. It is important to note that the thermal transmittance values specified for the model houses are known and were confirmed by control calculations. In both units, the external wall assembly consisted of steel sheet cladding on the outside, 50 mm mineral wool insulation, and an internal 8 mm laminated decor board finish. This configuration resulted in an approximate wall U-value of 0.55 W/m²K. The roof and floor assemblies

were also insulated with the same construction approach -but with a thicker rock wool insulation layer- in both houses, yielding U-values of 0.32 W/m²K (roof) and 0.45 W/m²K (floor), respectively.

To ensure that the observed thermal behavior reflected passive phenomena only, both model houses remained unoccupied throughout the measurement period; no internal heat sources were present, and no heating, cooling, or HVAC systems were operated. Windows and doors were kept closed and were excluded from the analysis, as no surface temperature or heat-flux sensors were installed on these elements.

Surface temperatures were measured using Type-K thermocouples on the external and internal surfaces of the north-, east-, south-, and west-facing walls, and also on the roof and floor surfaces. It should be emphasized that, although PCM was applied only on the side walls (and not in the roof or the floor), instrumentation was available for the roof and floor surfaces as well, because sensors were present on these surfaces. Multiple measurement points were used, and the mean surface temperature of each wall was derived from these point measurements. Indoor surface temperatures were measured by sensors mounted on the internal sides of the walls surface. External boundary conditions included time series of outdoor air temperature, global solar radiation, and wind speed.

Due to the small indoor volume of the model houses, thermal coupling between the inner surfaces could not be avoided. Convective heat exchange mediated by the indoor air and radiative coupling between interior surfaces implies that individual walls cannot be treated as fully independent “single-surface” systems. Consequently, the orientation-based separation cannot be regarded as a fully isolated comparison in a strict laboratory sense. Nevertheless, the approach remains informative because significant differences were observable during the measurements, and the dataset supports orientation-resolved interpretation through computable heat-transfer indicators.

During data processing, smoothing was applied to the raw temperature time series to reduce short-term noise and high-frequency fluctuations. A 3 h 45 min moving-average window was used for the 5 min sampled data, corresponding to a 45-point window. From a theoretical perspective, a moving average acts as a low-pass filter: rapid, small-timescale variations are attenuated, while the slower components associated with daily cycles are retained. The purpose of smoothing was therefore to enable more stable and reproducible

identification of daily profiles and extrema (maxima and minima), particularly under rapidly changing meteorological conditions.

From the smoothed time series, daily maximum and minimum surface temperatures were extracted for each measurement point on both the external and internal sides. Linear trend lines were fitted to the resulting daily-extrema series to separate the seasonal tendency along the whole period of measurements. Dispersion around the trend line was quantified using RMSE (root mean square error). RMSE is defined as the square root of the mean squared deviation between the observed values and the trend-estimated values; it is therefore sensitive to larger excursions and is suitable for quantifying how strongly daily extrema deviate from the longer-term trend. Within this framework, RMSE characterizes the magnitude of short-term meteorological variability reflected by each surface and supports orientation-based comparison of the measured thermal response.

4.3.3. The characteristic temperature difference through the walls and the estimation of characteristic heat flux density

In order to compute heat fluxes through the envelope surfaces without relying on complex and costly modeling software, an appropriately defined steady-state reference point is required, at which temperature can be treated as approximately steady state profiles within a given wall. For this purpose, the concept of *characteristic temperature* is introduced.

The question addressed here is how PCM plaster modifies heat transfer through the walls during daytime (inward-directed) and night-time (outward-directed) periods. The physical interpretation is that a portion of the heat flux transmitted through the wall assembly is effectively absorbed within the interior material layers; consequently, only the remaining fraction is transferred to the indoor air. During the cooling phase at night, the outward heat flow can be interpreted analogously: only part of it is associated with the energy balance of the indoor air, while the remainder heat flux may originate from the decrease of the interior plaster's sensible (and, in the case of PCM plaster, latent) heat energy content. This mechanism can manifest simultaneously as a delay and as a moderation in the indoor thermal response.

Based on the temperature time series, the coupling between exterior and interior surface temperatures is strong; however, it can be materially affected by the thermal resistances of the layer build-up, by the time-varying heat content of the structure (sensible heat and, for PCM plaster, latent heat), and by the temporal profile of the daily heating–cooling dynamics. The interior surface temperatures are also influenced by the mutual interaction of interior boundary surfaces mediated by the indoor air; this equalizing effect is particularly pronounced in the small model houses (≈18 m³). The lower level of interior surface temperatures suggests that only a limited portion of the inward-directed heat flow at the exterior surface reaches the indoor air directly, while a substantial share increases the energy content of the assemblies, and—in the house with PCM plaster—phase change can additionally store energy in latent form. During night-time hours, the outward heat transfer is predominantly attributable to the cooling of the wall structure, which, in the presence of PCM plaster, can be interpreted consistently with a moderation of indoor-space cooling.

For a robust comparison of the two configurations (reference wall assembly versus PCM-plastered assembly), the analysis is based on periods when the energy content of the original wall structure can be treated as approximately constant, i.e., when the mean wall temperature is nearly steady. This constraint is applied to the base wall structure; the interior plaster layer (and the PCM within it) can still undergo temperature changes, and thus changes in latent energy content, in response to the incoming and outgoing heat flows. Within a typical day, two-time windows can be identified in which the above condition is satisfied to a good approximation: a short daytime interval near the maximum of the mean wall temperature and a night-time interval near the minimum. Based on the measurements, these intervals are not instantaneous; they may persist for approximately 20-40 minutes and can therefore be selected reliably (Figure 20). A few representative days are shown in the figure to illustrate the concept clearly.

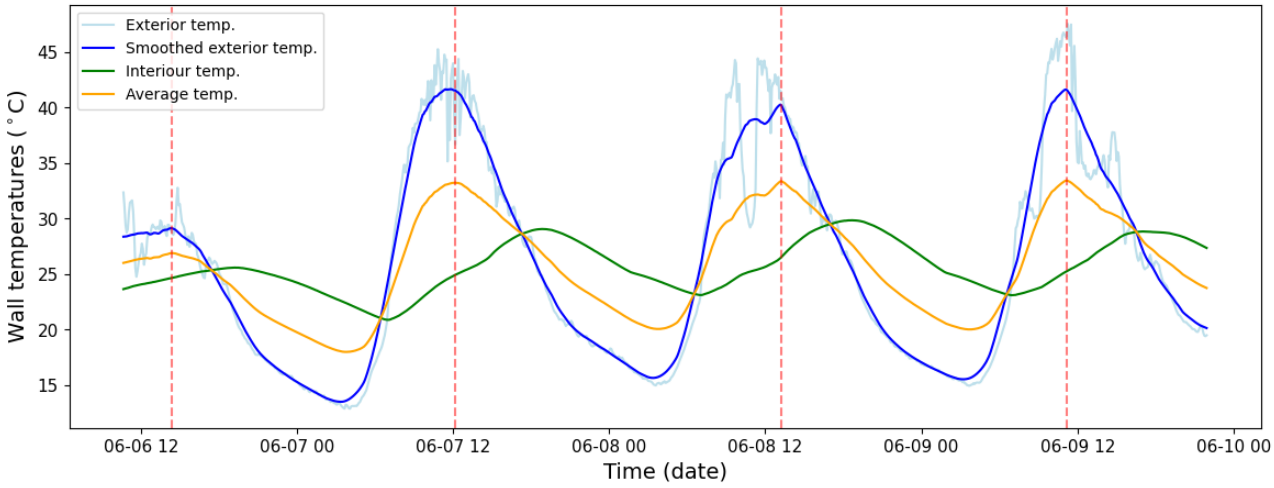

Figure 20: Exterior, interior and calculated average temperatures in the PCM model houses.

The characteristic temperature difference ($\Delta T_{x,s}$) is defined for envelope surface x as an exterior-to-interior surface temperature difference assigned to the selected characteristic daytime and night-time windows. Figure 20 illustrates the procedure: the exterior surface temperature exhibits a large-amplitude daily cycle (shown in both raw and smoothed form), while the interior surface temperature varies with a substantially smaller amplitude and with an evident time lag. The computed mean-temperature curve lies between the two and clearly indicates the vicinity of daily maxima and minima, which can be used to designate the characteristic windows. For a homogeneous wall, the mean temperature can be obtained as the arithmetic average of the exterior and interior surface temperatures; for multilayer assemblies, this is a practical approximation, but it remains suitable for the purpose of identifying characteristic windows.

Building on the characteristic temperature difference, a simplified estimate of a characteristic heat flux density ($q_{x,s}$) is introduced to approximate heat transfer at the key points of the daily cycle (daytime and night-time characteristic windows). The calculation assumes quasi-steady, one-dimensional heat conduction and uses the standard form of Fourier's law:

$$\mathbf{q_x = \Delta T_x / R_x} \qquad (2)$$

where:

- q_x is the estimated characteristic heat flux through surface x (W/m²),

- ΔT_x is the characteristic temperature difference between the exterior and interior wall surfaces (°C),
- R_x is the thermal resistance of the respective envelope element (m^2K/W), computed from the known layer build-up.

The R_x values are determined from the specified wall, roof, and floor assemblies, assuming identical geometry and material properties for the reference and the PCM-plastered unit. The PCM-containing plaster panels are treated as part of the interior lining. The plaster elements contained 22 wt% PCM microcapsules and were applied as a 25 mm thick indoor plaster layer over a total area of 15 m^2. Therefore, their role is interpreted primarily through additional heat capacity and, when activated, latent heat storage, rather than through a dominant change in steady-state thermal resistance.

Characteristic heat flux densities are computed separately for the daytime and night-time characteristic windows and for each orientation. This framework enables

- a consistent comparison of direction and magnitude of surface-level heat exchange,
- an orientation-resolved interpretation of the effect of external conditions particularly solar exposure—and
- a quantitative comparison of the modifying role of PCM plaster across façades.

Although the approach does not characterizes the full transient heat-flux dynamics or all details of the heat exchange, it provides a measurement-based and robust comparative framework for evaluating surface-level thermal interactions, and it supports the interpretation of cases in which the estimated heat flux appears larger in the PCM case at certain characteristic moments due to delay and buffering effects.

4.3.4. Orientation-dependent variability in daily surface-temperature extremes

Daily maximum and minimum surface temperatures were evaluated for each orientation over the full measurement period in order to capture orientation-specific thermal behavior under real boundary conditions. For this purpose, daily extreme values were extracted from the surface-temperature dataset and assessed in a trend-based framework to separate seasonal tendencies from short-term variability.

In Figures 21a–b, daily maximum values are shown for each orientation, and linear trend lines were fitted to the resulting point clouds. This representation condenses the dataset into:

- a seasonal tendency captured by the trend line, and
- day-to-day dispersion around that tendency, primarily driven by randomly changing meteorological boundary conditions.

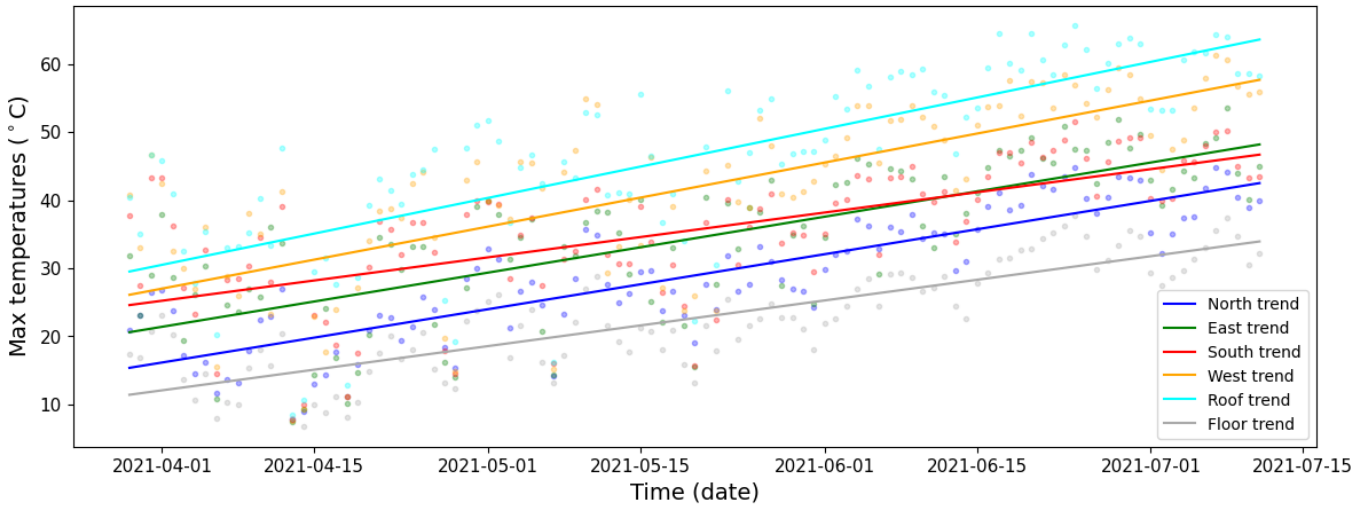

a.) Reference

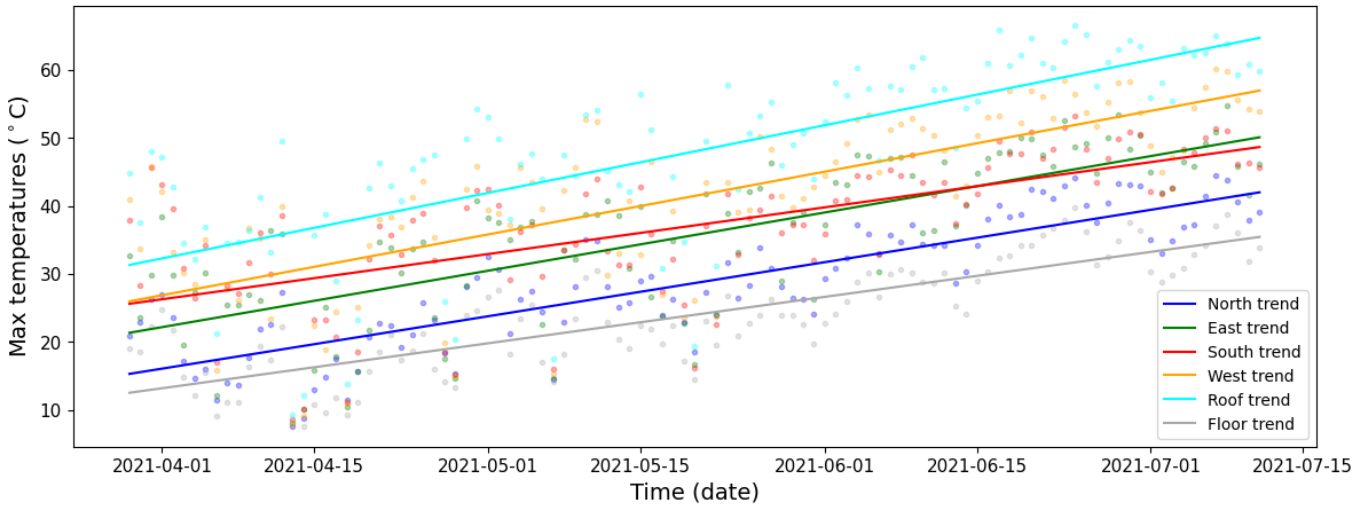

b.) PCM

Figure 21: Daily maximum surface temperatures by orientation with trendlines for model houses.

The relative position and slope of the trend lines make the role of orientation obvious at the level of daily peak surface temperatures.

To quantify the dispersion around the fitted trends, RMSE (root mean square error) was evaluated for the daily maxima and minima. In this context, RMSE represents the root of the mean squared deviation between the daily extreme values and the corresponding trend-line estimates. Higher RMSE values indicate stronger variability around the seasonal trend (i.e., greater sensitivity to short-term weather fluctuations), whereas lower RMSE values indicate a more uniform response around the trend.

Table 4: RMSE around linear trends for daily maximum and minimum surface temperatures by orientation (reference house vs. PCM-plastered house)

Orientation	*Max Ref (°C)*	*Max PCM (°C)*	*Min Ref (°C)*	*Min PCM (°C)*
North	4.86	4.79	3.21	3.19
East	7.38	7.43	3.14	3.19
South	7.41	7.55	3.15	3.20
West	8.72	8.45	3.22	3.23
Roof	8.52	8.94	3.97	3.82
Floor	4.22	4.40	2.89	2.80

The RMSE values reported in Table 4 are higher for daily maxima than for daily minima across all orientations, which is consistent with the stronger influence of short-term external loading during daytime peak conditions. Orientation effects are also more pronounced for the maxima: the highest RMSE values occur for the west orientation and the roof, whereas the north orientation and the floor show lower dispersion. For daily minima, RMSE values fall into a narrower range, although the roof remains relatively elevated, suggesting that its night-time behavior remains more sensitive to boundary-condition variability.

While the reference house and the PCM-plastered house exhibit RMSE values of similar order of magnitude across orientations, small differences can be observed, particularly for daily maxima. These differences are not treated as a strict quantitative comparison between houses; instead, they provide contextual support for separating:

- orientation- and weather-driven variability, and
- house-specific effects that may appear where peak-temperature regimes are more likely to activate phase-change processes.

4.3.5. Characteristic flux density derived from the characteristic temperature difference and interpretation of the apparent paradox

The purpose of introducing the characteristic temperature difference in Section 4.3.3 was to obtain an orientation-resolved, comparable quantity that can be linked directly to heat transfer through envelope elements under free-running conditions, without requiring more complex dynamic simulation. The definition of characteristic time windows was based on short intervals within the daily cycle in which the mean temperature of the base wall structure (i.e., the original layer build-up of the envelope) can be treated as approximately constant; therefore, a quasi-steady interpretation of the heat-flux estimate becomes acceptable. In parallel, the storage and delayed release or absorption of heat by the interior PCM plaster remains the governing mechanism; the approach does not remove this dynamic behavior but provides an interpretable framework for it.

Within this framework, the role of orientation is expressed primarily through the exterior-to-interior surface temperature difference (ΔT), as this quantity represents the driving potential relevant for conductive heat transfer. The ΔT time series and fitted trends for the PCM-plastered house are presented in Figure 22b, while the corresponding results for the reference house are shown in Figure 22a. Differences in ΔT magnitude and trend behavior across orientations provide the direct basis for differences in the computed characteristic heat-flux densities, because the subsequent estimation step is driven by the characteristic ΔT.

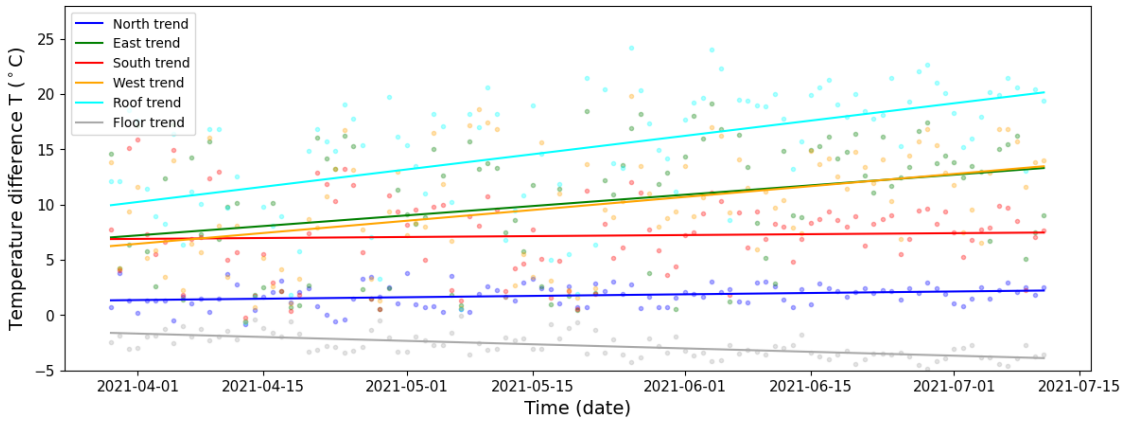

a.) Reference

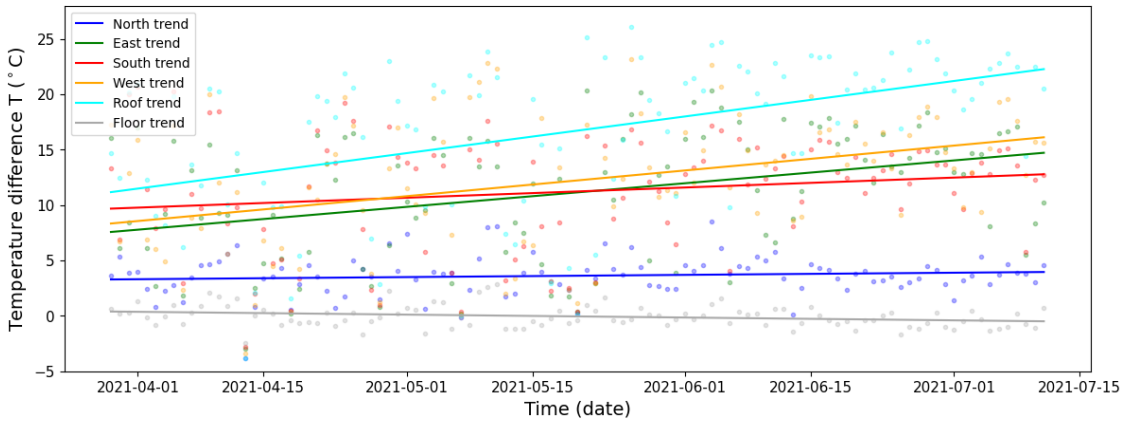

b.) PCM

Figure 22: Outer–inner surface temperature differences with trendlines for the model houses.

Characteristic heat-flux is determined using the previously defined relationship: the characteristic ΔT, evaluated within the selected daytime and night-time windows, is combined with the thermal resistance R of the given assembly (computed from the specified layer build-up). The calculation is applied by orientation and separately for daytime and night-time characteristic states, using the same procedure for both houses. This ensures methodological consistency, while allowing the resulting differences to reflect measured ΔT behavior and the presence of PCM plaster.

A key outcome is an apparently paradoxical situation: for several orientations, a higher instantaneous (external-side) driving potential and a correspondingly higher estimated characteristic heat-flux can occur with PCM plaster, without translating into higher indoor thermal stress. The resolution follows from the interpretation domain of the estimate. The

method characterizes the driving potential across the assembly and the associated heat-transfer tendency through the base structure; it does not directly represent the fraction of energy that appears immediately as indoor-air load. The PCM plaster acts as an interior-side thermal buffer, so peak exposure on the inner air temperature is moderated and shifted in time, even when the external-to-internal gradient—and thus the estimated characteristic flux—becomes larger at certain characteristic moments.

The implications differ between daytime and night-time characteristic states:

- During daytime characteristic states, the PCM plaster stores part of the incoming energy, thereby reducing and delaying indoor temperature peak exposure, while the exterior-to-interior gradient (and thus the estimated characteristic flux density) can be higher for several orientations.
- During night-time characteristic states, the estimated heat transfer is often lower, and in multiple cases the direction can reverse, particularly where the PCM releases stored heat more gradually after sunset.

In this sense, the characteristic flux approach makes the paradox physically explicit: a PCM layer can increase the instantaneous external-side driving potential while still contributing to a net reduction and temporal redistribution of heat load on the inner side (Figure 23).

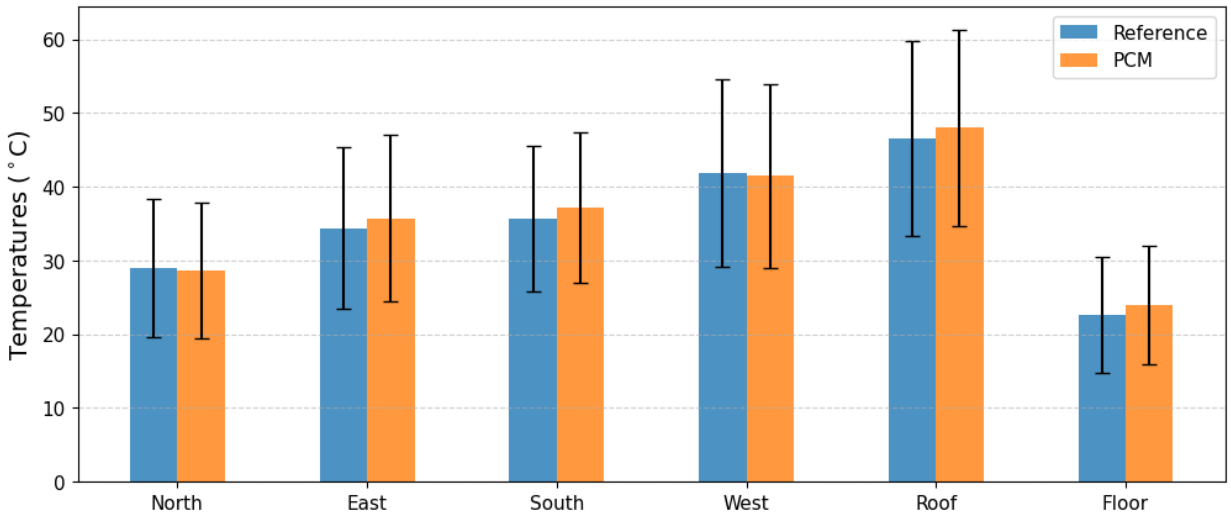

Figure 23: Comparison of average outside wall temperatures between the two model houses over the entire 105-day period - at temperature maxima

This redistribution means that, when heat flux is directed inward, a substantial fraction of the incoming flux is absorbed by the PCM layer, whereas during outward heat flux a significant portion of the released flux originates from latent heat released within the PCM rather than from cooling of the indoor air; in this way, the PCM layer mitigates the cooling of the indoor air.

Overall, the diurnal flux patterns indicate that PCM plaster primarily redistributes heat flow over time rather than simply blocking it; therefore, the orientation-resolved empirical results reported here provide a physically interpretable benchmark dataset for validating orientation-sensitive PCM simulations presented in previous numerical studies.

4.3.6. Orientation-resolved characteristic ΔT and heat-flux indicators

Evaluation of the characteristic heat-flux behavior over the diurnal cycle made it evident that the effectiveness of PCM plaster is fundamentally modulated by orientation.

The greatest practical benefit was observed on the west-facing façade. There, indoor peak temperatures were attenuated and the heating response was consistently delayed under the strong afternoon solar load typical of the monitored spring period. Similar effects were observed on the south-facing façade, although their magnitude was generally smaller. In contrast, PCM-related differences were more limited on the north-facing façade and on the floor, consistent with lower radiative exposure and more stable boundary conditions.

From an engineering perspective, characteristic heat-flux densities evaluated around daily maxima should not be interpreted as direct indoor thermal loads. For the most exposed orientations, the PCM-plastered house showed a moderated indoor peak response compared with the reference configuration. At the same time, characteristic gradients and the corresponding estimates derived from the external driving potential could be higher at selected characteristic moments. This does not imply increased indoor thermal stress. Heat storage and delayed release in the PCM plaster reduce peak exposure and shift it in time. The results therefore support an orientation-prioritized design approach: the highest

marginal benefit is expected on west- and south-facing façades and on the roof, while smaller effects are anticipated on the north façade and the floor.

The orientation-resolved summary of characteristic temperature differences already indicated material differences between the two houses. For the daytime, maximum-adjacent characteristic windows, larger characteristic temperature differences were obtained for the PCM-plastered house across all investigated envelope elements, while the floor constituted a special case: in the reference house, the daytime characteristic temperature difference was negative, whereas in the PCM-plastered house the value was close to zero; therefore, the characteristic ΔT was unambiguously higher in the PCM-plastered house when interpreted with sign (Figure 24). This can be explained by the fact that the daytime maximum indoor temperature is substantially higher in the reference house than in the house lined with PCM plaster. Consequently, relative to the given ground-adjacent external temperature, a larger characteristic temperature difference develops across the floor section. As a result, the characteristic temperature difference becomes negative in the reference house.

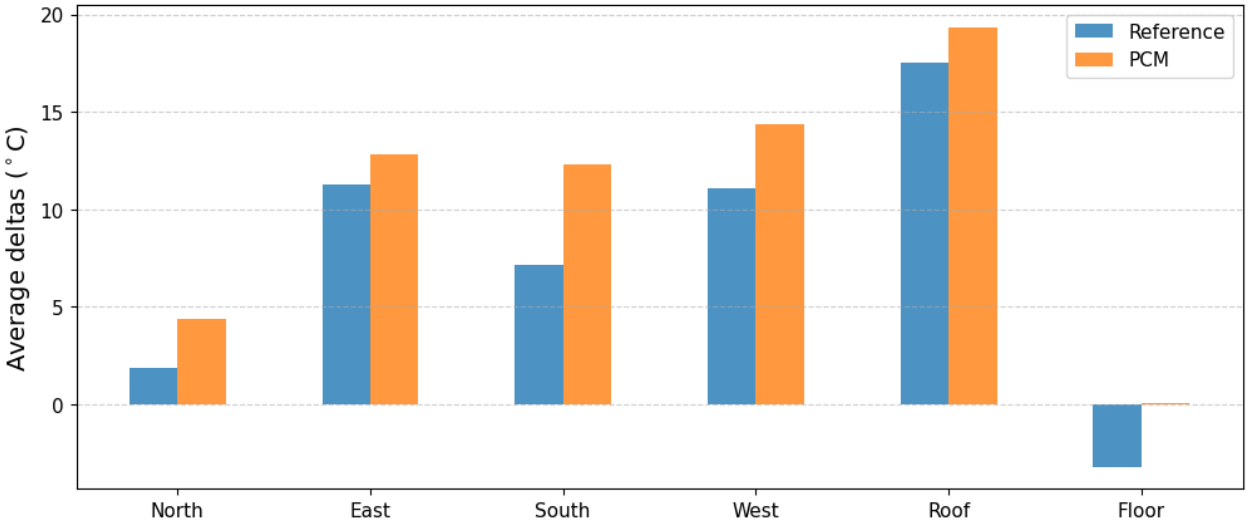

Figure 24: Comparison of average wall characteristic temperature difference (ΔT_{car}) between the two model houses over the entire 105-day period - at temperature maxima.

The evaluation was extended to the characteristic states associated with daily minima, because a core functional feature of PCM operation is the delayed and temporally distributed release of energy stored during daytime. Minimum-based characteristic states therefore provide additional information on the direction and magnitude of heat transfer

during the cooling phase, including cases in which the direction of the characteristic heat transfer can be modified by gradual post-sunset heat release (Figure 25).

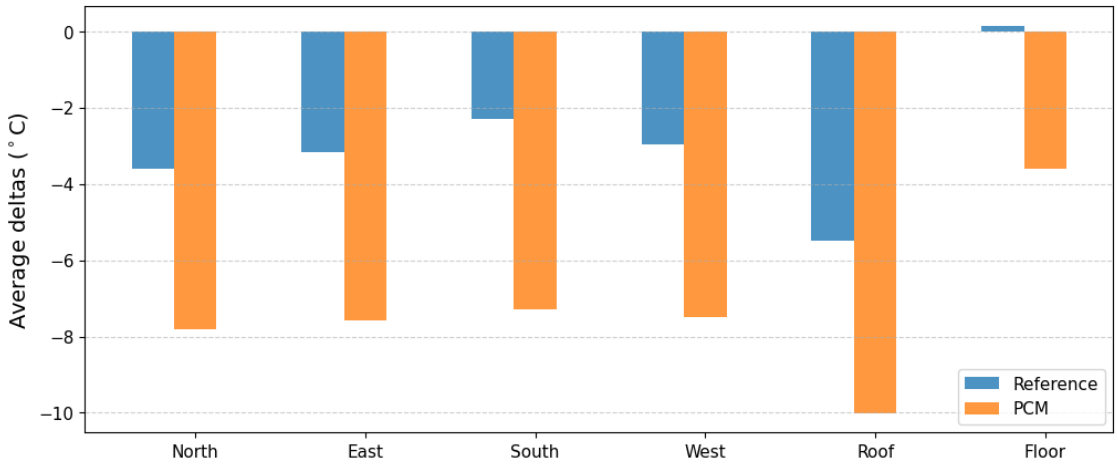

Figure 25: Comparison of average wall characteristic temperature difference (ΔT_{car}) between the two model houses over the entire 105-day period - at temperature minima.

The critical next step is the conversion of characteristic temperature differences into characteristic heat-fluxes. In this context, an apparently counterintuitive outcome was observed: the estimated characteristic heat fluxes in the PCM-plastered house were higher than those of the reference house for all orientations. This result can appear inconsistent with the concept of PCM plaster providing protection against overheating or overcooling. The inconsistency is resolved by specifying the interpretation domain of the estimate. By definition, the calculation characterizes heat transfer through the base wall structure (i.e., the layer build-up between the exterior steel sheet cladding and the interior OSB/finishing layer), rather than the portion of energy that reaches the indoor air immediately. As a consequence, a substantial fraction of the energy associated with the base-structure driving potential can be absorbed and stored by the interior plaster and PCM and subsequently released with delay. The quasi-steady characteristic-window concept is justified here, because the mean temperature of the base structure changes only negligibly within the selected windows, such that the sensible energy content of the base wall body can be treated as approximately constant.

The next step of the analysis was the calculation of orientation-resolved characteristic heat-fluxes from the characteristic temperature differences, using the layer-based thermal resistance(s) and assuming quasi-steady, one-dimensional heat conduction. The resulting

orientation-resolved characteristic heat-flux densities provide a compact engineering summary of where the driving potential across the base structure is highest and where it remains limited, while remaining consistent with the room-side mitigation effect introduced by PCM storage and delayed release (Figure 26).

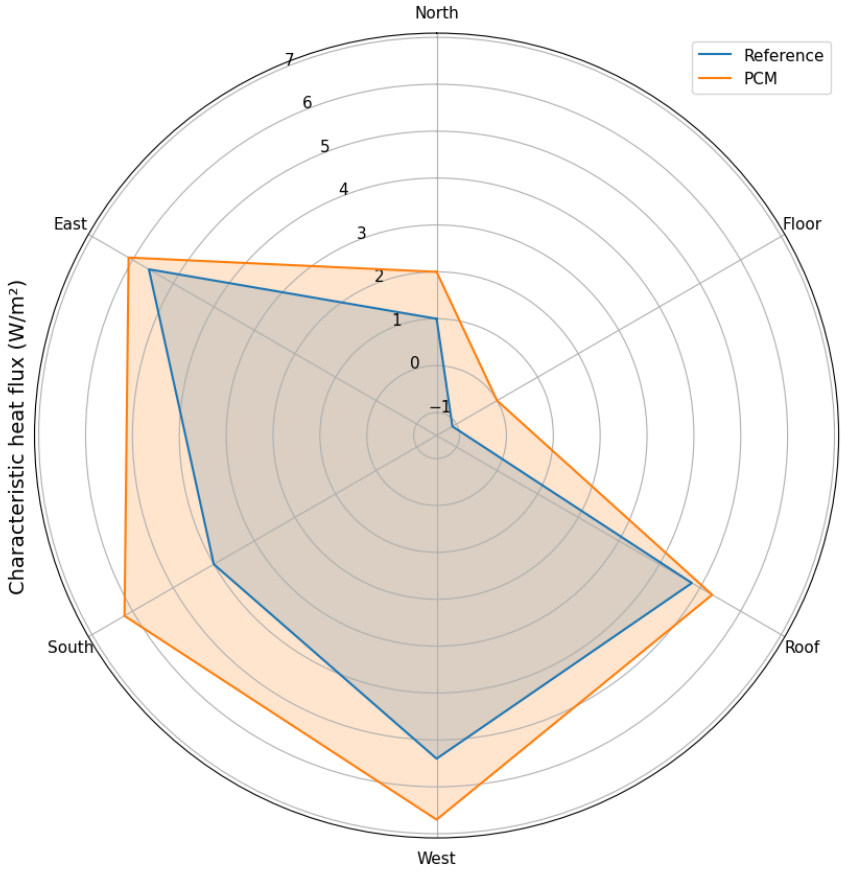

Figure 26: Characteristic heat fluxes for each orientation in individual model houses

Accordingly, the results are interpreted in terms of temporal redistribution rather than simple blocking: PCM plaster absorbs part of the incoming load and releases it later, so room-side peak exposure can be reduced and shifted even when the instantaneous external-side driving potential, and the corresponding characteristic heat-flux estimate across the base structure are higher. In this sense, the orientation-sensitive empirical dataset obtained here remains physically interpretable and can serve as a benchmark for validating previously reported numerical PCM simulations that explicitly account for orientation effects. [Ferster et al., 2017; Liu et al., 2022; Tunçbilek et al., 2025]

5. Summary and limitations

5.1 Summary

The dissertation examined the effect of plaster with incorporated microencapsulated phase change material on the dynamic thermal behavior of lightweight buildings. The study focused on how indoor PCM plaster modifies the daily indoor temperature profile, how it affects the magnitude and timing of peak temperatures, how it relates to overheating exposure and thermal comfort, and which orientations offer the greatest practical benefit based on measured data. The investigation was based on a 105-day measurement campaign conducted in 2021 in two identical lightweight model houses. The geometry and structural configuration of the two houses were the same. The difference was that the PCM-plastered model house was lined on the available inner surfaces of all four vertical walls, but not on the floor or roof, with 25 mm thick plaster panels containing microencapsulated paraffin-based PCM, covering a total area of 15 m², while the reference house had no additional PCM-containing plaster lining.

One important feature of the dissertation is that it is based not on simulation, but on the processing of a large, measured dataset. The large volume of raw sensor data was processed and evaluated through a Python-based, reproducible workflow, in several cases using statistical methods. This made it possible to draw conclusions not from a few selected days or isolated weather situations, but from the natural meteorological variability of the full monitoring period. This long time-series approach proved particularly important for interpreting the dynamic behavior of the lightweight system, since the effects under study appeared not in a single extreme value, but in the overall shape of the daily temperature profile.

The results confirmed that, under the investigated conditions, PCM plaster significantly reduced daily indoor temperature fluctuations. Compared with the reference house, lower daily amplitudes were observed, showing that PCM can moderate the effects of short-term thermal loads even under real conditions with strong solar radiation. Poincaré representation proved to be a particularly useful tool for interpreting the long time series, because it allowed the dynamic behavior of the two houses to be compared in a clear and consistent way. The investigation also showed that the model houses exhibited heat-trap-like behavior, meaning that indoor maximum temperatures, and in many cases indoor

mean temperatures as well, exceeded the corresponding outdoor air temperature. PCM did not eliminate this effect, but it reduced it, confirming that its influence remains meaningful under real loading conditions.

The second main group of findings concerned the temporal structure of the thermal response. The study showed that PCM affects not only the magnitude of indoor temperature peaks, but also shifts the timing of the daily maximum to a later hour. This peak delay can be interpreted as a distinct dynamic effect of PCM. The later occurrence of the peak proved favorable from a comfort perspective, since it increased the proportion of time spent within the comfort range and reduced overheating exposure. The dissertation therefore demonstrated that comparing daily maxima and minima alone is not sufficient to interpret the effect of PCM; the temporal profile of temperature and the position of the peaks also carry independent information.

The third group of findings related to practical applicability. Rather than seeking to define a general or average PCM effect, the study aimed to identify, on the basis of measured data, those orientations and building elements where PCM application is likely to be most beneficial. Characteristic temperature difference and characteristic heat flux density were used for the orientation-dependent evaluation. The results showed that the roof and the west-facing orientation represent the most critical loading conditions, while the role of the north-facing orientation is much smaller. This approach made it possible to treat PCM application not as a general measure, but as a targeted decision grounded in engineering considerations.

An important result of the dissertation is that, through a large-sample evaluation based on measured data, it confirmed the temperature-damping, peak-shifting, and comfort-improving effect of PCM plaster in a lightweight setting. The work contributed to a more precise understanding of PCM performance by placing the emphasis not only on absolute extremes, but also on the full daily temperature profile, temporal dynamics, and orientation-dependent applicability. On this basis, the dissertation provides not only new scientific findings, but also practical guidance for the targeted use of PCM in lightweight buildings.

5.2 Limitations

The results of the dissertation should be interpreted within the limits of the applied experimental framework. The study was based on measurements from two identical lightweight model houses. This provided a well-controlled basis for comparison, but it also limits direct generalization to full-scale occupied buildings. The findings are therefore directly valid mainly for the investigated structural configuration, geometry, and application method.

The measurement campaign was conducted under free-running conditions. This made it possible to reveal the natural dynamic thermal response of the structure. At the same time, the results cannot be transferred without qualification to buildings with active heating, cooling, ventilation, or shading systems, or to buildings where occupancy patterns and internal heat gains play a major role. Research plans in this direction are already well advanced and are aimed at a real lightweight building rather than a model container.

The investigated system did not include designed ventilation. For this reason, the measured indoor thermal behavior does not include the effects of controlled air exchange. This is especially important in small lightweight spaces, where ventilation can strongly influence the indoor temperature profile and overheating exposure. In addition, PCM was applied only in the indoor wall construction; the roof structure did not contain PCM. Since the roof proved to be one of the most heavily loaded surfaces in the study, this is important for the practical interpretation of the results.

The study was based on one 105-day measurement period in 2021. Although the size and density of the dataset provided a strong basis for the conclusions, the results still reflect the behavior of one specific meteorological period. The magnitude of the observed effects may therefore differ under other annual conditions, other climates, or more extreme weather situations. Consequently, the results should be interpreted within the validity domain of the 105-day free-running measurement period and the investigated model-house configuration, rather than as full-year performance indicators or directly transferable building-scale values.

The findings apply to the investigated plaster containing microencapsulated PCM, its specific location in the structure, and its thermal characteristics. Different PCM types, different phase-change ranges, different thicknesses, or different structural integration

may lead to different thermal behavior and different practical benefit. The conclusions should therefore not be treated as universally valid for all PCM systems.

The data-processing procedures used in the dissertation, including filtering, smoothing, and daily indicator extraction, form part of the interpretive framework. These steps were necessary for the consistent processing of the large sensor dataset. At the same time, the numerical values of some derived indicators may depend to some extent on the selected processing settings. This does not weaken the main findings, but it does justify interpreting them within the applied methodology.

The study did not cover the long-term aging of PCM, its mechanical durability, its economic performance, or its full life-cycle implications. These are important issues for practical implementation, but they were beyond the scope of the present dissertation. The results presented here should therefore be understood primarily as a contribution to the dynamic thermal behavior of the system and to its comfort-related effects.

New scientific results

The new scientific results are derived from the data of a 105-day free-running measurement campaign carried out in 2021. The investigation compared two lightweight model houses with identical geometry and structural design. One of the model houses had a plaster lining containing microencapsulated PCM on the internal vertical wall surfaces, while the reference house had no PCM-containing plaster lining.

The direct validity of the conclusions is limited to this measurement period, the given meteorological conditions, the applied PCM amount, the free-running mode of operation, and the investigated envelope configuration. The generalizable scientific contribution of the thesis statements lies in the fact that they quantify, on the basis of high-resolution measurement time series, the dynamic temperature attenuation, peak-time shifting, thermal comfort-related, and orientation-dependent effects of the PCM plaster. The specific quantitative results are interpreted within these boundary conditions; however, the applied data-processing and evaluation methodology can also be used in other PCM-related building physics studies with similar measurement arrangements.

1. I applied Poincare representation to the long indoor temperature time series recorded at 5-minute resolution in order to compare the dynamic temperature behavior over the full measurement period in an interpretable way. Using this method, the thermal behavior of the model houses could be compared both visually and mathematically through the evaluation of the standard deviations and the extent of the point cloud. Based on this representation, the indoor temperature response of the PCM-plastered house had a lower amplitude and was more balanced than that of the reference house [S1-S3].
2. I quantified the daily temperature attenuation effect of the PCM plaster over the full 105-day measurement period. The average daily indoor temperature amplitude was 6.3 °C in the reference house and 3.6 °C in the PCM-plastered house. This confirmed that, in the investigated lightweight model-house system, the latent heat storage effect of the PCM consistently reduced the daily indoor temperature fluctuation [S1].
3. I demonstrated the heat-trap-like behavior of the reference house through the combined analysis of daily indoor and outdoor maximum temperatures and solar

radiation over the full measurement period. Using 3D response surfaces constructed as functions of outdoor temperature and solar radiation, I showed that the daily maximum indoor temperatures in the reference house exceeded the outdoor air temperature to a greater extent than in the PCM-plastered house. Based on the difference between the two response surfaces, the applied PCM plaster reduced indoor overheating relative to the outdoor environment in the investigated experimental system [S1].

4. I quantified the peak-time shifting effect of the PCM plaster on a long measurement time series using a reproducible peak-detection procedure based on curve smoothing. In the PCM-plastered house, the average delay of the temperature peaks was approximately twice the value measured in the reference house. This showed that the effect of the PCM appeared not only in the reduction of peak temperatures, but also in the temporal rearrangement of the daily thermal response [S2].
5. I demonstrated that the peak-time shift caused by the PCM plaster also had a favorable effect from the perspective of thermal comfort. Based on the evaluation relative to the adaptive comfort range, the proportion of time spent within the comfort range increased in the PCM-plastered house. This confirmed that the effect of the PCM appears not only in the modification of daily extrema, but also in the more favorable temporal positioning of temperature peaks, and directly contributes to improved thermal comfort in the building [S2].
6. I determined the optimal orientation order for targeted PCM placement from measured surface temperature data, without simulation-based modeling. I calculated a characteristic temperature difference from the daily extrema and then estimated heat flux density from this value using Fourier's law of heat conduction. According to the resulting ranking, in the investigated experimental system, the roof and the western orientation proved to be the most favorable target surfaces, while the role of the northern orientation was substantially smaller [S3].

Tézisek

A tézisek egy 2021-ben végzett, 105 napos, szabadon futó mérési kampány adatain alapulnak. A vizsgálat két azonos geometriájú és szerkezeti kialakítású könnyűszerkezetes modellház összehasonlítására épült. Az egyik modellház belső oldali függőleges falfelületein mikrokapszulázott PCM-et tartalmazó vakolat-bélésréteg volt, míg a referenciaház PCM-es vakolat nélküli kialakítású volt.

A következtetések közvetlen érvényessége erre a mérési időszakra, az adott meteorológiai körülményekre, az alkalmazott PCM-mennyiségre, a szabadon futó üzemmódra és a vizsgált határolószerkezeti kialakításra vonatkozik. A tézisek általánosítható tudományos hozzájárulása abban áll, hogy nagyfelbontású mérési idősorok alapján számszerűsítik a PCM-vakolat dinamikus hőmérsékletcsillapító, csúcsidei eltolódást okozó, termikus komfortra gyakorolt és tájolásfüggő hatását. A konkrét számszerű eredmények e peremfeltételek között értelmezhetők, ugyanakkor az alkalmazott adatfeldolgozási és értékelési módszertan más, hasonló mérési elrendezésű PCM-es épületfizikai vizsgálatokban is alkalmazható.

1. A teljes mérési időszak dinamikus hőmérsékleti viselkedésének áttekinthető összehasonlítására Poincaré-ábrázolást alkalmaztam a hosszú, 5 perces felbontású beltéri hőmérsékleti idősorokon. A módszerrel a modellházak termikus viselkedése vizuálisan és matematikailag is összehasonlítható a szórások és a ponthalmaz kiterjedésének értékelésével. Az ábrázolás alapján a PCM-ház beltéri hőmérsékleti válasza kisebb amplitúdójú és kiegyenlítettebb volt, mint a referenciaházé.**[S1-S3]**.
2. A PCM-vakolat napi hőmérsékletcsillapító hatását a teljes, 105 napos mérési időszak alapján számszerűsítettem. Az átlagos napi beltéri hőmérséklet-amplitúdó a referenciaházban 6,3 °C, míg a PCM-házban 3,6 °C volt. Ez igazolta, hogy az adott könnyűszerkezetes modellházas rendszerben a PCM látens hőtároló hatása következetesen mérsékelte a napi beltéri hőmérséklet-ingadozást.**[S1]**.
3. A referenciaház hőcsapda-jellegű viselkedését a teljes mérési időszak napi belső és külső maximumhőmérsékleteinek, valamint a napsugárzásnak az együttes

elemzésével mutattam ki. A külső hőmérséklet és a napsugárzás függvényében képzett 3D válaszfelületek segítségével igazoltam, hogy a referenciaházban a napi beltéri maximumhőmérsékletek nagyobb mértékben haladták meg a külső léghőmérsékletet, mint a PCM-házban. A két válaszfelület különbsége alapján az alkalmazott PCM-vakolat az adott kísérleti rendszerben mérsékelte a külső környezethez viszonyított beltéri túlmelegedést.**[S1]**.

4. A PCM-vakolat csúcsidei eltoló hatását reprodukálható görbesimítást alkalmazó csúcskeresési eljárással, hosszú mérési idősoron számszerűsítettem. A PCM-házban a hőmérsékleti csúcsok átlagos késése megközelítőleg kétszerese volt a referenciaházban mért értéknek. Ez azt mutatta, hogy a PCM hatása nemcsak a csúcshőmérsékletek mérséklésében, hanem a napi hőválasz időbeli átrendezésében is megjelent.**[S2].**

5. Kimutattam, hogy a PCM-vakolat által okozott csúcsidei eltolódás a termikus komfort szempontjából is kedvező hatású. Az adaptív komforttartományhoz viszonyított értékelés alapján a PCM-házban nőtt a komfort-tartományon belül töltött idő aránya. Ez igazolta, hogy a PCM hatása nemcsak a napi szélsőértékek módosításában, hanem a hőmérsékleti csúcsok kedvezőbb időbeli elhelyezkedésében is megjelenik, és közvetlenül hozzájárul az épület jobb termikus komfortjához.**[S2]**.

6. Mért felületi hőmérsékleti adatokból, nem szimulációs modellezéssel határoztam meg a PCM célzott elhelyezése szempontjából optimális tájolási sorrendet. A napi szélsőértékekből karakterisztikus hőmérséklet-különbséget számítottam, majd ebből a Fourier-féle hővezetési összefüggés alapján hőáramsűrűséget becsültem. Az így kapott rangsor szerint az adott kísérleti rendszerben a tető és a nyugati tájolás bizonyult a legkedvezőbb célfelületnek, míg az északi tájolás szerepe lényegesen kisebb volt.**[S3]**.

Publications forming the basis of the theses

[S1] Ferencz, M., Németh, B., Gyenis, J., & Feczkó, T. (2025). Statistical evaluation of PCM plaster lining impact on indoor temperature fluctuation due to variability of outdoor temperature and solar radiation along a whole spring season. Journal of Building Engineering, 99, 111626. https://doi.org/10.1016/j.jobe.2024.111626 **D1, IF: 7.4**

[S2] Ferencz, M., Nagy, B., Németh, B., Gyenis, J., & Feczkó, T. (2025). Quantifying thermal time lag due to PCM plaster in model houses. Buildings, 15(22), 4120. https://doi.org/10.3390/buildings15224120 **Q2 IF: 3.1**

[S3] Ferencz, M., Nagy, B., Gyenis, J., Feczkó, T. (2026) Experimental study on the thermal behavior of PCM plaster lined model house walls during a whole spring season influenced by their orientation

Other own publications related to the dissertation

[S4] Németh, B., Ujhidy, A., Tóth, J., Ferencz, M., Kurdi, R., Gyenis, J., & Feczkó, T. (2023). Power consumption of model houses with and without PCM plaster lining using different heating methods. Energy and Buildings, 284, 112845. **D1, IF. 7.1**

https://doi.org/10.1016/j.enbuild.2023.112845

[S5] Németh, B., Ferencz, M., Kovács, S., Trif, L., Lendvai, J., Kolay, Kovács, Á., Király, K., & Feczkó, T. (2024). Fázisváltó hőtároló anyagok előállítása hulladék zsírból és használt növényi olajból. ENERGIAGAZDÁLKODÁS, 65(Hőhajó különszám), 26–33.

References

Al-Absi, Z. A., Mohd Hafizal, M. I., & Ismail, M. (2022). *Experimental study on the thermal performance of PCM-based panels developed for exterior finishes of building walls*. Journal of Building Engineering, 52, 104379. https://doi.org/10.1016/j.jobe.2022.104379

Al-Absi, Z. A., Mat, S., Sopian, K., Sulaiman, M. Y., & Zaidi, S. H. (2020). *Phase change materials (PCMs) and their optimum position in building walls*. Sustainability, 12(4), 1294. https://doi.org/10.3390/su12041294

Akeiber, H. J., Wahid, M. A., Hussen, H. M., & Mohammad, A. T. (2014). *Review of development survey of phase change material models in building applications*. The Scientific World Journal, 391690. https://doi.org/10.1155/2014/391690

Al-Rashed, A. A. A. A., Alnaqi, A. A., & Alsarraf, J. (2021). *Energy-saving of building envelope using passive PCM technique: A case study of Kuwait City climate conditions*. Sustainable Energy Technologies and Assessments, 46, 101254. https://doi.org/10.1016/j.seta.2021.101254

Al-Yasiri, Q., & Szabó, M. (2023). *Numerical analysis of thin building envelope-integrated phase change material towards energy-efficient buildings in severe hot location*. Sustainable Cities and Society, 89, 104365. https://doi.org/10.1016/j.scs.2022.104365

Anter, A. G., Sultan, A. A., Hegazi, A. A., & El Bouz, M. A. (2023). *Thermal performance and energy saving using phase change materials (PCM) integrated in building walls*. Journal of Energy Storage, 67, 107568. https://doi.org/10.1016/j.est.2023.107568

Aqilah, N., Rijal, H. B., & Zaki, S. A. (2022). *A review of thermal comfort in residential buildings: Comfort trends and energy saving potential*. Energies, 15, 9012. https://doi.org/10.3390/en15239012

Arıcı, M., Bilgin, F., Nižetić, S., & Karabay, H. (2020). *PCM integrated to external building walls: An optimization study on maximum activation of latent heat*. Applied Thermal Engineering, 165, 114560. https://doi.org/10.1016/j.applthermaleng.2019.114560

Arıcı, M., Bilgin, F., Krajčík, M., Nižetić, S., & Karabay, H. (2022). *Energy saving and CO_2 reduction potential of external building walls containing two layers of phase change material*. Energy, 252, 124010. https://doi.org/10.1016/j.energy.2022.124010

Arsad, F. S., Hod, R., Ahmad, N., Baharom, M., & Ja'afar, M. H. (2023). *Assessment of indoor thermal comfort temperature and related behavioural adaptations: A systematic*

review. *Environmental Science and Pollution Research, 30*, 73137–73149. https://doi.org/10.1007/s11356-023-27089-9

Ascione, F., Bianco, N., De Masi, R. F., de' Rossi, F., & Vanoli, G. P. (2014). *Energy refurbishment of existing buildings through the use of phase change materials: Energy savings and indoor comfort in the cooling season*. Applied Energy, 113, 990–1007. https://doi.org/10.1016/j.apenergy.2013.08.045

Baetens, R., Jelle, B. P., & Gustavsen, A. (2010). *Phase change materials for building applications: A state-of-the-art review*. Energy and Buildings, 42(9), 1361–1368. https://doi.org/10.1016/j.enbuild.2010.03.026

Biswas, K., & Abhari, R. (2014). *Low-cost phase change material as an energy storage medium in building envelopes: Experimental and numerical analyses*. Energy Conversion and Management, 88, 1020–1031. https://doi.org/10.1016/j.enconman.2014.09.003

Bruno, R., & Bevilacqua, P. (2023). *Bio-PCM to enhance dynamic thermal properties of dry-assembled wooden walls: Experimental results*. Building and Environment, 242, 110526. https://doi.org/10.1016/j.buildenv.2023.110526

Cabeza, L. F., Castell, A., Barreneche, C., de Gracia, A., & Fernández, A. I. (2011). *Materials used as PCM in thermal energy storage in buildings: A review*. Renewable and Sustainable Energy Reviews, 15(3), 1675–1695. https://doi.org/10.1016/j.rser.2010.11.018

Cabeza, L. F., Castellón, C., Nogués, M., Medrano, M., Leppers, R., & Zubillaga, O. (2007). *Use of microencapsulated PCM in concrete walls for energy savings*. Energy and Buildings, 39(2), 113–119. https://doi.org/10.1016/j.enbuild.2006.03.030

Carlucci, F., De Simone, M., & Firth, S. K. (2021). *Phase change material integration in building envelopes: A review of research trends and simulation methods*. Applied Sciences, 11(10), 4680. https://doi.org/10.3390/app11104680

Castell, A., Martorell, I., Medrano, M., Pérez, G., & Cabeza, L. F. (2010). *Experimental study of using PCM in brick constructive solutions for passive cooling*. Energy and Buildings, 42(4), 534–540. https://doi.org/10.1016/j.enbuild.2009.10.022

Childs, K. W., & Stovall, T. K. (2012). *Potential energy savings due to phase change material in a building wall assembly: An examination of two climates* (ORNL/TM-2012/6). Oak Ridge National Laboratory. https://doi.org/10.2172/1038077

Claude, V., Charron, S., de Barquin, F., & Dirkx, I. (2021). *Microencapsulated phase changing materials for gypsum plasters: A practical approach*. Construction Materials, 1(3), 188–202. https://doi.org/10.3390/constrmater1030012

de Gracia, A., Castell, A., Medrano, M., & Cabeza, L. F. (2011). *Dynamic thermal performance of alveolar brick construction system*. Energy Conversion and Management, 52(7), 2495–2500. https://doi.org/10.1016/j.enconman.2011.01.022

Drissi, S., Ling, T.-C., Mo, K. H., & Eddhahak, A. (2019). *A review of microencapsulated and composite phase change materials: Alteration of strength and thermal properties of cement-based materials*. Renewable and Sustainable Energy Reviews, 110, 467–484. https://doi.org/10.1016/j.rser.2019.04.072

EN 16798-1:2019. (2019). Energy performance of buildings—Ventilation for buildings—Part 1: Indoor environmental input parameters for design and assessment of energy performance of buildings addressing indoor air quality, thermal environment, lighting and acoustics—Module M1-6. Brussels: European Committee for Standardization.

Fan, Z., Zhao, Y., Shi, Y., Liu, X., & Jiang, D. (2023). *Thermal performance evaluation of a novel building wall for lightweight building containing phase change materials and interlayer ventilation: An experimental study*. Energy and Buildings, 278, 112677. https://doi.org/10.1016/j.enbuild.2022.112677

Ferdyn-Grygierek, J., Grygierek, K., Gumińska, A., Krawiec, P., Oćwieja, A., Poloczek, R., Szkarłat, J., Zawartka, A., Zobczyńska, D., & Żukowska-Tejsen, D. (2021). *Passive cooling solutions to improve thermal comfort in Polish dwellings*. Energies, 14, 3648. https://doi.org/10.3390/en14123648

https://doi.org/10.1016/j.jobe.2024.111626Ferster, B., Shen, H., & Rendall, J. D. (2017). *PCM (phase change material) optimization modeling for passive cooling in South Texas*. In *Proceedings of Building Simulation 2017 (15th IBPSA Conference)* (pp. 958–965). https://doi.org/10.26868/25222708.2017.255

Fořt, J., Trník, A., Pavlíková, M., Pavlík, Z., & Černý, R. (2018). *Fabrication of dodecanol/diatomite shape-stabilized PCM and its utilization in interior plaster*. International Journal of Thermophysics, 39(12), 137. https://doi.org/10.1007/s10765-018-2459-z

Gounni, A., & El Alami, M. (2017). *The optimal allocation of the PCM within a composite wall for surface temperature and heat flux reduction: An experimental approach*. Applied Thermal Engineering, 127, 1488–1494. https://doi.org/10.1016/j.applthermaleng.2017.08.168

Grygierek, K., & Sarna, I. (2020). *Impact of passive cooling on thermal comfort in a single-family building for current and future climate conditions*. Energies, 13, 5332. https://doi.org/10.3390/en13205332

Hepple, R., Zhao, Y., Yang, R., Zhang, Q., & Yang, S. (2024). *Investigating the effects of PCM-integrated walls on thermal performance for UK residential buildings of different typologies*. Buildings, 14, 3382. https://doi.org/10.3390/buildings14113382

Izquierdo-Barrientos, M. A., Belmonte, J. F., Rodríguez-Sánchez, D., Molina, A. E., & Almendros-Ibáñez, J. A. (2012). *A numerical study of external building walls containing phase change materials (PCM)*. Applied Thermal Engineering, 47, 73–85. https://doi.org/10.1016/j.applthermaleng.2012.02.038

Jin, X., Medina, M. A., & Zhang, X. (2016). *Numerical analysis for the optimal location of a thin PCM layer in frame walls*. Applied Thermal Engineering, 103, 1057–1063. https://doi.org/10.1016/j.applthermaleng.2016.04.056

Kalnæs, S. E., & Jelle, B. P. (2015). *Phase change materials and products for building applications: A state-of-the-art review and future research opportunities*. Energy and Buildings, 94, 150–176. https://doi.org/10.1016/j.enbuild.2015.02.023

Karaipekli, A., Sarı, A., & Biçer, A. (2016). *Thermal regulating performance of gypsum/(C18–C24) composite phase change material (CPCM) for building energy storage applications*. Applied Thermal Engineering, 107, 55–62. https://doi.org/10.1016/j.applthermaleng.2016.06.160

Khudhair, A. M., & Farid, M. M. (2004). *A review on energy conservation in building applications with thermal storage by latent heat using phase change materials*. Energy Conversion and Management, 45(2), 263–275. https://doi.org/10.1016/S0196-8904(03)00131-6

Kishore, R. A., Bianchi, M. V. A., Booten, C., Vidal, J., & Jackson, R. (2021). *Parametric and sensitivity analysis of a PCM-integrated wall for optimal thermal load modulation in lightweight buildings*. Applied Thermal Engineering, 187, 116568. https://doi.org/10.1016/j.applthermaleng.2021.116568

Konuklu, Y., Ostry, M., Paksoy, H. O., & Charvát, P. (2015). *Review on using microencapsulated phase change materials (PCM) in building applications*. Energy and Buildings, 106, 134–155. https://doi.org/10.1016/j.enbuild.2015.07.019

Kuznik, F., David, D., Johannes, K., & Roux, J.-J. (2011). *A review on phase change materials integrated in building walls*. *Renewable and Sustainable Energy Reviews, 15*(1), 379–391. https://doi.org/10.1016/j.rser.2010.08.019

Lachheb, M., Younsi, Z., Naji, H., Karkri, M., & Ben Nasrallah, S. (2017). *Thermal behavior of a hybrid PCM/plaster: A numerical and experimental investigation*. Applied Thermal Engineering, 111, 49–59. https://doi.org/10.1016/j.applthermaleng.2016.09.083

Lajimi, N., & Boukadida, N. (2023). *Effect of the position of the PCM on the thermal behavior of a multilayer wall of a building in summer period*. Frontiers in Environmental Science, 11, 1226454. https://doi.org/10.3389/fenvs.2023.1226454

Lee, A. K. (2022). *Application of PCM to shift and shave peak demand: Parametric studies* (Master's thesis). Concordia University, Montreal, Quebec, Canada. https://spectrum.library.concordia.ca/id/eprint/979032/

Lee, K. O., Medina, M. A., Raith, E., & Sun, X. (2015). *Assessing the integration of a thin phase change material (PCM) layer in a residential building wall for heat transfer reduction and management*. Applied Energy, 137, 699–706. https://doi.org/10.1016/j.apenergy.2014.09.003

Li, W., Rahim, M., Wu, D., El Ganaoui, M., & Bennacer, R. (2024). *Experimental study of dynamic PCM integration in building walls for enhanced thermal performance in summer conditions*. Renewable Energy, 237, 121891. https://doi.org/10.1016/j.renene.2024.121891

Liu, Z., Hou, J., Wei, D., Meng, X., & Dewancker, B. J. (2022). *Thermal performance analysis of lightweight building walls in different directions integrated with phase change materials (PCM)*. Case Studies in Thermal Engineering, 40, 102536. https://doi.org/10.1016/j.csite.2022.102536

Mahmoud, M., Yousef, B. A. A., Radwan, A., Alkhalidi, A., Abdelkareem, M. A., & Olabi, A. G. (2024). *Thermal assessment of lightweight building walls integrated with phase change material under various orientations*. Journal of Building Engineering, 85, 108614. https://doi.org/10.1016/j.jobe.2024.108614

Mavromatidis, L. E., El Mankibi, M., Michel, P., & Santamouris, M. (2012). *Numerical estimation of time lags and decrement factors for wall complexes including multilayer thermal insulation, in two different climatic zones*. Applied Energy, 92, 480–491. https://doi.org/10.1016/j.apenergy.2011.10.007

Németh, B., Ujhidy, A., Tóth, J., Gyenis, J., & Feczkó, T. (2021). *Testing of microencapsulated phase-change heat storage in experimental model houses under winter weather conditions*. Building and Environment, 204, 108119. https://doi.org/10.1016/j.buildenv.2021.108119

Nghana, B., & Tariku, F. (2016). *Phase change material's (PCM) impacts on the energy performance and thermal comfort of buildings in a mild climate*. Building and Environment, 99, 221–238. https://doi.org/10.1016/j.buildenv.2016.01.023

Pielichowska, K., & Pielichowski, K. (2014). *Phase change materials for thermal energy storage*. Progress in Materials Science, 65, 67–123. https://doi.org/10.1016/j.pmatsci.2014.03.005

Plytaria, M. T., Tzivanidis, C., Bellos, E., Alexopoulos, I., & Antonopoulos, K. A. (2019). *Thermal behavior of a building with incorporated phase change materials in the south and the north wall*. Computation, 7(1), 2. https://doi.org/10.3390/computation7010002

Pomianowski, M. Z., Heiselberg, P., & Zhang, Y. (2013). *Review of thermal energy storage technologies based on PCM application in buildings*. Energy and Buildings, 67, 56–69. https://doi.org/10.1016/j.enbuild.2013.08.006

Ranger, C. G., Rivera-Solorio, C. I., Gijón-Rivera, M., & Mousavi, S. (2022). *The effect on thermal comfort and heat transfer in naturally ventilated roofs with PCM in a semi-arid climate: An experimental research*. Energy and Buildings, 274, 112453. https://doi.org/10.1016/j.enbuild.2022.112453

Serrano, S., Barreneche, C., Navarro, A., Haurie, L., Fernandez, A. I., & Cabeza, L. F. (2016). *Use of multi-layered PCM gypsums to improve fire response: Physical, thermal*

and mechanical characterization. Energy and Buildings, 127, 1–9. https://doi.org/10.1016/j.enbuild.2016.05.056

Stejskalová, K., Bujdoš, D., Procházka, L., Smetana, B., Zlá, S., & Teslík, J. (2022). *Mechanical, thermal, and fire properties of composite materials based on gypsum and PCM*. Materials, 15(3), 1253. https://doi.org/10.3390/ma15031253

Sun, X., Medina, M. A., & Zhang, Y. (2019). *Potential thermal enhancement of lightweight building walls derived from using phase change materials (PCMs)*. Frontiers in Energy Research, 7, 13. https://doi.org/10.3389/fenrg.2019.00013

Thiele, A. M., Liggett, R. S., Sant, G., & Pilon, L. (2017). *Simple thermal evaluation of building envelopes containing phase change materials using a modified admittance method*. *Energy and Buildings, 145*, 238–250. https://doi.org/10.1016/j.enbuild.2017.03.046

Thermofoam Kft., Pannon University, & Centre for Energy Research. (2021). *Modern thermal energy storage in buildings using environmentally friendly phase change materials in construction and insulation elements* [Project booklet; in Hungarian: *Épületek korszerű hőtárolása környezetbarát fázisváltó anyagok alkalmazásával építő- és szigetelőelemekben*]. GINOP-2.2.1-15-2016-00010 project. http://biopcm.hu/assets/downloads/Kiadvany.pdf

Toure, P. M., Dieye, Y., Gueye, P. M., Sambou, V., Bodian, S., & Tiguampo, S. (2019). *Experimental determination of time lag and decrement factor*. Case Studies in Construction Materials, 11, e00298. https://doi.org/10.1016/j.cscm.2019.e00298

Tunçbilek, E., Arıcı, M., Krajčík, M., Li, D., Nižetić, S., & Papadopoulos, A. M. (2023). *Enhancing building wall thermal performance with phase change material and insulation: A comparative and synergistic assessment*. Renewable Energy, 218, 119270. https://doi.org/10.1016/j.renene.2023.119270

Xu, C., Zhang, Y., & Qiu, D. (2024). *The regulation of temperature fluctuations and energy consumption in buildings using phase change material–gypsum boards in summer*. Buildings, 14, 3387. https://doi.org/10.3390/buildings14113387

Zalba, B., Marín, J. M., Cabeza, L. F., & Mehling, H. (2003). *Review on thermal energy storage with phase change: Materials, heat transfer analysis and applications*. Applied Thermal Engineering, 23(3), 251–283. https://doi.org/10.1016/S1359-4311(02)00192-8

Zhang, Y., Lin, K., Jiang, Y., & Zhou, G. (2008). *Thermal storage and nonlinear heat-transfer characteristics of PCM wallboard*. Energy and Buildings, 40(9), 1717–1723. https://doi.org/10.1016/j.enbuild.2008.03.005

Zhou, G., Zhang, Y., Wang, X., Lin, K., & Xiao, W. (2007). *An assessment of mixed type PCM-gypsum and shape-stabilized PCM plates in a building for passive solar heating*. Solar Energy, 81(11), 1351–1360. https://doi.org/10.1016/j.solener.2007.01.014

Zhuang, S., Zhang, Y., Zhu, Q., Yan, R., & He, J. (2015). *Experimental study on the thermal response of PCM energy storage block with hole ventilation*. Advances in Materials Science and Engineering, 981854. https://doi.org/10.1155/2015/981854

Acknowledgments

I would like to express my gratitude to all those who contributed to the completion of this dissertation, whether through professional or personal support.

First and foremost, I am grateful to my supervisor, Tivadar Feczkó PhD, for the professional guidance, critical remarks, and support provided throughout the research. I would also like to express my sincere gratitude to János Gyenis DSc, Professor Emeritus of the University of Pannonia, for his devoted, patient, and indispensable support, advice, and encouragement.

I also thank all colleagues and co-authors with whom I had the opportunity to work during the individual publications and investigations. Their collaboration, professional discussions, and shared thinking contributed significantly to the final form of the dissertation.

I am especially grateful to my husband, Barna Nagy not only for his constant emotional support, but also for his help with the development and refinement of the Python codes.

Finally, I would like to thank all family members, friends, and supporters who stood by me with patience, understanding, and encouragement throughout this long period of work.

Last but not least, this work was funded by the 2020-1.1.2-PIACI-KFI-2021-00287 project provided by the National Research, Development and Innovation Fund of Hungary.

Annex 1: Software and Libraries Used

The analyses in this dissertation were conducted using Python 3.10.11. For data processing, the following Python libraries were employed:

- Matplotlib 3.10.6: Data visualization
- Pandas 2.2.3: Data analysis and manipulation
- NumPy 2.3.3: Numerical computing
- SciPy 1.16.3: Statistical analysis

All code is available upon request.

For the comparative computation of the 3D saddle surface, we used TIBCO Statistica 14.0 (StatSoft, Inc.).